

Representing and Learning Functions Invariant Under Crystallographic Groups

Ryan P Adams and Peter Orbanz

Abstract. Crystallographic groups describe the symmetries of crystals and other repetitive structures encountered in nature and the sciences. These groups include the wallpaper and space groups. We derive linear and nonlinear representations of functions that are (1) smooth and (2) invariant under such a group. The linear representation generalizes the Fourier basis to crystallographically invariant basis functions. We show that such a basis exists for each crystallographic group, that it is orthonormal in the relevant L_2 space, and recover the standard Fourier basis as a special case for pure shift groups. The nonlinear representation embeds the orbit space of the group into a finite-dimensional Euclidean space. We show that such an embedding exists for every crystallographic group, and that it factors functions through a generalization of a manifold called an orbifold. We describe algorithms that, given a standardized description of the group, compute the Fourier basis and an embedding map. As examples, we construct crystallographically invariant neural networks, kernel machines, and Gaussian processes.

1 Introduction

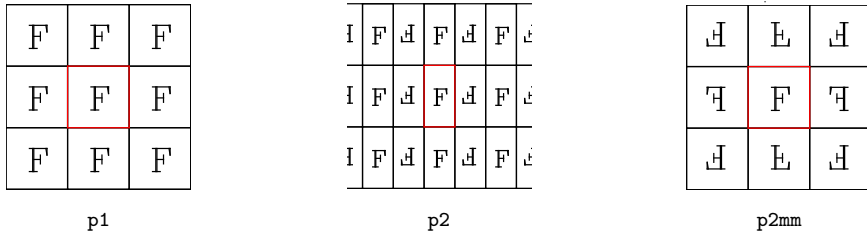
Among the many forms of symmetry observed in nature, those that arise from repetitive spatial patterns are particularly important. These are described by sets of transformations of Euclidean space called crystallographic groups [62, 65]. For example, consider a problem in materials science, where atoms are arranged in a crystal lattice. The symmetries of the lattice are then characterized by a crystallographic group \mathbb{G} . Symmetry means that, if we apply one of the transformations in \mathbb{G} to move the lattice—say to rotate or shift it—the transformed lattice is indistinguishable from the untransformed one. In such a lattice, the Coulomb potential acting on any single electron due to a collection of fixed nuclei does not change under any of the transformations in \mathbb{G} [12, 36, 42]. If we think of the potential field as a function on \mathbb{R}^3 , this is an example of a \mathbb{G} -invariant function, i.e., a function whose values do not change if its arguments are transformed by elements of the group. When solving the resulting Schrödinger equation for single particle states, members of the group commute with the Hamiltonian, and quantum observables are again \mathbb{G} -invariant [12, 26, 36, 37, 42, 57]. A different example are ornamental tilings on the walls of the Alhambra, which, when regarded as functions on \mathbb{R}^2 , are invariant under two-dimensional crystallographic groups [58]. The purpose of this work is to construct smooth invariant functions for any given crystallographic group in any dimension.

For finite groups, invariant functions can be constructed easily by summing over all group elements; for compact infinite groups, the sum can be replaced by an integral. This and related ideas have received considerable attention in machine learning [e.g., 14, 21, 38]. Such summations are not possible for crystallographic groups, which are neither finite nor compact, but their specific algebraic and geometric properties allow us to approach the problem in a different manner. We postpone a detailed literature review to Section 10, and use the remainder of this section to give a non-technical sketch of our results.

1.1. A non-technical overview

This section sketches our results in a purely heuristic way; proper definitions follow in Section 2.

Crystallographic symmetry. Crystallographic groups are groups that tile a Euclidean space \mathbb{R}^n with a convex shape. Suppose we place a convex polytope Π in the space \mathbb{R}^n , say a square or a rectangle in the plane. Now make a copy of Π , and use a transformation $\phi : \mathbb{R}^2 \rightarrow \mathbb{R}^2$ to move this copy to another location. We require that ϕ is an isometry, which means it may shift, rotate or flip Π , but does not change its shape or size. Here are some examples, where the original shape Π is marked in red:

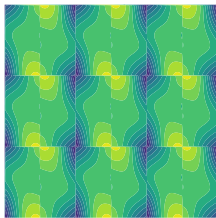


The descriptors **p1**, **p2**, and **p2mm** follow the naming standard for groups developed by crystallographers [31], and the symbol “F” is inscribed to clarify which transformations are used. The transformations in these examples are horizontal and vertical shifts (in **p1**), rotations around the corners of the rectangle in (**p2**), and reflections about its edges (**p2mm**). Suppose we repeat one of these processes indefinitely so that the copies of Π cover the entire plane and overlap only on their boundaries. That requires a countably infinite number of transformations, one per copy. Collect these into a set \mathbb{G} . If this set forms a group, this group is called crystallographic. Such groups describe all possible symmetries of crystals, and have been thoroughly studied in crystallography. For each dimension n , there is—up to a natural notion of isomorphism that we explain in Section 2—only a finite number of crystallographic groups: Two on \mathbb{R} , 17 on \mathbb{R}^2 , 230 on \mathbb{R}^3 , and so forth. Those on \mathbb{R}^2 are also known as wallpaper groups, and those on \mathbb{R}^3 as space groups.

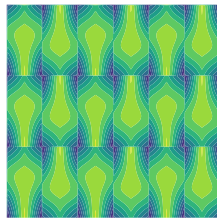
The objects of interest. A function f is invariant under \mathbb{G} if it satisfies

$$f(\phi x) = f(x) \quad \text{for all } \phi \in \mathbb{G} \text{ and all } x \in \mathbb{R}^n .$$

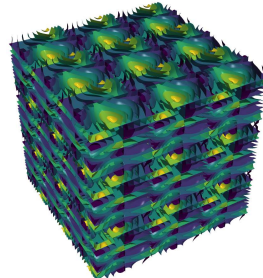
A simple way to construct such a function is to start with a tiling as above, define a function on Π , and then replicate it on every copy of Π . Here are two examples on \mathbb{R}^2 , corresponding to (ii) and (iii) above, and an example on \mathbb{R}^3 :



p2

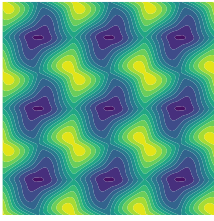


p2mm

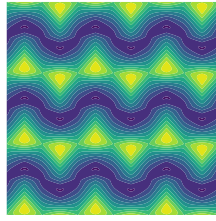


I4₁22

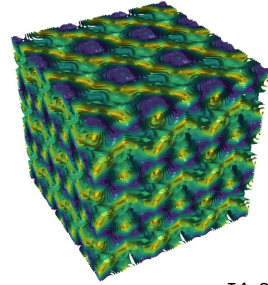
However, as the examples illustrate, functions obtained this way are typically not continuous. Our goal is to construct smooth invariant functions, such as these:



p2



p2mm



I₄22

We identify two representations of such functions, one linear and one nonlinear. Working with either representation algorithmically requires a data structure representing the invariance constraint. We construct such a structure, which we call an orbit graph, in Section 4. This graph is constructed from a description of the group (which can be encoded as a finite set of matrices) and of Π (a finite set of vectors).

Linear representations: Invariant Fourier transforms. We are primarily interested in two and three dimensions, but a one-dimensional example is a good place to start: In one dimension, a convex polytope is always an interval, say $\Pi = [0, 1]$. If we choose \mathbb{G} as the group \mathbb{Z} of all shifts of integer length, it tiles the line \mathbb{R} with Π . In this case, an invariant function is simply a periodic function with period 1. Smooth periodic functions can be represented as a Fourier series,

$$f(x) = \sum_{i=0}^{\infty} a_i \cos\left(\frac{ix}{2\pi}\right) + b_i \sin\left(\frac{ix}{2\pi}\right)$$

for sequences of scalar coefficients a_i and b_i . Note each sine and cosine on the right is \mathbb{G} -invariant and infinitely often differentiable. Now suppose we abstract from the specific form of these sines and cosines, and only regard them as \mathbb{G} -invariant functions that are very smooth. The series representation above then has the general form

$$f(x) = \sum_{i=0}^{\infty} c_i e_i(x),$$

where the e_i are smooth, \mathbb{G} -invariant functions that depend only on \mathbb{G} and Π , and the c_i are scalar coefficients that depend on f . (In the Fourier series, e_i is a cosine for odd and a sine for even indices.) In Section 5, we obtain generalizations of this representation to crystallographically invariant functions. To do so, we observe that the Fourier basis can be derived as the set of eigenfunctions of the Laplace operator: The sine and cosine functions above are precisely those functions $e : \mathbb{R} \rightarrow \mathbb{R}$ that solve

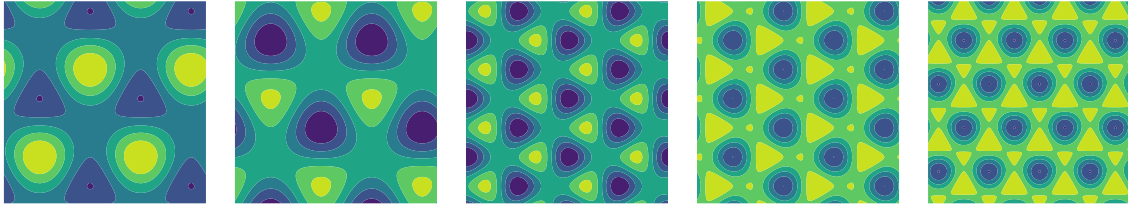
$$\begin{aligned} -\Delta e &= \lambda e \\ \text{subject to } & e \text{ is periodic with period 1} \end{aligned}$$

for some $\lambda \geq 0$. (The negative sign is chosen to make the eigenvalues λ non-negative.) The periodicity constraint is equivalent to saying that e is invariant under the shift group $\mathbb{G} = \mathbb{Z}$. The corresponding problem for a general crystallographic group \mathbb{G} on \mathbb{R}^n is hence

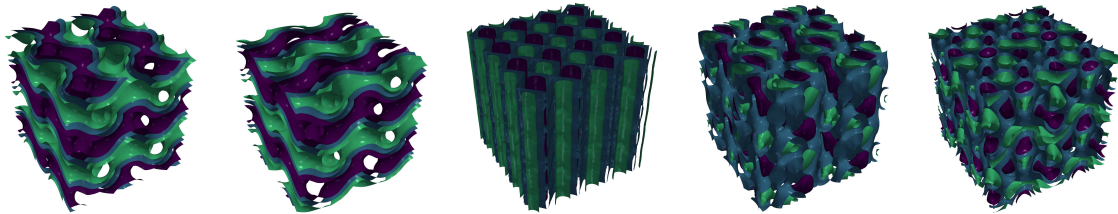
$$(1) \quad \begin{aligned} -\Delta e &= \lambda e \\ \text{subject to } & e = e \circ \phi \text{ for all } \phi \in \mathbb{G}. \end{aligned}$$

Theorem 7 shows that this problem has solutions for any dimension n , convex polytope $\Pi \subset \mathbb{R}^n$, and crystallographic group \mathbb{G} that tiles \mathbb{R}^n with Π . As in the Fourier case, the solution functions e_1, e_2, \dots are very smooth.

If we choose $\Pi \subset \mathbb{R}^2$ as the square $[0, 1]^2$ and \mathbb{G} as the group \mathbb{Z}^2 of discrete horizontal and vertical shifts—that is, the two-dimensional analogue of the example above—we recover the two-dimensional Fourier transform. The function e_0 is constant; the functions e_1, \dots, e_5 are shown in Figure 4. If the group also contains other transformations, the basis looks less familiar. These are the basis functions e_1, \dots, e_5 for a group (p3) containing shifts and rotations of order three:

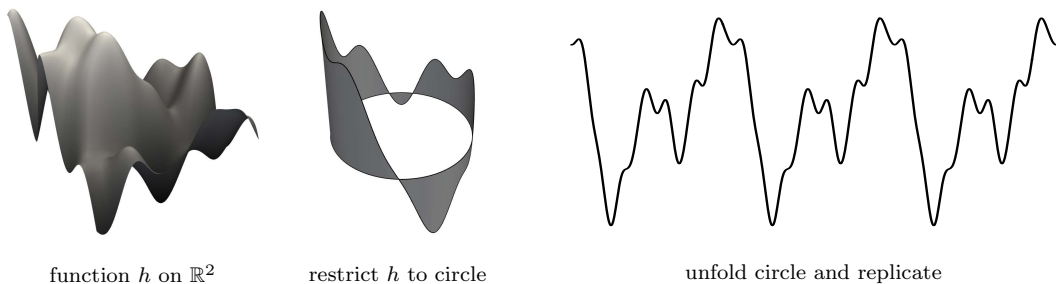


The same idea applies in any finite dimension n . For $n = 3$, the e_i can be visualized as contour plots. For instance, the first five non-constant basis elements for a specific three-dimensional group, designated $I4_1$ by crystallographers, look like this:



Our results show that any continuous invariant function can be represented by a series expansion in functions e_i . As for the Fourier transform, the functions form an orthonormal basis of the relevant \mathbf{L}_2 space. The functions e_i can hence be seen as a generalization of the Fourier transform from pure shift groups to crystallographic groups. All of this is made precise in Section 5.

Nonlinear representations: Factoring through an orbifold. The second representation, in Section 6, generalizes an idea of David MacKay [45], who constructs periodic functions on the line as follows: Start with a continuous function $h : \mathbb{R}^2 \rightarrow \mathbb{R}$. Choose a circle of circumference 1 in \mathbb{R}^2 , and restrict h to the circle. The restriction is still continuous. Now “cut and unfold the circle with h on it” to obtain a function on the unit interval. Since this function takes the same value at both interval boundaries, replicating it by shifts of integer length defines a function on \mathbb{R} that is periodic and continuous:



More formally, MacKay’s approach constructs a function $\rho : \mathbb{R} \rightarrow \text{circle} \subset \mathbb{R}^2$ such that f is continuous and periodic on $\mathbb{R} \iff f = h \circ \rho$ for some continuous $h : \mathbb{R}^2 \rightarrow \mathbb{R}$.

We show how to generalize this construction to any finite dimension n , any crystallographic group \mathbb{G} on \mathbb{R}^n , and any convex polytope with which \mathbb{G} tiles the space: For

each \mathbb{G} and Π , there is a continuous, surjective map

$$(2) \quad \rho : \mathbb{R}^n \rightarrow \Omega \quad \text{for some finite } N \geq n \text{ and a compact set } \Omega \subset \mathbb{R}^N$$

such that

$$f \text{ is continuous and invariant} \quad \Leftrightarrow \quad f = h \circ \rho \quad \text{for some continuous } h : \mathbb{R}^N \rightarrow \mathbb{R} .$$

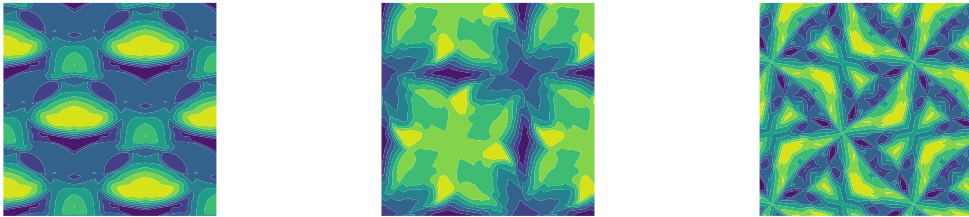
This is Theorem 15. Section 6.1 shows how to compute a representation of ρ using multidimensional scaling.

The set Ω can be thought of as an n -dimensional surface in a higher-dimensional space \mathbb{R}^N . If \mathbb{G} contains only shifts, this surface is completely smooth, and hence a manifold. That is the case in MacKay’s construction, where Ω is the circle, and the group $p1$ on \mathbb{R}^2 , for which Ω is the torus shown on the left:



For most crystallographic groups, Ω is not a manifold, but rather a more general object called an orbifold. The precise definition (see Appendix C) is somewhat technical, but loosely speaking, an orbifold is a surface that resembles a manifold almost everywhere, except at a small number of points at which it is not smooth. That is illustrated by the orbifold on the right, which represents a group containing rotations, and has several “sharp corners”.

Applications I: Neural networks. We can now define \mathbb{G} -invariant models by factoring through ρ . To define an invariant neural network, for example, start with a continuous neural network $h_\theta : \mathbb{R}^N \rightarrow Y$ with weight vector θ and some output space Y . Then $\rho \circ h_\theta$ is a continuous and invariant neural network $\mathbb{R}^n \rightarrow Y$. Here are examples for three groups (cm , $p4$, and $p4gm$) on \mathbb{R}^2 , with three hidden layers and randomly generated weights:



Applications II: Invariant kernels. We can similarly define \mathbb{G} -invariant reproducing kernels on \mathbb{R}^n , by starting with a kernel $\hat{\kappa}$ on \mathbb{R}^N and defining a function on \mathbb{R}^n as

$$\kappa(x, y) = \hat{\kappa} \circ (\rho \otimes \rho)(x, y) = \hat{\kappa}(\rho(x), \rho(y)) .$$

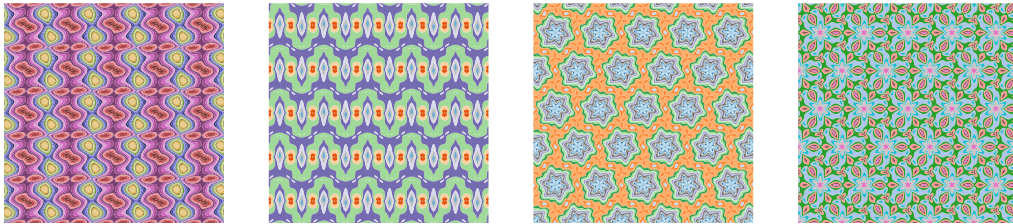
This function is again a kernel. In Section 7, we show that its reproducing kernel Hilbert space consists of continuous \mathbb{G} -invariant functions on \mathbb{R}^n . We also show that, even though \mathbb{R}^n is not compact, κ behaves essentially like a kernel on a compact domain (Proposition 23). In particular, it satisfies a Mercer representation and a compact embedding property, both of which usually require compactness. This behavior is specific to kernels invariant under crystallographic groups, and does not extend to more general

groups of isometries on \mathbb{R}^n .

Applications III: Invariant Gaussian processes. There are two ways in which a Gaussian process (GP) can be invariant under a group: A GP is a distribution on functions, and we can either ask for each function it generates to be invariant, or only require that its distribution is invariant (see Section 8 for definitions). The former implies the latter. Both types of processes can be constructed by factoring through an orbifold: Suppose we start with a kernel $\hat{\kappa}$ (a covariance function) and a real-valued function $\hat{\mu}$ (the mean function), both defined on \mathbb{R}^N . If we then generate a random function F on \mathbb{R}^n as

$$F := H \circ \rho \quad \text{where} \quad H \sim \text{GP}(\hat{\mu}, \hat{\kappa}),$$

the function F is \mathbb{G} -invariant with probability 1. The following are examples of such random functions, rendered as contour plots with non-smooth colormaps.



If we instead generate F as

$$F \sim \text{GP}(\mu, \kappa) \quad \text{where} \quad \mu := \hat{\mu} \circ \rho \quad \text{and} \quad \kappa := \hat{\kappa} \circ (\rho \otimes \rho),$$

the distribution of F is \mathbb{G} -invariant. See Section 8.

Properties of the Laplace operator. Section 9 studies differentials and Laplacians of crystallographically invariant functions $f : \mathbb{R}^n \rightarrow \mathbb{R}$. The results are then used in the proof of the Fourier representation. Consider a vector field F , i.e., a function $F : \mathbb{R}^n \rightarrow \mathbb{R}^n$. An example of such a vector field is the gradient $F = \nabla f$. Lemma 27 shows that the gradient transforms under elements ϕ of \mathbb{G} as

$$\nabla f(\phi x) = (\text{linear part of } \phi) \cdot \nabla f \quad \text{or abstractly} \quad F \circ \phi = (\text{linear part of } \phi) \circ F.$$

Proposition 28 shows that, for any vector field F that transforms in this way, the total flux through the boundary of the polytope Π vanishes,

$$\int_{\partial\Pi} F(x)^\top (\text{normal vector of } \partial\Pi \text{ at } x) dx = 0.$$

We can combine this fact with a result from the theory of partial differential equations, the so-called Green identity, which decomposes the Laplacian on functions on Π as

$$-\Delta f = \text{self-adjoint component on interior of } \Pi \quad - \quad \text{correction term on } \partial\Pi.$$

Fact 29 makes the statement precise. Using the fact that the flux vanishes, we can show that the correction term on $\partial\Pi$ vanishes, and from that deduce that the Laplace operator on invariant functions is self-adjoint (Theorem 30). That allows us to draw on results from the spectral theory of self-adjoint operators to solve (1).

Background and reference results. Since our methods draw on a number of different fields, the appendix provides additional background on groups of isometries (App. A), functional analysis (App. B), and orbifolds (App. C), and spectral theory (App. D).

2 Preliminaries: Crystallographic groups

Throughout, we consider a Euclidean space \mathbb{R}^n , and write d_n for Euclidean distance in n dimensions. Euclidean volume (that is, Lebesgue measure on \mathbb{R}^n) is denoted vol_n . As we work with both sets and their boundaries, we must carefully distinguish dimensions: The span of a set $A \subset \mathbb{R}^n$ is the smallest affine subspace that contains it. We define the **dimension** and **relative interior** of A as

$$\dim A := \dim \text{span } A \quad \text{and} \quad A^\circ := \text{largest subset of } A \text{ that is open in span } A .$$

The **boundary** of A is the set $\partial A := A \setminus A^\circ$. If A has dimension $k < n$, then $\text{vol}_k(A)$ denotes Euclidean volume in span A . For example: If $A \subset \mathbb{R}^3$ is a closed line segment, then $\dim A = 1$, and $\text{vol}_1(A)$ is the length of the line segment, whereas $\text{vol}_3(A) = \text{vol}_2(A) = 0$. Taking the relative interior A° removes the two endpoints, whereas interior of A in \mathbb{R}^3 is the empty set. (No such distinction is required for the closure \bar{A} , since A is closed in span A if and only if it is closed in \mathbb{R}^n .)

2.1. Defining crystallographic groups

Consider a group \mathbb{G} of isometries of \mathbb{R}^n . (See Appendix A for a brief review of definitions.) Every isometry ϕ of \mathbb{R}^n is of the form

$$(3) \quad \phi x = A_\phi x + b_\phi \quad \text{for some orthogonal } n \times n \text{ matrix } A_\phi \text{ and some } b_\phi \in \mathbb{R}^n .$$

Let $M \subset \mathbb{R}^n$ be a set. We say that \mathbb{G} **til**es the space \mathbb{R}^n with M if the image sets ϕM completely cover the space so that only their boundaries overlap:

$$\bigcup_{\phi \in \mathbb{G}} \phi M = \mathbb{R}^n \quad \text{and} \quad \phi M \cap \psi M \subset \partial(\phi M) \quad \text{whenever } \phi \neq \psi .$$

Each set ϕM is a **tile**, and the collection $\mathbb{G}M := \{\phi M \mid \phi \in \mathbb{G}\}$ is a **tiling** of \mathbb{R}^n .

By a **convex polytope**, we mean the convex hull of a finite set of points [70]. Let $\Pi \subset \mathbb{R}^n$ be an n -dimensional convex polytope. The boundary $\partial\Pi$ consists of a finite number of $(n-1)$ -dimensional convex polytopes, called the **facets** of Π . Thus, if \mathbb{G} tiles \mathbb{R}^n with Π , only points on facets are contained in more than one tile.

Definition 1. A **crystallographic group** is a group of isometries that tiles \mathbb{R}^n with an n -dimensional convex polytope Π .

The polytope Π is then also called a **fundamental region** (in geometry) or an **asymmetric unit** (in materials science) for \mathbb{G} . This definition of crystallographic groups differs from those given in the literature, but we clarify in Appendix A.2 that it is equivalent.

2.2. Basic properties

Some properties of \mathbb{G} can be read right off the definition: Since \mathbb{G} tiles the entire space with a set Π of finite diameter, we must have $|\mathbb{G}| = \infty$. Since Π is n -dimensional and convex, it contains an open metric ball of positive radius. Each tile contains a copy of this ball, and these copies do not overlap. It follows that

$$(4) \quad d(\phi(x), \psi(x)) > \varepsilon \quad \text{for all distinct } \phi, \psi \in \mathbb{G} \text{ and all } x \in \Pi^\circ .$$

A group of isometries that satisfies (4) for some $\varepsilon > 0$ is called **discrete**, in contrast to groups which contain, e.g., continuous rotations. Discreteness implies \mathbb{G} is countable, but not all countable groups of isometries are discrete (the group \mathbb{Q}^n of rational-valued shifts

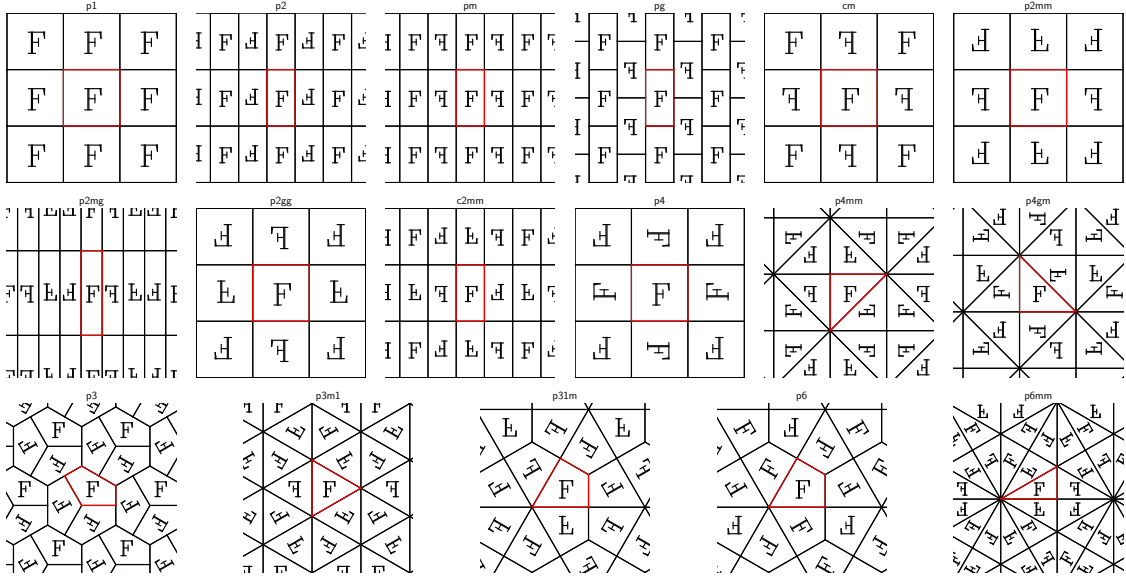


Figure 1: Tiling behavior of the 17 crystallographic groups on \mathbb{R}^n (the wallpaper groups).

is a non-example). In summary, every crystallographic group is an infinite, discrete (and hence countable) subgroup of the Euclidean group on \mathbb{R}^n .

Suppose we choose one of the tilings in Figure 1, and rotate or shift the entire plane with the tiling on it. Informally speaking, that changes the tiling, but not the tiling mechanism, and it is natural to consider the two tilings isomorphic. More formally, two crystallographic groups \mathbb{G} and \mathbb{G}' are **isomorphic** if there is an orientation-preserving, invertible, and affine (but not necessarily isometric) map $\gamma : \mathbb{R}^n \rightarrow \mathbb{R}^n$ such that $\mathbb{G}' = \gamma\mathbb{G}$, where $\gamma\mathbb{G} := \{\gamma\phi\gamma^{-1} \mid \phi \in \mathbb{G}\}$.

Fact 2 ([62, 4.2.2]). *Up to isomorphism, there are only finitely many crystallographic groups on \mathbb{R}^n for each $n \in \mathbb{N}$. Specifically, there 17 such groups for $n = 2$, and 230 for $n = 3$.*

3 Preliminaries: Invariant functions

A function $f : \mathbb{R}^n \rightarrow \mathbf{X}$, with values in some set \mathbf{X} , is **ϕ -invariant** if it satisfies

$$f(\phi x) = f(x) \quad \text{for all } x \in \mathbb{R}^n \quad \text{or in short} \quad f \circ \phi = f.$$

It is **\mathbb{G} -invariant** if it is ϕ -invariant for all $\phi \in \mathbb{G}$. We are specifically interested in \mathbb{G} -invariant functions that are continuous, and write

$$\mathbf{C}(M) := \{f : \mathbb{R}^n \rightarrow \mathbb{R} \mid f \text{ continuous}\} \quad \text{and} \quad \mathbf{C}_{\mathbb{G}} := \{f \in \mathbf{C}(\mathbb{R}^n) \mid f \text{ is } \mathbb{G}\text{-invariant}\}.$$

More generally, a function $f : (\mathbb{R}^n)^k \rightarrow \mathbf{X}$ is **\mathbb{G} -invariant in each argument** if

$$(5) \quad f(\phi_1 x_1, \dots, \phi_k x_k) = f(x_1, \dots, x_k) \quad \text{for all } \phi_1, \dots, \phi_k \in \mathbb{G} \text{ and } x_1, \dots, x_k \in \mathbb{R}^n.$$

3.1. Tiling with functions

To construct a \mathbb{G} -invariant function, we may start with a function h on Π and “replicate it by tiling”. For that to be possible, h must in turn be the restriction of a \mathbb{G} -invariant

function to Π . It must then satisfy $h(\phi x) = h(x)$ if both ϕx and x are in Π . We hence define the relation

$$x \sim y \quad :\iff \quad x, y \in \Pi \text{ and } y = \phi(x) \text{ for some } \phi \in \mathbb{G} \setminus \{\mathbf{1}\}.$$

We note immediately that $x \sim y$ implies each point is also contained in an adjacent tile, so both must be on the boundary $\partial\Pi$ of Π . The requirement

$$(6) \quad h(x) = h(y) \quad \text{whenever } x \sim y$$

is therefore a **periodic boundary condition**. If it holds, the function

$$(7) \quad f(x) := h(\phi^{-1}x) \quad \text{for } x \in \phi(\Pi) \text{ and each } \phi \in \mathbb{G}$$

is well-defined on \mathbb{R}^n , and is \mathbb{G} -invariant. Conversely, every \mathbb{G} -invariant function f can be obtained this way (by choosing h as the restriction $f|_{\Pi}$). Informally, (7) says that we stitch together function segments on tiles that are all copies of h , and these segments overlap on the tile boundaries. The boundary condition ensures that wherever such overlaps occur, the segments have the same value, so that (7) produces no ambiguities. The special case of (6) for pure shift groups—where A_ϕ is the identity matrix for all $\phi \in \mathbb{G}$ —is known as a **Born-von Karman boundary condition** (e.g., Ashcroft and Mermin [7]).

3.2. Orbits and quotients

An alternative way to express invariance is as follows: A function is \mathbb{G} -invariant if and only if it is constant on each set of the form

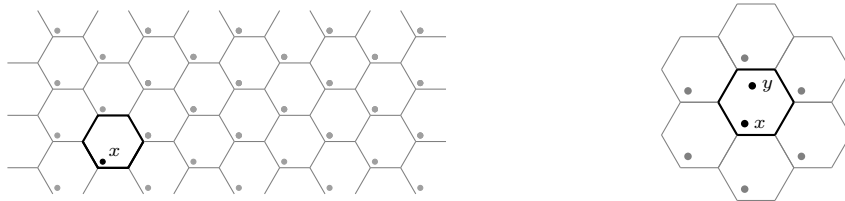
$$\mathbb{G}(x) := \{\phi x \mid \phi \in \mathbb{G}\} \quad \text{for each } x \in \mathbb{R}^n.$$

The set $\mathbb{G}(x)$ is called the **orbit** of x . We see immediately that each orbit of a crystallographic group is countably infinite, but locally finite: The definition of discreteness in (4) implies that every bounded subset of \mathbb{R}^n contains only finitely many points of each orbit. We also see that each point $x \in \mathbb{R}^n$ is in one and only one orbit, which means the orbits form a partition of \mathbb{R}^n . The assignment $x \mapsto \mathbb{G}(x)$ is hence a well-defined map

$$q(x) := \mathbb{G}(x) \quad \text{with image} \quad \mathbb{R}^n/\mathbb{G} := q(\mathbb{R}^n) = \{\mathbb{G}(x) \mid x \in \mathbb{R}^n\}.$$

The orbit set \mathbb{R}^n/\mathbb{G} is also called the **quotient set** or just the **quotient** of \mathbb{G} , and q is called the **quotient map** (e.g., Bonahon [15]). Since the orbits are mutually disjoint, we can informally think of q as collapsing each orbit into a single point, and \mathbb{R}^n/\mathbb{G} is the set of such points.

Figure 2: *Left:* A point x and points on its orbit $\mathbb{G}(x)$ in a shift tiling of \mathbb{R}^2 . *Right:* The infimum in the definition of $d_{\mathbb{G}}(\mathbb{G}(x), \mathbb{G}(y))$ may be attained by the Euclidean distance $d_n(x, y)$ between a point y in Π and a point ϕx in a different tile $\phi\Pi$.



Quotient spaces are abstract but useful tools for expressing invariance properties: For any function $f : \mathbb{R}^n \rightarrow \mathbb{R}$, we have

$$(8) \quad f \text{ is } \mathbb{G}\text{-invariant} \iff f = \hat{f} \circ q \quad \text{for some function } \hat{f} : \mathbb{R}^n/\mathbb{G} \rightarrow \mathbb{R},$$

since each point of \mathbb{R}^n/\mathbb{G} represents an orbit and f is invariant iff it is constant on orbits. We can also use the quotient to express continuity, by equipping it with a topology that satisfies

$$(9) \quad f \in \mathbf{C}_{\mathbb{G}} \iff f = \hat{h} \circ q \quad \text{for some continuous } \hat{h} : \mathbb{R}^n/\mathbb{G} \rightarrow \mathbb{R}.$$

There is exactly one such topology, called the **quotient topology** in the literature. Its definition can be made more concrete by metrizing it:

Fact 3 (see Bonahon [15], Theorem 7.7). *If \mathbb{G} is crystallographic, the function*

$$d_{\mathbb{G}}(\omega_1, \omega_2) := \inf \{d(x, y) \mid x \in \omega_1, y \in \omega_2\} \quad \text{for } \omega_1, \omega_2 \in \mathbb{R}^n/\mathbb{G}$$

is a valid metric on \mathbb{R}^n/\mathbb{G} , and it metrizes the quotient topology. A subset $U \subset \mathbb{R}^n/\mathbb{G}$ is open if and only if its preimage $q^{-1}U$ is open in \mathbb{R}^n .

Since \mathbb{G} is discrete, the infimum in $d_{\mathbb{G}}$ is a minimum. The distance of two orbits (considered as points in \mathbb{R}^n/\mathbb{G}) is hence the shortest Euclidean distance between points in these orbits (considered as sets in \mathbb{R}^n), see Figure 2 (right). If x and y are points in the polytope Π , we have

$$x \sim y \iff d_{\mathbb{G}}(\mathbb{G}(x), \mathbb{G}(y)) = 0.$$

Informally speaking, $d_{\mathbb{G}}$ implements the periodic boundary condition (6). The metric space $(\mathbb{R}^n/\mathbb{G}, d_{\mathbb{G}})$ is also called the **quotient space** or **orbit space** of \mathbb{G} . A very important property of crystallographic groups is that they have compact quotient spaces:

Fact 4 ([65, Proposition 1.6]). *If a discrete group \mathbb{G} of isometries tiles \mathbb{R}^n with a set M , the quotient space $(\mathbb{R}^n/\mathbb{G}, d_{\mathbb{G}})$ is homeomorphic to the quotient space M/\mathbb{G} . If \mathbb{G} is crystallographic and tiles with a convex polytope, then $(\mathbb{R}^n/\mathbb{G}, d_{\mathbb{G}})$ is compact.*

3.3. Transversals and projections

Since orbit spaces are abstract objects, we can only work with them implicitly. One way to do so is by representing each orbit by one of its points in \mathbb{R}^n . A subset of \mathbb{R}^n that contains exactly one point of each orbit is called a **transversal**. In general, transversals can be exceedingly complex sets [9], but crystallographic groups always have simple transversals. Algorithm 2 in the next section constructs a transversal explicitly. In the following, we will always write $\tilde{\Pi}$ to mean

$$\tilde{\Pi} := \text{a transversal contained in } \Pi \text{ computed by Algorithm 2.}$$

Given such a transversal, we can define the **projector** $p : \mathbb{R}^n \rightarrow \Pi$ as

$$(10) \quad p(x) := \text{the unique element of } \mathbb{G}(x) \cap \tilde{\Pi}.$$

If we think of each point in $\tilde{\Pi}$ as a concrete representative of an element of \mathbb{R}^n/\mathbb{G} , then p is similarly a concrete representation of the quotient map q , and we can translate the

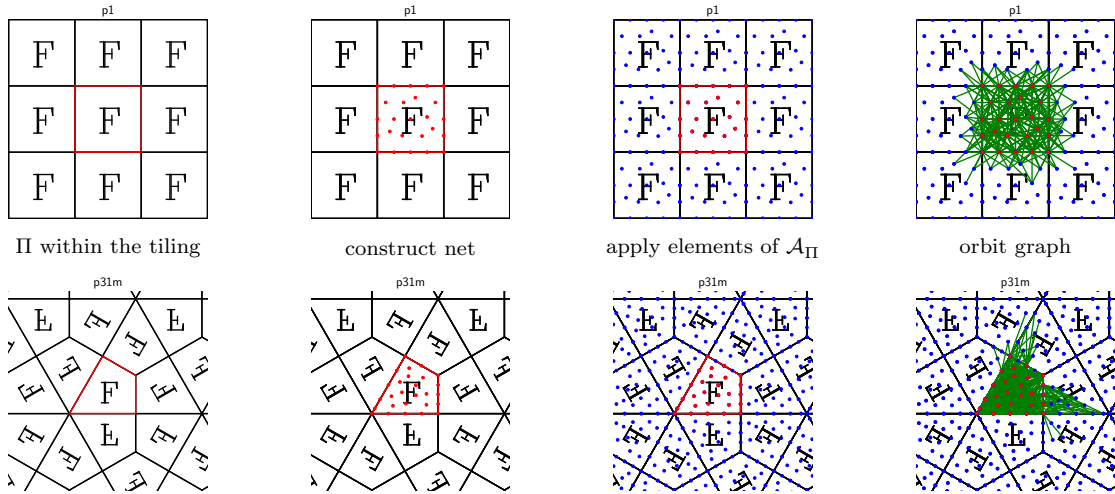


Figure 3: Orbit graph construction for two plane groups: $p1$ and $p31m$. Starting with the fundamental region (left), place points to construct an ϵ -net (middle left), apply local group operations to these points (middle right), then add edges which may include vertices outside the fundamental region (right).

identities above accordingly: The projector is by definition \mathbb{G} -invariant, since we can write f in (7) as $f = h \circ p$. That shows

$$(11) \quad f : \mathbb{R}^n \rightarrow \mathbb{R} \text{ is } \mathbb{G}\text{-invariant} \iff f = h \circ p \text{ for some } h : \Pi \rightarrow \mathbb{R} \text{ satisfying (6)} .$$

Although p is not continuous as a function $\mathbb{R}^n \rightarrow \Pi$, continuity only fails at the boundary, and p behaves like a continuous function when composed with h :

Lemma 5. *Let $h : \Pi \rightarrow \mathbf{X}$ be a continuous function with values in a topological space \mathbf{X} . If h satisfies (6), then $h \circ p$ is a continuous \mathbb{G} -invariant function $\mathbb{R}^n \rightarrow \mathbf{X}$. It follows that*

$$(12) \quad f \in \mathbf{C}_{\mathbb{G}} \iff f = h \circ p \quad \text{for some continuous } h : \Pi \rightarrow \mathbb{R} \text{ satisfying (6)} .$$

Since p exists for any choice of \mathbb{G} and Π , and since it can be evaluated algorithmically, we have hence reduced the problem of constructing continuous invariant functions to the problem of finding functions that satisfy the periodic boundary condition (6).

4 Taking quotients algorithmically: Orbit graphs

To work with invariant functions computationally, we must approximate the quotient metric. We do so using a data structure that we call an orbit graph, in which two points are connected if their orbits are close to each other. More formally, any undirected graph is a metric space when equipped with path length as distance. The metric space defined by the graph \mathcal{G} below discretizes the metric space $(\mathbb{R}^n/\mathbb{G}, d_{\mathbb{G}})$. To define \mathcal{G} , fix constants $\epsilon, \delta > 0$. A finite set Γ is an ϵ -net in Π if each point lies within distance ϵ of Γ ,

$$\Gamma \text{ is an } \epsilon\text{-net} \quad :\Leftrightarrow \quad \text{for each } x \in \Pi \text{ there exists } z \in \Gamma \text{ such that } d_n(x, z) < \epsilon ,$$

see e.g., Cooper et al. [23]. If Γ is an ϵ -net in Π , we call the graph

$$\mathcal{G} = \mathcal{G}(\epsilon, \delta) = (\Gamma, E) \quad \text{where} \quad E := \{(x, y) \mid d_{\mathbb{G}}(\mathbb{G}(x), \mathbb{G}(y)) < \delta\}$$

an **orbit graph** for \mathbb{G} and Π .

4.1. Computing orbit graphs

Algorithmically, an orbit graph can be constructed as follows: Constructing an ε -net is a standard problem in computational geometry and can be solved efficiently (e.g., Haussler and Welzl [33]). Having done so, the problem we have to solve is:

$$\text{Given points } x, y \in \Pi, \text{ determine } d_{\mathbb{G}}(\mathbb{G}(x), \mathbb{G}(y)).$$

Since Π is a polytope, its diameter

$$\text{diam}(\Pi) := \max \{d_n(x, y) \mid x, y \in \Pi\} < \infty$$

can also be evaluated computationally. By definition of $d_{\mathbb{G}}$, we have

$$d_{\mathbb{G}}(\mathbb{G}(x), \mathbb{G}(y)) = \min_{\phi \in \mathbb{G}} d_n(x, \phi y) \leq d_n(x, y) \leq \text{diam}(\Pi).$$

That shows the minimum is always attained for a point ϕy on a tile $\phi\Pi$ that lies within distance $\text{diam}(\Pi)$ of x . The set of transformations that specify these tiles is

$$\mathcal{A}_{\Pi} = \{\phi \in \mathbb{G} \mid d_n(x, \phi z) \leq \text{diam}(\Pi) \text{ for some } z \in \Pi\}.$$

This set is always finite, since \mathbb{G} is discrete and the ball of radius $\text{diam}(\Pi)$ is compact. We can hence evaluate the quotient metric as

$$d_{\mathbb{G}}(\mathbb{G}(x), \mathbb{G}(y)) = \min \{d_n(x, \phi y) \mid \phi \in \mathcal{A}_{\Pi}\},$$

which reduces the construction of E to a finite search problem. In summary:

Algorithm 1 (Constructing the orbit graph).

- 1.) Construct the ε -net Γ .
- 2.) Find local group elements \mathcal{A}_{Π} .
- 3.) For each pair $x, y \in \Gamma$, find $d_{\mathbb{G}}(\mathbb{G}(x), \mathbb{G}(y)) = \min \{d_n(x, \phi y) \mid \phi \in \mathcal{A}_{\Pi}\}$.
- 4.) Add an edge between x and y if $d_{\mathbb{G}}(\mathbb{G}(x), \mathbb{G}(y)) < \delta$.

The construction is illustrated in Figure 3.

4.2. Computing a transversal

Recall that the **faces** of a polytope are its vertices, edges, and so forth; the facets are the $(n - 1)$ -dimensional faces. The polytope itself is also a face, of dimension n . See [70] for a precise definition. Given Π and \mathbb{G} , we will call two faces S and S' \mathbb{G} -equivalent if $S' = \phi S$ for some $\phi \in \mathbb{G}$. Thus, if $S = \Pi$, its equivalence class is $\{\Pi\}$. If S is a facet, it is equivalent to at most one distinct facet, so its equivalence class has one or two elements. The equivalence classes of lower-dimensional faces may be larger—if \mathbb{G} is $\mathfrak{p}1$ and Π a square, for example, all four vertices of Π are \mathbb{G} -equivalent.

Algorithm 2 (Constructing a transversal).

- 1) Start with an exact tiling. Enumerate all faces of Π .
- 2) Sort faces into \mathbb{G} -equivalence classes.
- 3) Select one face from each class and take its relative interior.
- 4) Output the union $\tilde{\Pi}$ of these relative interiors.

Lemma 6. *The set $\tilde{\Pi}$ constructed by Algorithm 2 is a transversal.*

Proof. The relative interiors of the faces of a convex polytope are mutually disjoint and their union is Π , so each point $x \in \Pi$ is on exactly one such relative interior. Let S be the face with $x \in S^\circ$, and consider any $\phi \in \mathbb{G}$. Since the tiling is exact, ϕS is either a face of Π or $\phi S \cap \Pi = \emptyset$. If $\phi x \in \Pi$, the intersection cannot be empty, so ϕS is a face and hence \mathbb{G} -equivalent to S . It follows that the interior of a face of Π intersect the orbit $\mathbb{G}x$ if and only if it is in the equivalence class of S . Since we select exactly one element of this class, exactly one point of $\mathbb{G}x$ is contained in $\tilde{\Pi}$. \square

4.3. Computing the projector

Since \mathbb{G} is crystallographic, it contains shifts in n linearly independent directions, and these shifts hence specify a coordinate system of \mathbb{R}^n . More precisely: There are n elements ϕ_1, \dots, ϕ_n of \mathbb{G} that (1) are pure shifts (satisfy $A_{\phi_i} = \mathbb{I}$), (2) are linearly independent, and (3) are the shortest such elements (in terms of the Euclidean norm of b_{ϕ_i}). Up to a sign, each of these elements is uniquely determined. We refer to the vectors ϕ_1, \dots, ϕ_n as the **shift coordinate** system of \mathbb{G} .

Algorithm 3 (Computing the projector).

- 1.) Perform a basis change from the shift coordinates to the standard basis of \mathbb{R}^n .
- 2.) Set $\tilde{x} = (x_1 \bmod 1, \dots, x_n \bmod 1)$.
- 3.) Find $\phi \in \mathbb{G}$ such that $\phi \tilde{x} \in \tilde{\Pi}$.
- 4.) Apply the reverse change of basis from standard to shift coordinates.

5 Linear representation: Invariant Fourier transforms

In this section, we obtain a basis representation for invariant functions: given a crystallographic group \mathbb{G} , we construct a sequence of \mathbb{G} -invariant functions e_1, e_2, \dots on \mathbb{R}^n such that any \mathbb{G} -invariant continuous function can be represented as a (possibly infinite) linear combination $\sum_{i \in \mathbb{N}} c_i e_i$. If \mathbb{G} is generated by n orthogonal shifts, the functions e_i are an n -dimensional Fourier basis. Theorem 7 below obtains an analogous basis for each crystallographic group \mathbb{G} .

5.1. Representation theorem

For any open set $M \subseteq \mathbb{R}^n$, we define the Laplace operator on twice differentiable functions $h : M \rightarrow \mathbb{R}$ as

$$\Delta h := \frac{\partial^2 h}{\partial x_1^2} + \dots + \frac{\partial^2 h}{\partial x_n^2} = \nabla^\top (\nabla h).$$

Now consider specifically functions $e : \mathbb{R}^n \rightarrow \mathbb{R}$. Fix some $\lambda \in \mathbb{R}$, and consider the constrained partial differential equation

$$(13) \quad \begin{aligned} -\Delta e &= \lambda e && \text{on } \mathbb{R}^n \\ \text{subject to } e &= e \circ \phi && \text{for } \phi \in \mathbb{G}. \end{aligned}$$

Clearly, there is always a trivial solution, namely the constant function $e = 0$. If (13) has a non-trivial solution e , we call this e a **\mathbb{G} -eigenfunction** and λ a **\mathbb{G} -eigenvalue** of the linear operator $-\Delta$. Denote the set of solutions by

$$\mathcal{V}(\lambda) := \{e : \mathbb{R}^n \rightarrow \mathbb{R} \mid e \text{ satisfies (13)}\}.$$

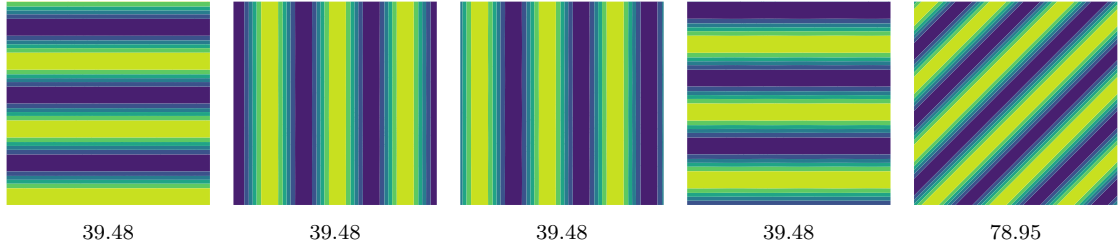


Figure 4: The first five non-constant basis functions e_2, \dots, e_6 in Theorem 7, with their eigenvalues λ_i , for the group $p1$. The eigenbasis in this case is precisely the standard Fourier basis on \mathbb{R}^2 .

Since 0 is a solution, and any linear combination of solutions is again a solution, $\mathcal{V}(\lambda)$ is a vector space, called the **eigenspace** of λ . Its dimension

$$k(\lambda) := \dim \mathcal{V}(\lambda)$$

is the **multiplicity** of λ .

Theorem 7 (Crystallographically invariant Fourier basis). *Let \mathbb{G} be a crystallographic group that tiles \mathbb{R}^n with a convex polytope Π . Then the constrained problem (13) has solutions for countably many distinct values $\lambda_1, \lambda_2, \dots$ of λ , and these values satisfy*

$$0 = \lambda_1 < \lambda_2 < \lambda_3 < \dots \quad \text{and} \quad \lambda_i \xrightarrow{i \rightarrow \infty} \infty.$$

Every solution function e is infinitely often differentiable. There is a sequence e_1, e_2, \dots of solutions whose restrictions $e_1|_{\Pi}, e_2|_{\Pi}, \dots$ to Π form an orthonormal basis of the space $\mathbf{L}_2(\Pi)$, and satisfy

$$|\{j \in \mathbb{N} \mid e_j \in \mathcal{V}(\lambda_i)\}| = k(\lambda_i) \quad \text{for each } i \in \mathbb{N}.$$

A function $f : \mathbb{R}^n \rightarrow \mathbb{R}$ is \mathbb{G} -invariant and continuous if and only if

$$f = \sum_{i \in \mathbb{N}} c_i e_i \quad \text{for some sequence } c_1, c_2, \dots \in \mathbb{R},$$

where the series converges in the supremum norm.

Proof. See Appendix G. □

Remark 8. The space $\mathbf{L}_2(\mathbb{R}^n)$ contains no non-trivial \mathbb{G} -invariant functions, since for every $f \in \mathbf{C}_{\mathbb{G}}$

$$\|f\|_{\mathbf{L}_2(\mathbb{R}^n)} = \sum_{\phi \in \mathbb{G}} \|f|_{\phi\Pi}\|_{\mathbf{L}_2(\phi\Pi)} = \begin{cases} 0 & f = 0 \text{ almost everywhere} \\ \infty & \text{otherwise} \end{cases}.$$

On the other hand, the restriction $f|_{\Pi}$ is in $\mathbf{L}_2(\Pi)$, and completely determines f . That makes $\mathbf{L}_2(\Pi)$ the natural \mathbf{L}_2 -space in the context of crystallographic invariance, and is the reason why the restrictions $e_i|_{\Pi}$ are used in the theorem. Since $\mathbf{L}_2(\phi\Pi)$ is isometric to $\mathbf{L}_2(\Pi)$ for all $\phi \in \mathbb{G}$, it does not matter which tile we restrict to.

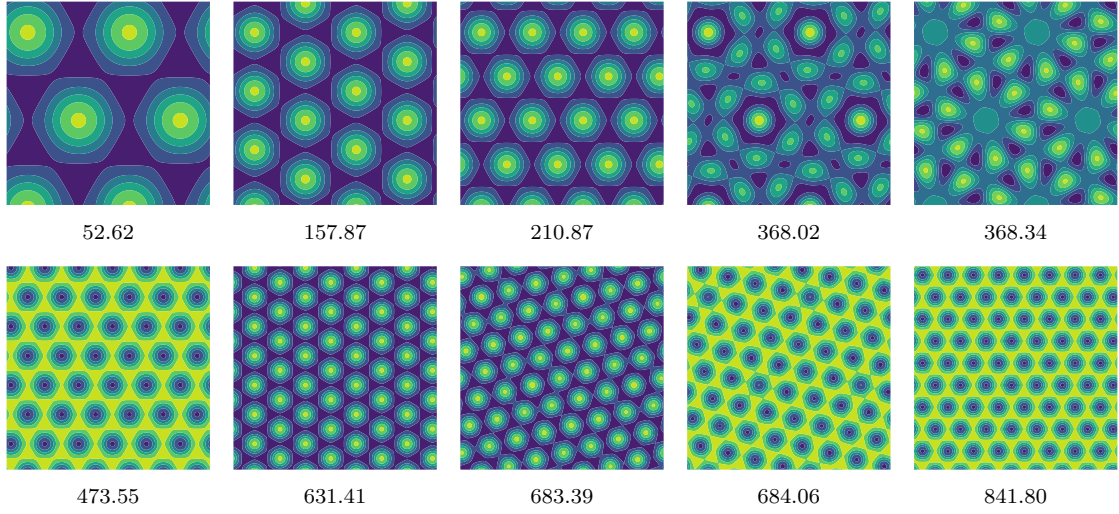


Figure 5: The first ten non-constant basis functions e_2, \dots, e_{11} in Theorem 7, with their approximate eigenvalues λ_i , for the group $\mathfrak{p6}$. In this case, the multiplicities $k(\lambda_i)$ are not $2n = 4$ as for the standard Fourier transform.

5.2. Relationship to Fourier series

The standard Fourier bases for periodic functions on \mathbb{R}^n can be obtained as the special cases of Theorem 7 for shift groups: Fix some edge width $c > 0$, and choose Π and \mathbb{G} as

$$\Pi = [0, c]^n \quad \text{and} \quad \mathbb{G} = \{x \mapsto x + c(i_1, \dots, i_n)^\top \mid i_1, \dots, i_n \in \mathbb{Z}\}.$$

For these groups, all eigenvalue multiplicities are $k(\lambda_i) = 2n$ for each $i \in \mathbb{N}$. For $n = 2$, the group \mathbb{G} is $\mathfrak{p1}$ (see Figure 1). Its eigenfunctions are shown in Figure 4.

To clarify the relationship in more detail, consider the case $n = 1$: Since Δ is a second derivative, the functions $e(x) = \cos(\nu x)$ and $e(x) = \sin(\nu x)$ satisfy

$$\Delta e(x) = -\nu^2 e(x) \quad \text{for each } \nu \geq 0,$$

and are hence eigenfunctions of $-\Delta$ with eigenvalue $\lambda = \nu^2$. For this choice of Π and \mathbb{G} , the invariance constraint in (13) holds iff $e(x) = e(x + c)$ for every $x \in \mathbb{R}$. That is true iff

$$\nu(x + c) = \nu x + 2\pi(i - 1) \quad \text{for some } i \in \mathbb{N}, \text{ and hence } \lambda_i = \nu^2 = \left(\frac{2\pi(i-1)}{c}\right)^2.$$

The eigenspaces are therefore the two-dimensional vector spaces

$$\mathcal{V}(\lambda_i) = \text{span}\{\sin(\sqrt{\lambda_i} \cdot), \cos \sqrt{\lambda_i} \cdot\} \quad \text{with} \quad k(\lambda_i) = 2 \quad \text{for all } i \in \mathbb{N}.$$

Any continuous function f that is \mathbb{G} -invariant (or, equivalently, c -periodic) can be expanded as

$$(14) \quad f(x) = \sum_{i \in \mathbb{N}} a_i \cos(\sqrt{\lambda_i} x) + b_i \sin(\sqrt{\lambda_i} x).$$

In the notation of Theorem 7, the coefficients are $c_{2i} = a_i$ and $c_{2i+1} = b_i$, and

$$e_{2i}(x) = \cos(\sqrt{\lambda_{2i}} x) \quad \text{and} \quad e_{2i+1}(x) = \sin(\sqrt{\lambda_{2i+1}} x).$$

Note that the unconstrained equation has solutions for all λ in the uncountable set $[0, \infty)$. The invariance constraint limits possible values to the countable set $\lambda_1, \lambda_2, \dots$. If f was continuous but not invariant, the expansion (14) would hence require an integral on the right. Since f is invariant, a series suffices.

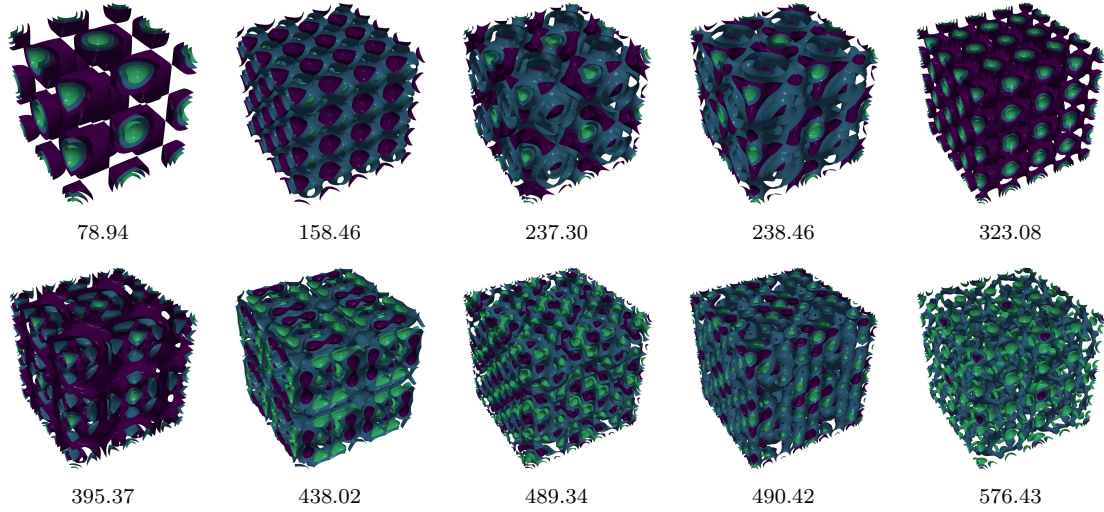


Figure 6: The first ten non-constant basis functions e_2, \dots, e_{11} in Theorem 7, with their approximate eigenvalues λ_i , for the group $I23$ on \mathbb{R}^3 .

Remark 9 (Multiplicities and real versus complex coefficients). Fourier series, in particular in one dimension, are often written using complex-valued functions as

$$f(x) = \sum_{i \in \mathbb{N}} \gamma_i \exp(J\lambda_i x) \quad \text{where } \gamma_i \in \mathbb{C} \text{ and } J := \sqrt{-1}.$$

Since Euler's formula $\exp(Jx) = \cos(x) + J \sin(x)$ shows

$$\gamma_i \exp(J\sqrt{\lambda_i}x) = a_i \cos(\sqrt{\lambda_i}x) + b_i \sin(\sqrt{\lambda_i}x) \quad \text{for } (a_i - Jb_i) = \gamma_i,$$

that is equivalent to (14). The complex plane \mathbb{C} is not inherent to the Fourier representation, but rather a convenient way to parameterize the two-dimensional eigenspace $\mathcal{V}(\lambda_i)$. For general crystallographic groups, the complex representation is less useful, since the multiplicities $k(\lambda_i)$ may not be even, as can be seen in Figure 5.

5.3. Spectral algorithms

The eigenfunctions in Theorem 7 can be approximated by eigenvectors of a suitable graph Laplacian of the orbit graph as follows. We first compute an orbit graph $\mathcal{G} = (\Gamma, E)$ as described in Section 4. We weight each edge (x, y) of the graph by

$$(15) \quad w(x, y) = \begin{cases} \exp\left(-\frac{d_{\mathbb{G}}^2(\mathbb{G}(x), \mathbb{G}(y))}{2\epsilon^2}\right) & \text{if } (x, y) \in E \\ 0 & \text{otherwise} \end{cases}.$$

The normalized Laplacian of the weighted graph is

$$(16) \quad L = \mathbb{I} - D^{-1}W \quad \text{where } W_{xy} = w(x, y),$$

and D is the diagonal matrix containing the sum of each row of W . See e.g., Chung [20] for more on the matrix L . Our estimates of the eigenvalues and -functions of Δ are the eigenvalues and eigenvectors of L ,

$$\hat{\lambda}_i := \textit{ith eigenvalue of } L \quad \text{and} \quad \hat{e}_i := \textit{ith eigenvector of } L.$$

These approximate the spectrum of Δ in the sense that

$$\lambda_i \approx \frac{2}{\epsilon} \hat{\lambda}_i \quad \text{and} \quad e_i(x) \approx \frac{2}{\epsilon} (\hat{e}_i)_x \quad \text{for } x \in \Gamma,$$

see Singer [56]. Once an eigenvector \hat{e}_i is computed, values of e_i at points $x \notin \Gamma$ can be estimated using standard interpolation methods.

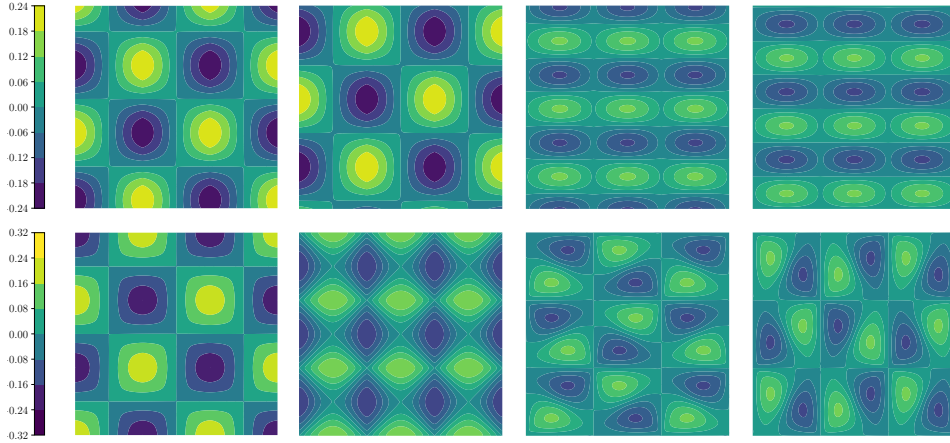


Figure 7: Visualizations of four-dimensional orbifold embeddings for wallpaper groups cm (top) and $p2gg$ (bottom). Compare the $p2gg$ embedding to the three-dimensional visualization in Figure 9.

Algorithm 4 (Computing Fourier basis).

- 1.) Construct the orbit graph (Γ, E) .
- 2.) Compute the normalized Laplacian matrix L according to (16).
- 3.) Compute eigenvectors \hat{e}_i and eigenvalues $\hat{\lambda}_i$ of L .
- 4.) Return eigenvalues and interpolated eigenfunctions.

Alternatively, the basis can be computed using a Galerkin approach, which is described in Section 9.5. The functions in Figures 4, 5 and 6 are computed using the Galerkin method.

Remark 10 (Reflections and Neumann boundary conditions). The orbit graph automatically enforces the boundary condition (6), since it measures distance in terms of $d_{\mathbb{G}}$. The exception are group elements that are reflections, since these imply an additional property that the graph does not resolve: If ϕ is a reflection over a facet S , x a point on S (and hence $\phi x = x$), and f a ϕ -invariant smooth function, we must have $\nabla f(x) = -\nabla f(\phi x)$, and hence $\nabla f = 0$ on S . In the parlance of PDEs, this is a **Neumann boundary condition**, and can be enforced in several ways:

- 1) For each point $x_j \in \Gamma$ that is on S , add a point $x_{j'}$ to Γ and the edge $(x_j, x_{j'})$ to E . Then constrain each eigenvector e_i in Algorithm 4 to satisfy $e_{ij} = e_{ij'}$. This approach is common in spectral graph theory (e.g., Chung [20]).
- 2) Alternatively, one may symmetrize the orbit graph: For vertex x_j that is close to S , add its reflection $x_{j'} := \phi(x_j)$ to Γ . Now construct the edge set according to $d_{\mathbb{G}}$ using the augmented vertex set, and again constrain eigenvectors to satisfy $e_{ij} = e_{ij'}$. Either constrained eigenvalue problem can be solved using techniques of Golub [29].

6 Nonlinear representation: Factoring through an orbifold

We now generalize MacKay’s construction, as sketched in the introduction, from shifts to crystallographic groups. The construction defines a map

$$\rho|_{\Pi} : \Pi \rightarrow \Omega \subset \mathbb{R}^N \quad \text{which in turn defines} \quad \rho := \rho_{\Pi} \circ p : \mathbb{R}^n \rightarrow \Omega .$$

In MacKay’s case, Π is an interval and $\Omega \in \mathbb{R}^2$ a circle. The circle can be obtained from Π by “gluing” the ends of the interval to each other. To generalize this idea, we proceed as

follows: Starting with the polytope Π , we find any pair of points x and y on the same orbit of \mathbb{G} , and “bend” Π so that we can glue x to y . That results in a surface Ω in \mathbb{R}^N , where $N \geq n$ since we have bent Π . If we denote the point on Ω that corresponds to $x \in \Pi$ by $\rho|_{\Pi}(x)$, we obtain the maps above. We first show how to implement this construction numerically, and then consider its mathematical properties. In mathematical terms, the surface Ω is an **orbifold**, a concept that generalizes the notion of a manifold. The term \mathbb{G} -orbifold is made precise in Appendix C, but can be read throughout this section as a surface in \mathbb{R}^N that is “smooth almost everywhere”.

6.1. Gluing algorithms

The gluing algorithm constructs numerical approximations $\hat{\rho}$ of ρ and $\hat{\Omega}$ of Ω . Here, $\hat{\Omega}$ is a surface in \hat{N} dimensions, where (as we explain below) \hat{N} may be larger than N . As in the linear formulation of Section 5, we start with the orbit graph $\mathcal{G} = (\Gamma, E)$, but in this case weight the edges to obtain a weighted graph

$$\mathcal{G}_w = (\Gamma, E_w) \quad \text{with} \quad \text{weight}(x, y) := \begin{cases} d_{\mathbb{G}}(x, y) & \text{if } (x, y) \in E \\ 0 & \text{if } (x, y) \notin E \end{cases}.$$

The weighted graph provides approximate distances in quotient space. The surface $\hat{\Omega}$ is constructed from this graph by multidimensional scaling (MDS) [40]. MDS proceeds as follows: Let R be the matrix of squared geodesic distances, with entries

$$R_{ij} = (\text{weighted path length from } x_i \text{ to } x_j \text{ in } \mathcal{G}_w)^2.$$

Let $0 < \delta_1 \leq \dots \leq \delta_{|\Gamma|}$ be the eigenvalues and $v_1, \dots, v_{|\Gamma|}$ the eigenvectors of the matrix

$$\tilde{R} = -\frac{1}{2} \left(\mathbb{I} - \frac{1}{|\Gamma|} \mathbb{J} \right) R \left(\mathbb{I} - \frac{1}{|\Gamma|} \mathbb{J} \right) \quad \text{where } \mathbb{I} = \text{diag}(1, \dots, 1) \text{ and } \mathbb{J} = \begin{pmatrix} 1 & \dots & 1 \\ \vdots & \dots & \vdots \\ 1 & \dots & 1 \end{pmatrix}.$$

The embedding of each point x_i in the ε -net Γ is then given by

$$\hat{\rho}(x_i) := \begin{pmatrix} \sqrt{\delta_{|\Gamma|}} v_{|\Gamma|,i} \\ \sqrt{\delta_{|\Gamma|-1}} v_{|\Gamma|-1,i} \\ \vdots \\ \sqrt{\delta_{|\Gamma|-\hat{N}}} v_{|\Gamma|-\hat{N},i} \end{pmatrix}.$$

The dimension \hat{N} is chosen to minimize error in the distances. From $\hat{\rho}(x_1), \dots, \hat{\rho}(x_{|\Gamma|})$, the surface $\hat{\Omega}$ and the map $\hat{\rho}|_{\Pi}$ are obtained by interpolation.

Algorithm 5 (Gluing with multidimensional scaling).

- 1.) Construct the weighted orbit graph \mathcal{G}_w .
- 2.) Compute the eigenvalues δ_i and eigenvectors v_i of \tilde{R} .
- 3.) Compute vertex embeddings $\hat{\rho}(x_1), \dots, \hat{\rho}(x_{|\Gamma|})$.
- 4.) Return interpolated vertex embeddings.

Once $\hat{\rho}|_{\Pi}$ can be computed, we can also compute $\hat{\rho} := \hat{\rho}|_{\Pi} \circ p$, since the projector p can be evaluated using Algorithm 3.

Remark 11. The procedure satisfies two desiderata for constructing the orbifold map: 1) facets to be glued will be brought together, and 2) distances between interior points in Π will be approximately preserved. The embedding is unique up to isometric transformations. The embedding step is similar to the Isomap [61] algorithm, but unlike Isomap embeds into a higher-dimensional space rather than a lower-dimensional one.

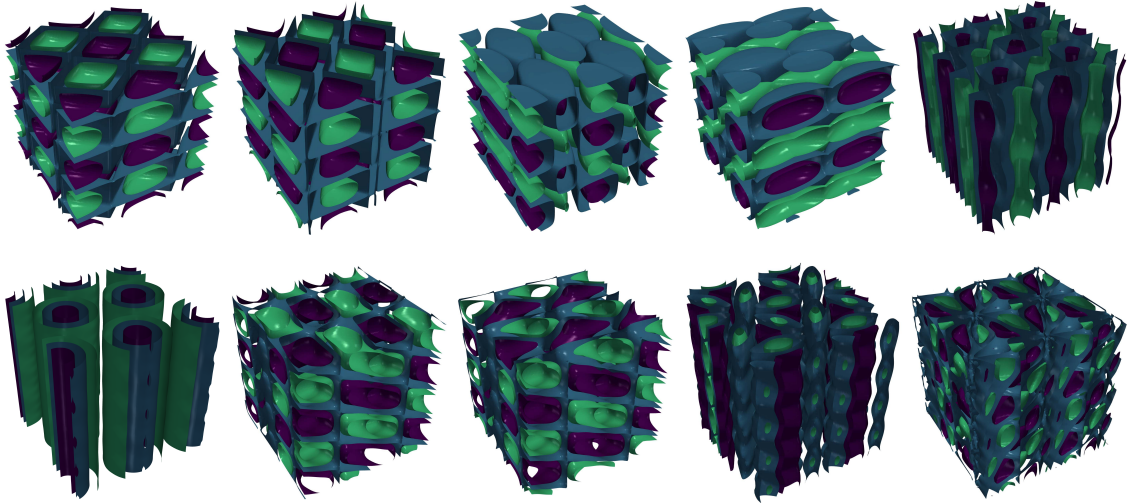


Figure 8: Visualizations of five-dimensional orbifold embeddings for $\text{Imm}2$ (top) and $\text{P}6_5$ (bottom).

6.2. Example: Invariant neural networks

Given \mathbb{G} and Π , compute $\hat{\rho}$ and $\hat{\Omega}$ using Algorithm 5. Choose a neural network

$$h_\theta : \mathbb{R}^{\hat{N}} \rightarrow \mathbb{R} \quad \text{with parameter vector } \theta \text{ and set } f_\theta := h_\theta \circ \hat{\rho}.$$

Then f_θ is a real-valued neural network on \mathbb{R}^n . Figure 10 shows examples of f_θ for $n = 3$, where h_θ has three hidden layers of ten units each, with rectified linear (relu) activations, although the input dimension \hat{N} may vary according to the choice of \mathbb{G} and Π . The parameter vector is generated at random.

Remark 12. Since most ways of performing interpolation in the construction of $\hat{\rho}$ are amenable to automatic differentiation tools, this representation is easy to incorporate into machine learning pipelines. Moreover, universality results for neural networks (e.g., Hornik et al. [35]) carry over: If a class of neural networks h_θ approximates to arbitrary precision in $\mathbf{C}(\mathbb{R}^N)$, then the resulting functions f_θ approximate to arbitrary precision in $\mathbf{C}_{\mathbb{G}}$ (though the approximation rate may change under composition with ρ). See Corollary 17.

6.3. Exact tilings

Although the properties of general orbifolds constitute one of the more demanding problems of modern mathematics, orbifolds of crystallographic groups are particularly well-behaved, and are well-understood. That we can draw directly on this theory is due to the fact that it uses a notion of gluing very similar to that employed by our algorithms as a proof technique [15, 53]. The two notions align under an additional condition: A convex polytope Π is **exact** for \mathbb{G} if \mathbb{G} tiles with Π , and if each face S of Π can be represented as

$$S = \Pi \cap \phi\Pi \quad \text{for some } \phi \in \mathbb{G}.$$

Not every Π with which \mathbb{G} tiles is exact—in Figure 1, for example, the polytopes shown for pg and $\text{p}3$ are not exact, though all others are. However, given Π and \mathbb{G} , we can always construct an exact surrogate as follows: Choose any point $x \in \mathbb{R}$ that is not a fixed point

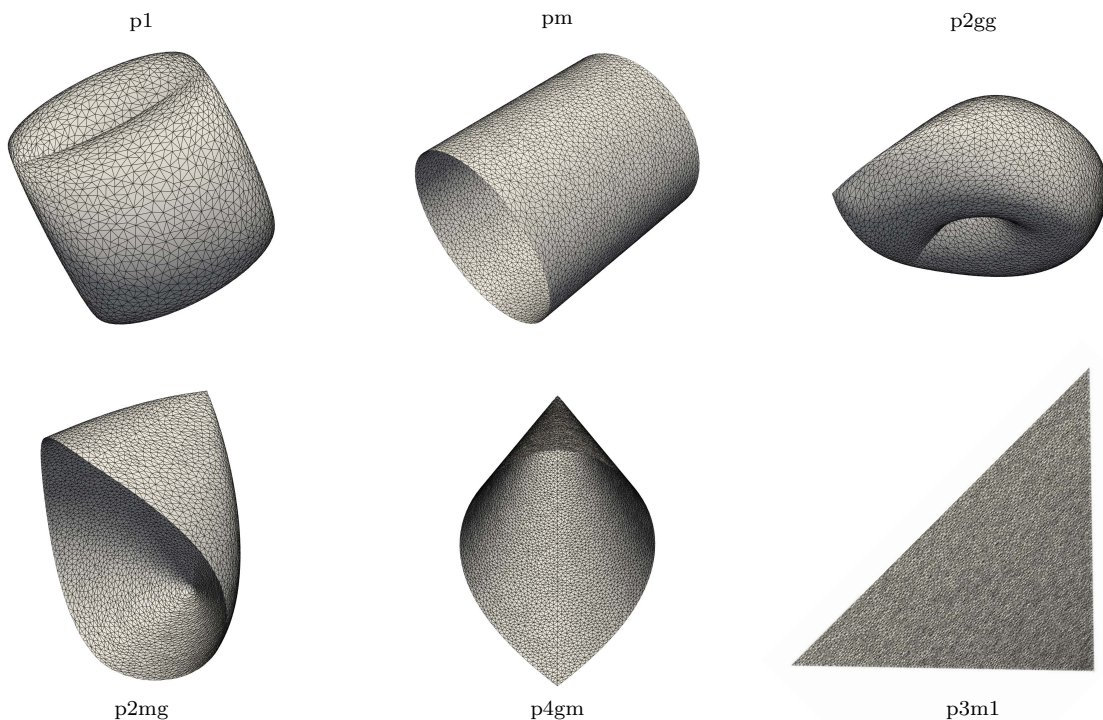


Figure 9: Visualization of several plane group orbifolds in three dimensions, computed as embeddings of orbit graphs as described in Section 6.1. The mesh on each orbifold is the image of the orbit graph. Note that reflections result in boundaries for pm , $p2mg$, $p4mg$, and $p3m1$, and that in particular all of the edges for $p3m1$ are boundaries. The self-intersections visible for $p2gg$ are an artifact of visualizing in three dimensions—for a sufficiently high dimension, the surface does not self-intersect.

for any $\phi \in \mathbb{G} \setminus \{1\}$. If \mathbb{G} is crystallographic, that is true for every point in the interior of Π . For each $\phi \in \mathbb{G}$, the set

$$R_\phi(x) := \{y \in \mathbb{R}^n \mid d_n(y, x) \leq d_n(y, \phi x)\},$$

is a half-space in \mathbb{R}^n (see Figure 11/left). The intersection

$$\mathbf{D}(x) := \bigcap_{\phi \in \mathbb{G}} R_\phi(x) = \bigcap_{\phi \mid \phi\Pi \cap \Pi \neq \emptyset} R_\phi(x)$$

of these half-spaces is called a **Dirichlet domain** for \mathbb{G} (Figure 11/right).

Fact 13 ([53, 6.7.4]). *If \mathbb{G} is crystallographic, $\mathbf{D}(x)$ is an exact convex polytope for \mathbb{G} .*

Example 14. For illustration, consider the group pg : We start with a rectangle Π . The group is generated by two glide reflections ϕ and ψ , each of which shifts Π horizontally and then reflects it about one of its long edges (Figure 12/left). Exactness fails because the set $\Pi \cap \phi\Pi$, marked in black, is not a complete edge of Π . A Dirichlet domain for this tiling differs significantly from Π (Figure 12/right). Although substituting $\mathbf{D}(x)$ for Π changes the look of the tiling, it does not change the group—that is, we still work with the same set of transformations (rather than another group in the same isomorphism class), and the axes of reflections are still defined by the faces of Π rather than those of $\mathbf{D}(x)$.

6.4. Properties of embeddings

Algorithm 5 can be interpreted as computing a numerical approximation $\hat{\rho}$ to a “true” embedding map ρ , namely the map in (2) in the introduction. Our main result on the

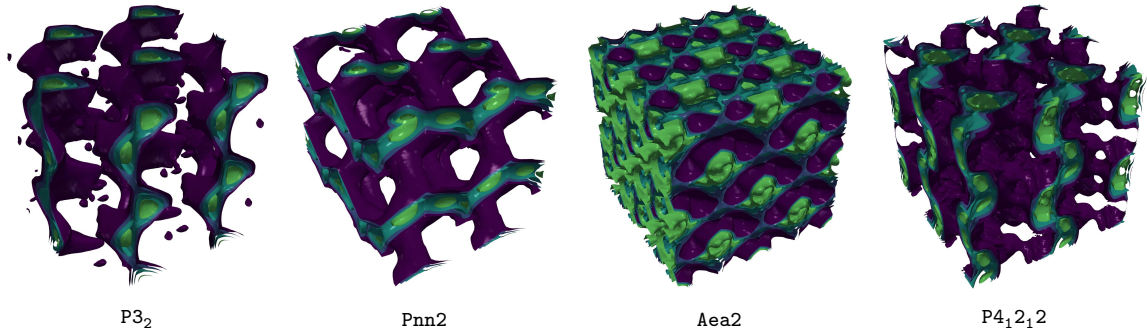


Figure 10: Four random neural networks for four different space groups, each with three hidden layers of ten units each and relu activations.

nonlinear representation, Theorem 15 below, shows that this map indeed exists for every crystallographic group, and describes some of its properties. The proof of the theorem shows that ρ and the set Ω can be constructed by the following abstract gluing algorithm.

Abstract gluing construction.

- 1.) Glue: Identify each $x \in \partial\Pi$ with the unique point $y \in \partial\Pi$ satisfying $x \sim y$.
- 2.) Equip the glued set M with metric $d_{\mathbb{G}}$.
- 3.) Embed the metric space $(M, d_{\mathbb{G}})$ as a subset $\Omega \subset \mathbb{R}^N$ for some $N \in \mathbb{N}$.
- 4.) For each $x \in \Pi$, define $\rho|_{\Pi}(x)$ as the representative of x on Ω .
- 5.) Set $\rho := \rho|_{\Pi} \circ p$.

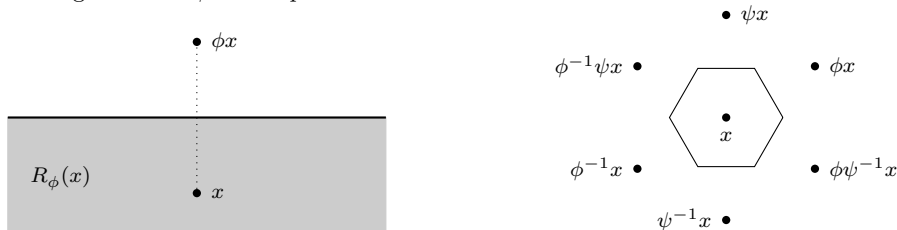
Since Π contains at least one point of each orbit, and the gluing step identifies all points identifies all points on the same orbit with each other, the glued set M can be regarded as the quotient set \mathbb{R}^n/\mathbb{G} . Recall that an **embedding** is a map $M \rightarrow \Omega \subset \mathbb{R}^N$ that is a homeomorphism (a continuous bijection with continuous inverse) of the metric spaces $(M, d_{\mathbb{G}})$ and (Ω, d_N) .

The state the theorem, we need one additional bit of terminology: The **stabilizer** of x in \mathbb{G} is the set of all ϕ that leave x invariant,

$$\text{Stab}(x) := \{\phi \in \mathbb{G} \mid \phi x = x\}$$

see Bonahon [15], Ratcliffe [53], Vinberg and Shvartsman [65]. We explain the role of the stabilizer in more detail in the next subsection.

Figure 11: Dirichlet domains. *Left:* The set $R_{\phi}(x)$, shown in gray, is the closed half space of all points at least as close to x as to ϕx . (In machine learning terms, the boundary of $R_{\phi}(x)$ orthogonally intersects the connecting line between x and ϕx at its center, and is hence the support vector classifier with two support vectors x and ϕx .) *Right:* A Dirichlet domain $\mathbf{D}(x)$ defined by the group generated by a vertical shift ϕ and a diagonal shift ψ in the plane.



Theorem 15. *Let \mathbb{G} be a crystallographic group that tiles \mathbb{R}^n with an exact convex polytope Π . Then the set M constructed by gluing is a compact \mathbb{G} -orbifold that is isometric to \mathbb{R}^n/\mathbb{G} . This orbifold can be embedded into \mathbb{R}^N for some*

$$n \leq N < 2(n + \max_{x \in \Pi} |\text{Stab}(x)|) < \infty,$$

that is, there is compact subset $\Omega \subset \mathbb{R}^N$ such that the metric space (Ω, d_N) is homeomorphic to $(\mathbb{R}^n/\mathbb{G}, d_{\mathbb{G}})$. In particular, every point $x \in \Pi$ is represented by one and only one point $\rho_{\Pi}(x)$. We can hence define a map

$$\rho : \mathbb{R}^n \rightarrow \Omega \subset \mathbb{R}^N \quad \text{as} \quad \rho(x) := \rho_{\Pi}(p(x)).$$

The map ρ is continuous, surjective, and \mathbb{G} -invariant. A function $f : \mathbb{R}^n \rightarrow Y$, with values in some topological space Y , is \mathbb{G} -invariant and continuous if and only if

$$f = h \circ \rho \quad \text{for some continuous } h : \mathbb{R}^N \rightarrow Y.$$

Ω is smooth almost everywhere, in the sense that

$$\text{vol}_n\{x \in \Pi \mid \Omega \cap B_{\varepsilon}(\rho(x)) \text{ is not a manifold for any } \varepsilon > 0\} = 0$$

where $B_{\varepsilon}(z)$ denotes the open Euclidean metric ball of radius ε centered at $z \in \mathbb{R}^N$.

Proof. See Appendix H. □

Remark 16. (a) Note carefully what the theorem does and does not show about the embedding algorithm in Section 6.1: It does say that the glued set constructed by the algorithm discretizes an orbifold, and that an N -dimensional embedding of this orbifold exists. It does *not* show that the embedding computed by MDS matches this dimension—indeed, since MDS attempts to construct an embedding that is also isometric (rather than just homeomorphic), we must in general expect the MDS embedding dimension to be larger, and we have at present no proof that an isometric embedding always exists.

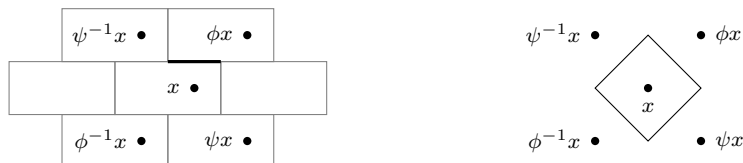
(b) If the tiling defined by \mathbb{G} and Π is not exact, we can nonetheless define an embedding ρ that represents continuous functions that are invariant functions with respect to this tiling: Construct a Dirichlet domain \mathbf{D} , and then construct ρ by applying the gluing algorithm to \mathbf{D} . Functions constructed as $h \circ \rho$ are then invariant for the tiling (\mathbb{G}, Π) .

We have now seen different representations of continuous \mathbb{G} -invariant functions on \mathbb{R}^n , respectively by continuous functions on Π , on the abstract space \mathbb{R}^n/\mathbb{G} , and on Ω . On Π , we must explicitly impose the periodic boundary condition, so we are using the set

$$\mathbf{C}_{\text{pbc}}(\Pi) := \{\hat{f} \in \mathbf{C}(\Pi) \mid \hat{f} \text{ satisfies (6)}\}.$$

In these representations, the projector p , the quotient map q , and the embedding map ρ play very similar roles. We can make that observation more rigorous:

Figure 12: The Dirichlet domain of a tiling may differ from the convex polytope defining the tiling. *Left:* A group generated by two glide reflections ϕ and ψ that tiles with a rectangle Π . Both glides shift the rectangle and then reflect it about one of its long edges. The set $\Pi \cap \phi\Pi$, marked black, is not a face of Π . *Right:* The Dirichlet domain $\mathbf{D}(x)$. When \mathbb{G} tiles with $\mathbf{D}(x)$, the axes of reflection are still defined by the edges of Π .



Corollary 17. *Given a crystallographic group \mathbb{G} that tiles with a convex polytope Π , consider the maps*

$$I_{\Pi} : \mathbf{C}_{\text{pbc}}(\Pi) \rightarrow \mathbf{C}_{\mathbb{G}} \quad \text{and} \quad I_{\mathbb{R}^n/\mathbb{G}} : \mathbf{C}(\mathbb{R}^n/\mathbb{G}) \rightarrow \mathbf{C}_{\mathbb{G}} \quad \text{and} \quad I_{\Omega} : \mathbf{C}(\Omega) \rightarrow \mathbf{C}_{\mathbb{G}}$$

$$\hat{f} \mapsto \hat{f} \circ p \qquad \hat{g} \mapsto \hat{g} \circ q \qquad \hat{h} \mapsto \hat{h} \circ \rho$$

where I_{Ω} is only defined if Π is exact. Equip all spaces with the supremum norm. Then I_{Π} and $I_{\mathbb{R}^n/\mathbb{G}}$ are isometric isomorphisms, and if Π is exact, so is I_{Ω} . In particular, $\mathbf{C}_{\mathbb{G}}$ is always a separable Banach space.

Proof. By Lemma 5, (8) and Theorem 15, all three maps are bijections. We also have

$$\|\hat{f}\|_{\text{sup}} = \sup_{x \in \Pi} |\hat{f}(x)| = \sup_{x \in \mathbb{R}^n} |\hat{f}(p(x))| = \|\hat{f} \circ p\|_{\text{sup}} \quad \text{for } \hat{f} \in \mathbf{C}_{\text{pbc}}(\Pi),$$

and the same holds mutatis mutandis on \mathbb{R}^n/\mathbb{G} and Ω , so all maps are isometries. Since Π is compact, $\mathbf{C}(\Pi)$ is separable [3, 3.99]. The same hence holds for the closed subspace $\mathbf{C}_{\text{pbc}}(\Pi)$, and by isometry for $\mathbf{C}_{\mathbb{G}}$. \square

6.5. Why the glued surface may not be smooth

Whether or not the glued surface is smooth depends on whether the transformations in \mathbb{G} leave any points invariant. It is a known fact in geometry (and made precise in the proof of Theorem 15) that

$$\text{glued surface is a manifold} \quad \Leftrightarrow \quad \phi x \neq x \quad \text{for all } \phi \in \mathbb{G} \setminus \{\mathbf{1}\} \text{ and } x \in \mathbb{R}^n.$$

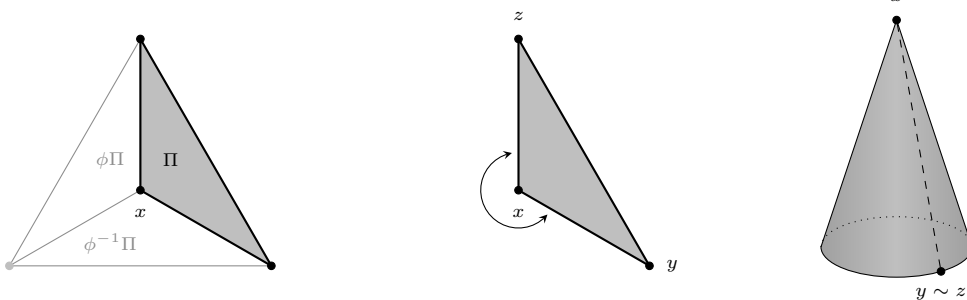
That can be phrased in terms of the stabilizer as

$$\text{glued surface is a manifold} \quad \Leftrightarrow \quad \text{Stab}(x) = \{\mathbf{1}\} \quad \text{for all } x \in \mathbb{R}^n.$$

It is straightforward to check that $\text{Stab}(x)$ is a group [65]. Since each ϕ is an isometry, and shifts of \mathbb{R}^n have no fixed points, $\phi(x) = x$ can only hold if $b_{\phi} = 0$. Thus, $\text{Stab}(x)$ is always a subset of the point group \mathbb{G}_o (in the terminology of Appendix A), which means it is finite. To illustrate its effect on the surface, consider the following examples.

Example 18. (a) Recall that MacKay's construction [45], as sketched in the introduction, can be translated to crystallographic groups by setting $\Pi = [0, 1]$ and choosing \mathbb{G} as shifts. In this case, $\text{Stab}(x) = \{\mathbf{1}\}$ for each $x \in \mathbb{R}$, and the glued surface is a circle, which is indeed

Figure 13: Fixed points become non-smooth under gluing. *Left:* A triangular polytope Π is transformed by a rotation ϕ , which rotates by 120° around the vertex x of Π . Note that $\phi^2 = \phi^{-1}$ and $\phi^3 = \mathbf{1}$. *Middle:* The gluing defined by ϕ identifies the edge (x, z) and the edge (x, y) . *Right:* The resulting glued surface is a cone, with x mapped to the tip. Locally around x , the cone is not a manifold.



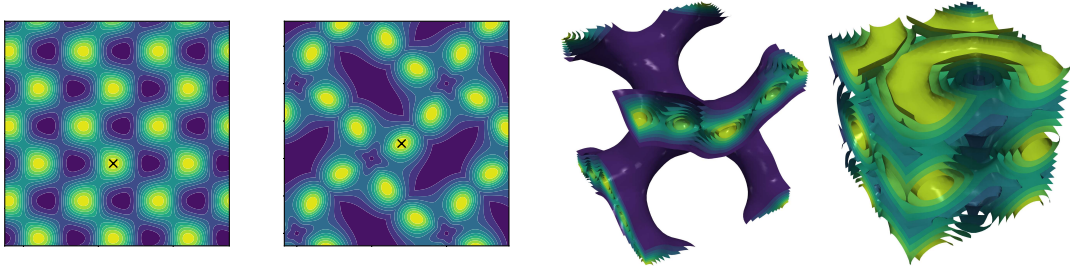


Figure 14: Invariant kernel functions using the kernel in (21), for groups on \mathbb{R}^2 and \mathbb{R}^3 : pg with $\ell = 0.1$, p4gm with $\ell = 0.01$, I4_1 with $\ell = 0.01$, and $\text{P6}_3/\text{m}$ with $\ell = 0.05$ (from left to right).

a manifold. The two-dimensional analogue is to choose $\Pi = [0, 1]^2$ and \mathbb{G} as the group p1 in Figure 1, in which case the glued surface is a torus as shown in Figure 9, and hence again a manifold.

(b) Now suppose Π is a triangle, x one of its corners, and ϕ a 120° rotation around x , as illustrated in Figure 13. Then $\text{Stab}(x) = \{\mathbf{1}, \phi, \phi^2 = \phi^{-1}\}$, and the glued surface $\Omega = \rho(\Pi)$ is a cone with $\rho(x)$ as its tip. That means Ω is not a manifold, because no neighborhood of the tip can be mapped isometrically to a neighborhood in \mathbb{R}^2 .

7 Invariant kernels

Throughout this section, $\kappa : \mathbb{R}^n \times \mathbb{R}^n \rightarrow \mathbb{R}$ is a kernel, i.e., a positive definite function, and \mathbb{H} is its reproducing kernel Hilbert space, or RKHS. Appendix B reviews definitions. We consider kernels that are \mathbb{G} -invariant in both arguments in the sense of (5), that is,

$$\kappa(\phi x, \psi y) = \kappa(x, y) \quad \text{for all } \phi, \psi \in \mathbb{G} \text{ and all } x, y \in \mathbb{R}^n .$$

That is the natural notion of invariance for most purposes, since such kernels are precisely those that define spaces of \mathbb{G} -invariant functions:

Proposition 19. *If and only if κ is \mathbb{G} -invariant in each argument, all functions $f \in \mathbb{H}$ are \mathbb{G} -invariant. If κ is also continuous, all $f \in \mathbb{H}$ are continuous, and hence $\mathbb{H} \subset \mathbf{C}_{\mathbb{G}}$.*

Theorem 15 implies that, to define an invariant kernel, we can start with any kernel $\hat{\kappa}$ on the embedding space \mathbb{R}^N , and compose it with the embedding map ρ :

Corollary 20. *Let $\hat{\kappa}$ be a kernel on \mathbb{R}^N . Then the function*

$$\kappa(x, y) := \hat{\kappa}(\rho(x), \rho(y)) \quad \text{or in short} \quad \kappa = \hat{\kappa} \circ (\rho \otimes \rho)$$

is a kernel on \mathbb{R}^n that is \mathbb{G} -invariant in both arguments. If $\hat{\kappa}$ is continuous, so is κ .

That follows immediately from Theorem 15 and the fact that the restriction of a kernel to a subset is again a kernel [59].

Example 21. Suppose $\hat{\kappa}$ is an radial basis function (RBF) kernel with length scale ℓ on \mathbb{R}^N , and hence of the form $\hat{\kappa}(z, z') = \exp(-\|z - z'\|^2/\ell^2)$. Then κ is simply

$$\kappa(x, y) = \hat{\kappa}(\rho(x), \rho(y)) = \exp\left(-\frac{\|\rho(x) - \rho(y)\|^2}{2\ell^2}\right).$$

Figure 14 illustrates this kernel the two-dimensional groups pg and p4gm and the three-dimensional groups I4_1 and $\text{P6}_3/\text{m}$.

Once we have constructed an invariant kernel, its application to machine learning problems is straightforward. That becomes obvious if we define $\Phi(x) = \kappa(x, \cdot)$, often called the **feature map** of κ [59]. Using the definition of the scalar product on \mathbb{H} and the reproducing property (see Appendix B.4), we then have

$$\Phi : \mathbb{R}^n \rightarrow \mathbb{H} \quad \text{and} \quad \kappa(x, y) = \langle \Phi(x), \Phi(y) \rangle_{\mathbb{H}} .$$

If κ is \mathbb{G} -invariant, then Φ is also \mathbb{G} -invariant by construction. Recall that most kernel methods in machine learning are derived by substituting a Euclidean scalar product by $\langle \Phi(x), \Phi(y) \rangle_{\mathbb{H}}$, thereby making a linear method nonlinear. Using a \mathbb{G} -invariant kernel results in a \mathbb{G} -invariant method.

Example 22 (Invariant SVM). A support vector machine (SVM) with kernel κ is determined by two finite sets of points \mathcal{X} and \mathcal{Y} in \mathbb{R}^n . To train the SVM, one maps these points into \mathbb{H} via Φ , finds the shortest connecting line between the convex hulls of $\Phi(\mathcal{X})$ and $\Phi(\mathcal{Y})$, and determines a hyperplane F that is orthogonal to this line and intersects its center—equivalently, in dual formulation, the unique hyperplane that separates the convex hulls of $\Phi(\mathcal{X})$ and $\Phi(\mathcal{Y})$ and maximizes the \mathbb{H} -norm distance to both. The set of points x in \mathbb{R}^n whose image $\Phi(x)$ lies on F is the **decision surface** of the SVM in \mathbb{R}^n . The hyperplane can be specified by two functions g (an offset vector) and h (a normal vector) in \mathbb{H} : A function $f \in \mathbb{H}$ lies on F if and only if

$$\langle f - g, h \rangle_{\mathbb{H}} = 0 \quad \text{or equivalently} \quad \langle f, h \rangle_{\mathbb{H}} = \langle g, h \rangle_{\mathbb{H}} .$$

Let x be a point in \mathbb{R}^n . If y and z are points with $g = \Phi(y)$ and $h = \Phi(z)$, then

$$x \text{ is on decision surface} \quad \iff \quad \kappa(x, z) = \kappa(y, z) .$$

Since invariance of κ implies $\kappa(\phi x, z) = \kappa(x, z)$, that shows the decision surface is \mathbb{G} -invariant. Figure 15 shows examples. In these figures the data were randomly generated with regions assigned labels using a random function generated as in Section 8. The support vectors are highlighted and illustrate the effects of symmetry constraints: the decision surface can be determined by data observed far away.

Two of the most important results on kernels are Mercer’s theorem and the compact inclusion theorem [59, Chapter 4]. The latter shows the inclusion map $\mathbb{H} \hookrightarrow \mathbf{C}$ is compact, and is used in turn to establish good statistical properties of kernel methods, such as oracle inequalities and finite covering numbers [59]. Both results assume that κ has compact support. If κ is invariant under a crystallographic group, its support is necessarily non-compact, but the next result shows that versions of both theorems hold nonetheless:

Proposition 23. *If κ is continuous and \mathbb{G} -invariant in both arguments, the inclusion map $\mathbb{H} \hookrightarrow \mathbf{C}_{\mathbb{G}}$ is compact. There exist functions $f_1, f_2, \dots \in \mathbb{H}$ and scalars $c_1 \geq c_2 \geq \dots > 0$ such that*

$$\kappa(x, y) = \sum_{i \in \mathbb{N}} c_i f_i(x) f_i(y) \quad \text{for all } x, y \in \mathbb{R}^n ,$$

and the scaled sequence $(\sqrt{c_i} f_i)$ is an orthonormal basis of \mathbb{H} . With this basis,

$$\mathbb{H} = \{ f = \sum_{i \in \mathbb{N}} a_i \sqrt{c_i} f_i \mid a_1, a_2, \dots \in \mathbb{R} \text{ with } \sum_i |a_i|^2 < \infty \} ,$$

where each series converges in \mathbb{H} and hence (by compactness of inclusion) also uniformly.

Intuitively, that is the case because every \mathbb{G} -invariant kernel is the pullback of a kernel on Ω , and Ω is compact. Figure 15 shows an application of such a kernel to generate a two-class classifier with an \mathbb{G} -invariant decision surface.

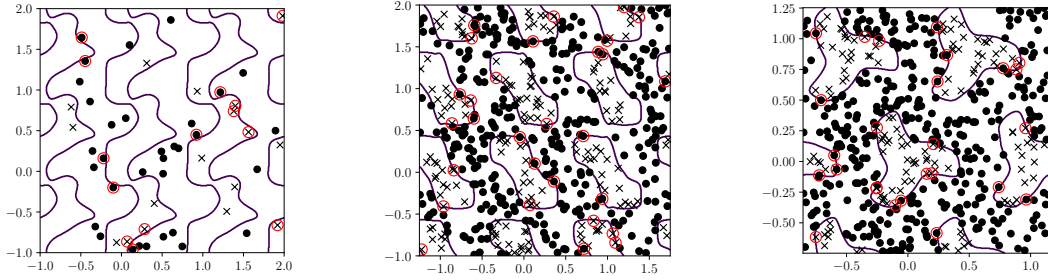


Figure 15: Support vector machine decision surfaces for \mathbb{G} -invariant kernels constructed as in Corollary 20. The groups used are p1 (left), p2 (middle), and p3 (right). Support vectors are highlighted with red circles.

8 Invariant Gaussian processes

We now consider the problem of generating random functions $F : \mathbb{R}^n \rightarrow \mathbb{R}$ such that each instance of F is continuous and \mathbb{G} -invariant with probability 1. That can be done linearly using the generalized Fourier representation, by generating the coefficients c_i in Theorem 7 at random. Here, we consider the nonlinear representation instead: If we set

$$F := H \circ \rho \quad \text{for a random continuous function } H : \mathbb{R}^N \rightarrow \mathbb{R} ,$$

Theorem 15 implies that F is indeed continuous and \mathbb{G} -invariant with probability 1, and hence a random element of $\mathbf{C}_{\mathbb{G}}$. Conversely, the result also implies that every random element of $\mathbf{C}_{\mathbb{G}}$ is of this form, for some random element H of $\mathbf{C}(\mathbb{R}^N)$.

8.1. Almost surely invariant processes

Recall that a random function $F : M \subseteq \mathbb{R}^n \rightarrow \mathbb{R}$ is a **Gaussian process** if the joint distribution of the random vector $(F(x_1), \dots, F(x_k))$ is Gaussian for any finite set of points $x_1, \dots, x_k \in M$. The **mean** and **covariance function** of a Gaussian process are defined as

$$\mu(x) := \mathbb{E}[F(x)] \quad \text{and} \quad \kappa(x, y) := \mathbb{E}[(F(x) - \mu(x))(F(y) - \mu(y))] \quad \text{for } x, y \in M .$$

The covariance function is always positive definite, and hence a kernel on M . The distribution of a Gaussian process is completely determined by μ and κ , and conditions for F to satisfy continuity or stronger regularity conditions can be formulated in terms of κ . See e.g., Marcus and Rosen [46] for more background.

Proposition 24. *Let H be a continuous Gaussian process on \mathbb{R}^N , with mean μ and covariance function κ . Then $F := H \circ \rho$ is a continuous random function on \mathbb{R}^n , and is \mathbb{G} -invariant with probability 1. Consider any finite set of points*

$$x_1, \dots, x_k \in \mathbb{R}^n \quad \text{such that } x_i \not\sim x_j \text{ for all distinct } i, j \leq k .$$

Then $(F(x_1), \dots, F(x_k))$ is a Gaussian random vector, with mean and covariance

$$\mathbb{E}[F(x_i)] = \mu(\rho(x_i)) \quad \text{and} \quad \text{Cov}[F(x_i), F(x_j)] = \kappa(\rho(x_i), \rho(x_j)) \quad \text{for } i, j \leq k .$$

Clearly, F cannot be a Gaussian process on \mathbb{R}^n : Since F is invariant, $F(x)$ completely determines $F(\phi(x))$, so $(F(x), F(\phi(x)))$ cannot be jointly Gaussian. Put differently, conditioning F on its values on Π renders F non-random. Loosely speaking, the proposition hence says that F is “as Gaussian” as a \mathbb{G} -invariant random function can be. Figure 16 illustrates random functions generated by such a process.

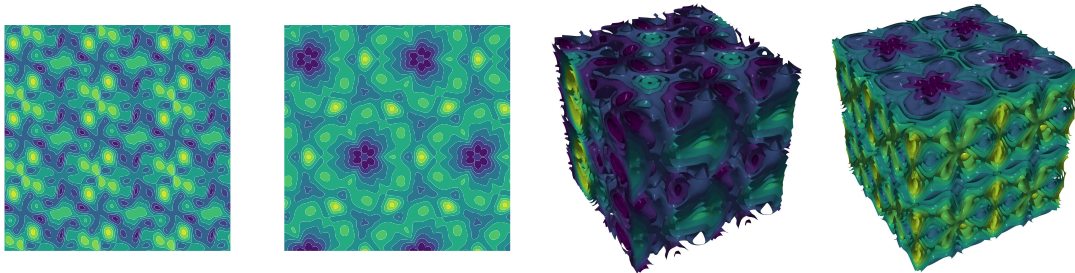


Figure 16: Random invariant functions on \mathbb{R}^2 and \mathbb{R}^3 , generated by Gaussian processes as described in Example 25. The groups are, from left to right, p2, p31m, P-6, and P422.

Example 25. The construction of MacKay [45] described in the introduction was designed specifically for Gaussian processes, to generate periodic functions at random. We can now generalize these processes from periodicity to crystallographic invariance: Given \mathbb{G} and Π , construct the embedding map $\rho: \mathbb{R}^n \rightarrow \mathbb{R}^N$. Choose $\hat{\kappa}$ as the RBF kernel (21) on \mathbb{R}^N , and $\hat{\mu}$ as the constant function 0 on \mathbb{R}^N . Then generate F as

$$H \sim \text{GP}(\hat{\mu}, \hat{\kappa}) \quad \text{and} \quad F := H \circ \rho.$$

For visualization, draws can be approximated by the randomized feature scheme of Rahimi and Recht [51]. Figure 16 shows examples for \mathbb{G} chosen as p2 and p31m on \mathbb{R}^2 , and for P-6 and P422 on \mathbb{R}^3 .

8.2. Distributionally invariant processes

Another type of invariance that random functions can satisfy is **distributional \mathbb{G} -invariance**, which holds if

$$F \stackrel{d}{=} F \circ \phi \quad \text{for all } \phi \in \mathbb{G}.$$

Here, $\stackrel{d}{=}$ denotes equality in distribution. That is equivalent to requiring that the distribution P of F satisfies $P(\phi A) = P(A)$ for every measurable set A . For crystallographic groups, distributionally invariant Gaussian processes can be constructed by factoring the parameters, rather than the random function F , through the embedding in Theorem 15:

Corollary 26. *Let μ be a real-valued function and κ a kernel on \mathbb{R}^N . If F is the Gaussian process on \mathbb{R}^n with mean $\mu \circ \rho$ and covariance function $\kappa \circ (\rho \otimes \rho)$, then F is distributionally \mathbb{G} -invariant, i.e. $F \circ \phi \stackrel{d}{=} F$ for all $\phi \in \mathbb{G}$.*

Almost sure invariance implies distributional invariance; distributional invariance is typically a much weaker property. Frequently encountered examples of distributional invariance are all forms of stationarity (distributional invariance under shift groups) and of exchangeability (permutation groups).

9 The Laplace operator on invariant functions

The results in this section describe the behavior of the Laplace operator on \mathbb{G} -invariant functions. All of these are ingredients in the proof of the Fourier representation. We first describe the transformation behavior of differentials of invariant functions, in Section 9.1. Gradients turn out to be invariant under shifts and equivariant under orthogonal transformations. Gradient vector fields, and more generally vector fields with the same

transformation behavior as gradients, have a cancellation property—their integral orthogonal to the tile boundary vanishes (Section 9.2). We then define the relevant solution space for the spectral problem, which has Hilbert space structure (so that we can define orthogonality and self-adjointness) but has smoother elements than \mathbf{L}_2 , in Section 9.3. Once the Laplacian has been properly defined on this space, we can use the cancellation property to show it is self-adjoint.

9.1. Differentials and gradients of invariant functions

Given a differentiable function $f : \mathbb{R}^n \rightarrow \mathbb{R}^m$, denote the differential at x as

$$Df(x) = \left(\frac{\partial f_j}{\partial x_i} \right)_{i \leq n, j \leq m} \in \mathbb{R}^{n \times m}.$$

The next result summarizes how invariance of f under a transformation ϕ affects Df . Note the order of operations matters: $D(f \circ \phi)$ is the differential of the function $f \circ \phi$, whereas $(Df) \circ \phi$ transforms the differential Df of f by ϕ .

Lemma 27. *If $f : \mathbb{R}^n \rightarrow \mathbb{R}^m$ is invariant under an isometry $\phi x = A_\phi x + b_\phi$ and differentiable, then*

$$(17) \quad (Df)(\phi x) = Df(x) \cdot A_\phi^\top.$$

If in particular $f : \mathbb{R}^n \rightarrow \mathbb{R}$, the gradient satisfies

$$(18) \quad \nabla f(\phi x) = A_\phi \cdot \nabla f(x) \quad \text{for all } x \in \mathbb{R}^n.$$

The Hessian matrix H_f and the Laplacian satisfy

$$(19) \quad H_f(\phi x) = A_\phi H_f(x) A_\phi^\top \quad \text{and} \quad \Delta f(\phi x) = \Delta f(x) \quad \text{for all } x \in \mathbb{R}^n.$$

Proof. Since ϕ is affine, its differential $(D\phi)(x) = A_\phi$ is constant. The chain rule shows

$$D(f \circ \phi) = (Df) \circ \phi \cdot (D\phi) = ((Df) \circ \phi) \cdot A_\phi.$$

By invariance, $f \circ \phi$ and f are the same function, and hence $D(f \circ \phi) = Df$. Substituting into the identity above shows (17), since $A_\phi^\top = A_\phi^{-1}$. For $m = 1$, the transpose $D^\top = \nabla$ is the gradient, and (17) becomes (18). Using (18), the Hessian can be written as

$$H_f = D(\nabla f) = D(A_\phi \nabla f \circ \phi^{-1}).$$

Another application of the chain rule then shows

$$H_f = D(A_\phi \nabla f) \circ \phi^{-1} \cdot D\phi^{-1} = A_\phi (D\nabla f) \circ \phi^{-1} \cdot A_{\phi^{-1}} = A_\phi (H_f \circ \phi^{-1}) A_\phi^\top,$$

which is the first statement in (19). Since the Laplacian is the trace of H_f , and the trace is invariant under change of basis, that implies

$$\Delta f(\phi x) = \text{tr}(H_f(\phi x)) = \text{tr}(A_\phi H_f(x) A_\phi^\top) = \text{tr}(H_f(x)) = \Delta f(x). \quad \square$$

9.2. Flux through the tile boundary

The next result is the key tool we use to prove self-adjointness of the Laplacian. We have seen above that the gradient of a \mathbb{G} -invariant function transforms under \mathbb{G} according to (18). We now abstract from the specific function ∇f , and consider any vector field $F : \Pi \rightarrow \mathbb{R}^n$ that transforms like the gradient on the tile boundary, i.e.

$$(20) \quad F(y) = A_\phi F(x) \quad \text{whenever } y = \phi x .$$

For a polytope Π with facets S_1, \dots, S_k , we define the normal field on the boundary as

$$\mathbf{N}_\Pi : \partial\Pi \rightarrow \mathbb{R}^n \quad \text{given by} \quad \mathbf{N}_\Pi(x) := \begin{cases} \mathbf{N}_i & \text{if } x \in S_i^\circ \\ 0 & \text{otherwise} \end{cases}$$

where \mathbf{N}_i is the unit normal vector of the facet S_i , directed outward with respect to Π . In vector analysis, the projection $F^\top \mathbf{N}_\Pi$ of a vector field onto the direction orthogonal to $\partial\Pi$ is known as the **flux** of F through the boundary.

Proposition 28 (Flux). *Let \mathbb{G} be a crystallographic group that tiles \mathbb{R}^n with a convex polytope Π . If a vector field $F : \Pi \rightarrow \mathbb{R}^n$ is integrable on $\partial\Pi$ and satisfies (20), then*

$$\int_{\partial\Pi} F(x)^\top \mathbf{N}_\Pi(x) \text{vol}_{n-1}(dx) = 0 .$$

Proof. See Appendix E. □

9.3. The Sobolev space of invariant functions

The proof of Theorem 7 follows a well-established strategy in spectral theory: The relevant spectral results hold for self-adjoint operators, and self-adjointness can only be defined with respect to an inner product. Since the space \mathbf{C}^2 on which the Laplace operator is defined is a Banach space, but has no inner product, one must hence first embed the problem into a suitable Hilbert space. For the Laplacian, this is generally a first-order Sobolev space; see Appendix B for a review of definitions, and Brezis [19], Maz'ya [47], McLean [48] for more on spectral theory and the general approach.

In our case, we proceed as follows: Since invariant functions are completely determined by their values on Π , we can equivalently solve the problem on the bounded domain Π rather than the unbounded domain \mathbb{R}^n . That gives us access to a number of results specific to bounded domains. We also observe that the invariance constraint $e = e \circ \phi$ is a linear constraint—if two functions satisfy it, so do their linear combinations—so the feasible set of this constraint is a vector space, and we can encode the constraint by restriction to a suitable subspace. We start with the vector space

$$(21) \quad \mathcal{H} := \{f|_{\Pi^\circ} \mid f : \mathbb{R}^n \rightarrow \mathbb{R} \text{ infinitely often differentiable and } \mathbb{G}\text{-invariant}\} .$$

The elements of \mathcal{H} are hence infinitely often differentiable on Π° , and their continuous extensions to the closure Π satisfy the periodic boundary condition (6). We then define the Sobolev space of candidate solutions as

$$\mathbf{H}_\mathbb{G} := \text{closure of } \mathcal{H} \text{ in } \mathbf{H}^1(\Pi^\circ) ,$$

equipped with the norm and inner product of $\mathbf{H}^1(\Pi^\circ)$. As a closed subspace of a Hilbert space, it is a Hilbert space.

9.4. The Laplace operator on $\mathbf{H}_{\mathbb{G}}$

We now have to extend Δ to all elements of $\mathbf{H}_{\mathbb{G}}$. In general, a linear operator Λ on a closed subspace $V \subset \mathbf{H}^1(\Pi^\circ)$ is an **extension** of Δ to V if it satisfies

$$(22) \quad \Lambda f = \Delta f \quad \text{for all } f \in V \cap \mathbf{C}^2(\Pi^\circ).$$

The extended operator is **self-adjoint** on V if

$$\langle \Lambda f, h \rangle_{\mathbf{H}^1} = \langle f, \Lambda h \rangle_{\mathbf{H}^1} \quad \text{for all } f, h \in V.$$

To prove self-adjointness, one decomposes Λ as

$$\langle -\Delta f, h \rangle_{\mathbf{L}_2} = (\text{integral over } \Gamma^\circ \text{ that is symmetric in } f \text{ and } h) - (\text{integral over } \partial\Gamma).$$

This is the Green identity alluded to in the introduction. To make it precise, we need two quantities: One is the **energy form** or **energy product**

$$(23) \quad a(f, h) := \int_{\Gamma} \nabla f(x)^\top \nabla h(x) \text{vol}_n(dx).$$

Since it only involves first derivatives, and both appear under the integral, it is well-defined for any $f, h \in \mathbf{H}^1(\Pi^\circ)$, and is hence a symmetric bilinear form $a : \mathbf{H}^1 \times \mathbf{H}^1 \rightarrow \mathbb{R}$. It is positive definite, since

$$(24) \quad a(f, h) = \sum_{i \leq n} \langle \partial_i f, \partial_i h \rangle_{\mathbf{L}_2} \quad \text{and hence} \quad a(f, f) = \sum_{i \leq n} \|\partial_i f\|_{\mathbf{L}_2}^2 \geq 0.$$

Substituting the definition of a into that of the \mathbf{H}^1 scalar product in (B.6) shows that

$$(25) \quad \langle f, h \rangle_{\mathbf{H}^1} = \langle f, h \rangle_{\mathbf{L}_2} + a(f, h) \quad \text{for all } f, h \in \mathbf{H}^1(\Gamma^\circ).$$

The second quantity is the **conormal derivative**

$$\partial_{\mathbf{N}} f(x) := \nabla f(x)^\top \mathbf{N}_{\Pi}(x).$$

The precise statement of the decomposition above is then as follows.

Fact 29 (Green's identity). *If the domain Π is sufficiently regular—in particular, if Π is a convex polytope—then*

$$\langle -\Delta f, h \rangle_{\mathbf{L}_2} = a(f, h) - \int_{\partial\Gamma} \partial_{\mathbf{N}} f(x) h(x) \text{vol}_{n-1}(dx) \quad \text{for } f, h \in \mathbf{H}^1(\Pi^\circ).$$

Informally, this shows that Δ “behaves self-adjointly” in the interior of Π , where derivatives can be computed in all directions around a point. At points on $\partial\Pi$, the boundary truncates derivatives in some direction, and that requires a correction term $\partial_{\mathbf{N}} f$.

Theorem 30 (Properties of the Laplacian). *Let \mathbb{G} be a crystallographic group that tiles \mathbb{R}^n with a convex polytope Π . Then Δ has a unique extension to a linear operator Λ on $\mathbf{H}_{\mathbb{G}}$. This operator is self-adjoint and continuous on $\mathbf{H}_{\mathbb{G}}$, and satisfies*

$$(26) \quad \text{(i) } \langle -\Lambda f, h \rangle_{\mathbf{L}_2} = a(f, h) \quad \text{and} \quad \text{(ii) } \langle -\Lambda f, f \rangle_{\mathbf{H}^1} \geq \|f\|_{\mathbf{H}^1}^2 - \|f\|_{\mathbf{L}_2}^2$$

for all $f, h \in \mathbf{H}_{\mathbb{G}}$.

The proof uses the flux property to show that crystallographic symmetry makes the boundary term cancel. Since a is symmetric, that makes Λ self-adjoint. In the parlance of elliptic differential equations, (26ii) says that Λ is **coercive** on $\mathbf{H}_{\mathbb{G}}$ (see [48]).

Proof. See Appendix F. □

9.5. Linear representations from a nonlinear ansatz

The properties of Laplace operators lead naturally to a class of numerical approximations known as Galerkin methods (e.g., Braess [18]). Using the embedding map ρ , we can derive a Galerkin method that can be used to compute the Fourier basis functions in Theorem 7—that is, we can use the nonlinear representation approach in the numerical approximation of the linear representation. The Galerkin method can be more accurate than the spectral approach in Algorithm 4, and was used to render Figures 4, 5 and 6.

Galerkin methods posit basis functions χ_1, \dots, χ_m and approximate an infinite dimensional function space by the finite-dimensional subspace $\text{span}\{\chi_1, \dots, \chi_m\}$. In our case, we approximate solutions e of (13) by approximating their restrictions $e|_{\Pi}$. We hence need functions $\chi_i : \Pi \rightarrow \mathbb{R}$. We start with functions $\tilde{\chi}_i : \mathbb{R}^N \rightarrow \mathbb{R}$, and set $\chi_i := \tilde{\chi}_i \circ \rho$. We then assume $e|_{\Pi}$ of (13) is in the span, and hence of the form

$$(27) \quad e|_{\Pi} = \sum_{i \leq m} c_i \chi_i .$$

If e solves the eigenvalue problem (13), $e|_{\Pi}$ satisfies

$$\langle -\Delta e|_{\Pi}, \chi_j \rangle_{\mathbf{L}_2} = \lambda \langle e|_{\Pi}, \chi_j \rangle_{\mathbf{L}_2} \quad \text{for all } j \leq m .$$

Applying (26) and substituting in (27) shows

$$a(e|_{\Pi}, \chi_j) = \lambda \langle e|_{\Pi}, \chi_j \rangle_{\mathbf{L}_2} \quad \text{and} \quad \sum_i c_i a(\chi_i, \chi_j) = \lambda \sum_i c_i \langle \chi_i, \chi_j \rangle_{\mathbf{L}_2} .$$

If we define matrices with entries $A_{ij} := a(\chi_i, \chi_j)$ and $B_{ij} := \langle \chi_i, \chi_j \rangle_{\mathbf{L}_2}$, that becomes

$$Ac = \lambda Bc \quad \text{where } c = (c_1, \dots, c_m)^{\top} .$$

The entries of A and B can be computed with off-the-shelf cubature methods, and we can then solve for the pair (λ, c) .

Remark 31. (a) If ρ and the basis functions are implemented with JAX [17] or a similar automatic differentiation tool, the gradients in (23) are available, which avoids finite difference approximation and explicit computation of second derivatives.

(b) Neumann boundary conditions for reflections (see Remark 10) can be enforced using the methods of Golub [29].

(c) The basis functions $\tilde{\chi}_i$ can be almost any basis on \mathbb{R}^N . Figures 4–6 were rendered by placing points x_1, x_2, \dots uniformly on Π , and centering radial basis functions at the points $\rho(x_i)$ in \mathbb{R}^N .

10 Related work and additional references

In machine learning. There has been substantial work on group invariance and equivariance in machine learning, with a focus on finite and compact groups. Most salient has been work on approximate translation invariance and equivariance in convolutional neural networks for images [39, 44] and speech [1], although this work has not been framed in a group-theoretic way. To our knowledge the earliest explicit consideration of compact and finite group structure in machine learning was from a Fourier perspective by Kondor [38]; this was primarily in the context of Hilbert-space formalisms of learning. The current perspective on compact and finite group equivariance in deep learning arose largely from Cohen and Welling [21]. There has been widespread application of machine learning models when group invariance or equivariance is desired, e.g., permutation invariance for sets

[69] and equivariance for neural auction design [52]. In the natural sciences, rotation invariance has been used for astronomy [25] and $E(3)$ equivariance has proved important for molecular applications [8]. Permutation equivariance of transformer architectures plays a crucial role in large language model [64].

In crystallography. Crystallographers have completely described the 17 two-dimensional and 230 three-dimensional crystallographic groups and various tilings they describe, and tabulated many of their properties [31]. The emphasis in this work differs somewhat from that in mathematics—in particular, work in crystallography emphasizes polytopes Π that occur in crystal structures (and which are not necessarily exact in the terminology used in Theorem 15), whereas more abstract work in geometry tends to work with Dirichlet domains or other exact tilings. A long line of work in the context of X-ray crystallography modifies the matrices that occur in fast Fourier transforms (FFTs) to speed up computation if a crystallographic symmetry is present in the data. This starts with the work of Bienenstock and Ewald [13] and Ten Eyck [60], see also An et al. [5]. The introduction of Seguel and Burbano [55] gives an overview. This work does not attempt to derive invariant Fourier bases.

In Fourier and PDE analysis. As we have already explained in some detail, the special case of Theorem 7 for $\Pi = [0, 1]^n$ and $\mathbb{G} = \mathbb{Z}^n$ yields the Fourier transform. For this problem, the periodic boundary condition can be replaced by a Neumann condition, and spectral problems with Neumann conditions are standard material in textbooks [19, 43]. For shifts that are not axis-parallel, the periodic boundary condition is known as a **Born-von Karman boundary condition** [7]. We are not aware of extensions to crystallographic groups. An introduction to the PDE techniques used in our proofs can be found in Brezis [19]. The conditions imposed there are too restrictive for our problems, however; a treatment general enough to cover all results we use is given by McLean [48].

In geometry. Thurston [e.g., 62] coined the term orbifold in the 1970s. Commonly cited references include Bonahon and Siebenmann [16], Scott [54], Thurston [62]; Apanasov [6] has a detailed bibliography. These all focus on general groups, however, for which the theory is much harder than in our case. The quotient space structure of crystallographic groups was already understood much earlier by the Göttingen and Moscow schools [65]. A readable introduction to isometry groups and their quotients is given by Bonahon [15]. The comprehensive account of Ratcliffe [53] is more demanding, but covers all results needed in our proofs. Vinberg and Shvartsman [65] cover the geometric aspects of crystallographic groups. Conway, Burgiel, and Goodman-Strauss [22] explain the geometry of orbifolds heuristically, with many illustrations.

11 Some open problems

Our approach raises a range of further questions well beyond the scope of the present paper, including in particular those concerning numerical and statistical accuracy. We briefly discuss some aspects of this problem.

Linear representation. Suppose we represent a \mathbb{G} -invariant continuous function f by evaluating the generalized Fourier basis in Theorem 7 using the spectral algorithm in Section 5.3. The algorithm returns numerical approximations $\hat{e}_1, \hat{e}_2, \dots$ of the basis functions. We may then expand f as

$$f \approx \sum_{i=1}^m c_i \hat{e}_i.$$

There are three principal sources of error in this representation:

1. The truncation error, since m is finite.
2. Any error incurred in computation of the coefficients c_i .
3. The error incurred by approximating the actual basis functions e_i by \hat{e}_i .

The truncation error (1) concerns the question how well the vector space $\text{span}\{e_1, \dots, e_m\}$ approximates the space $\mathbf{C}_{\mathbb{G}}$ or $\mathbf{L}_2(\Pi)$. This problem is studied in approximation theory. Depending on the context, one may choose the first m basis vectors (a strategy called “linear approximation” in approximation theory), or greedily choose those m basis vectors that minimize some error measure (“nonlinear approximation”), see DeVore [24]. Problem (2) depends on the function f , and on how it is represented computationally. If f must itself be reconstructed from samples, the coefficients are themselves estimators and incur statistical errors.

The error immediately related to our method is (3), and for the method of Section 5 depends on how well the graph Laplacian used in Section 5.3 approximates the Laplacian Δ . This problem has been studied in a number of fields, including machine learning in the context of dimensionality reduction [10] and numerical mathematics in the context of homogenous Helmholtz equations [32], and is the subject of a rich literature [11, 27, 28, 34, 41, 56]. Available results show that, as $\varepsilon \rightarrow 0$ in the ε -net, the matrix L converges to Δ , where the approximation can be measured in different notions of convergence, in particular pointwise and spectral convergence. The cited results all concern the manifold case. We are not aware of similar results for orbifolds.

For the method of Section 9.5, the error depends largely on the choice of basis in \mathbb{R}^N and the accuracy of the numerical integrals, as well as the orbifold map approximation itself (see below). Error analysis of the Rayleigh-Ritz method has a long history, see, e.g., Weinberger [66, 67], Wendroff [68].

Nonlinear representation. If we define a \mathbb{G} -invariant statistical or machine learning model on \mathbb{R}^n by factoring it through an orbifold, one may ask approximation questions of a more statistical flavor: Suppose we define a class $\mathcal{H} = \{h_\theta | \theta \in T\}$ of functions $h_\theta : \mathbb{R}^N \rightarrow \mathbb{R}$ on the embedding space \mathbb{R}^N , with some parameter space T . We then define a class \mathcal{F} of \mathbb{G} -invariant functions on \mathbb{R}^n as

$$\mathcal{F} := \{f_\theta | \theta \in T\} \quad \text{where} \quad f_\theta := h_\theta \circ \rho.$$

Depending on the context, we may think of the functions f_θ e.g., as neural networks or regressors. The task is then to conduct inference, i.e., to compute a point estimate $\hat{\theta}$ of θ (say by maximum likelihood estimation or empirical risk minimization), or to compute a posterior on T in a Bayesian setup. Since \mathcal{H} and \mathcal{F} share the same parameter space, any such inference task can be “pushed forward” forward to the embedding space, that is,

$$\text{inference under } \mathcal{F} \text{ given } x_1, \dots, x_n = \text{inference under } \mathcal{H} \text{ given } \rho(x_1), \dots, \rho(x_n)$$

The error can again be separated into components:

1. The statistical error associated with fitting $\{h_\theta | \theta \in T\}$.
2. The “forward distortion” introduced by the map $x_j \mapsto \rho(x_j)$.
3. The “backward distortion” introduced by the map $h_\theta \mapsto h_\theta \circ \rho$.

Problem (1) reduces to the statistical properties of \mathcal{H} , and depends on both the model and the chosen inference method. Problem (2) and (3), however, raise a number of new questions: The map ρ is, by Theorem 15, bijective (which means it does not introduce identifiability problems) and continuous. As the proof of Proposition 23 shows, it also

preserves density properties of certain function spaces, which can be thought of as a qualitative approximation result. Quantitative results are different matter: To bound the effect of transformations on statistical errors typically requires a stronger property than continuity, such as differentiability or at least a Lipschitz property. In results on manifold learning, the curvature of Ω often plays an explicit role. Orbifolds introduce a further challenge, since smoothness properties fail at the tips and edges introduced by points with non-trivial stabilizers. On the other hand, non-differentiabilities of crystallographic orbifolds have lower-bounded opening angles [62]—note the tip of the cone in Figure 13, for example, is not a cusp—so it may be possible to mitigate these problems.

Acknowledgements

The authors would like to thank Elif Ertekin and Eric Toberer for valuable discussions. RPA is supported in part by NSF grants IIS-2007278 and OAC-2118201. PO is supported by the Gatsby Charitable Foundation.

References

- [1] O. Abdel-Hamid, A.-R. Mohamed, H. Jiang, L. Deng, G. Penn, and D. Yu. Convolutional neural networks for speech recognition. *IEEE/ACM Trans. Audio Speech Lang. Process.*, 22:1533–1545, 2014.
- [2] R. A. Adams and J. J. F. Fournier. *Sobolev Spaces*. Academic Press, 2003.
- [3] C. D. Aliprantis and K. C. Border. *Infinite-Dimensional Analysis*. Springer, 2006.
- [4] C. D. Aliprantis and O. Burkinshaw. *Positive Operators*. Springer, 2006.
- [5] M. An, J. W. Cooley, and R. Tolimieri. Factorization method for crystallographic Fourier transforms. *Adv. Appl. Math*, 11:358–371, 1990.
- [6] B. Apanasov. *Conformal geometry of discrete groups and manifolds*. de Gruyter, 2000.
- [7] N. W. Ashcroft and N. D. Mermin. *Solid State Physics*. Harcourt, 1976.
- [8] S. Batzner, A. Musaelian, L. Sun, M. Geiger, J. P. Mailoa, M. Kornbluth, N. Molinari, T. E. Smidt, and B. Kozinsky. E (3)-equivariant graph neural networks for data-efficient and accurate interatomic potentials. *Nature Communications*, 13(1):2453, 2022.
- [9] H. Becker and A. S. Kechris. *The descriptive set theory of Polish group actions*. Cambridge Univ. Press, 1996.
- [10] M. Belkin and P. Niyogi. Laplacian eigenmaps for dimensionality reduction and data representation. *Neural Comput.*, 15(6):1373–1396, 2003.
- [11] M. Belkin and P. Niyogi. Towards a theoretical foundation for Laplacian-based manifold methods. *J. Comput. System Sci.*, 74(8):1289–1308, 2008.
- [12] D. G. Bell. Group theory and crystal lattices. *Rev. of Modern Phys.*, 26(3):311, 1954.
- [13] A. Bienenstock and P. P. Ewald. Symmetry of Fourier space. *Acta Cryst.*, 15:1253–1261, 1962.
- [14] B. Bloem-Reddy and Y. W. Teh. Probabilistic symmetries and invariant neural networks. *J. Mach. Learn. Res.*, 21(90):1–61, 2020.
- [15] F. Bonahon. *Low-Dimensional Geometry*. Amer. Math. Soc., 2009.
- [16] F. Bonahon and L. Siebenmann. Seifert orbifolds and their role as natural crystalline parts of arbitrary compact irreducible 3-orbifolds. In *London Math. Soc. Lect. Notes*, volume 95, pages 18–85. Cambridge Univ. Press, 1985.
- [17] J. Bradbury, R. Frostig, P. Hawkins, M. J. Johnson, C. Leary, D. al Maclaurin, G. Necula, A. Paszke, J. VanderPlas, S. Wanderman-Milne, and Q. Zhang. JAX: composable transformations of Python+NumPy programs, 2018. URL <http://github.com/google/jax>.
- [18] D. Braess. *Finite Elements*. Springer, 2007.
- [19] H. Brezis. *Functional Analysis, Sobolev Spaces, and Partial Differential Equations*. Springer, 2011.
- [20] F. Chung. *Spectral graph theory*. Amer. Math. Soc., 1997.
- [21] T. Cohen and M. Welling. Group equivariant convolutional networks. In *Int. Conf. Machine Learning*, pages 2990–2999. PMLR, 2016.
- [22] J. H. Conway, H. Burgiel, and C. Goodman-Strauss. *The Symmetries of Things*. CRC Press, 2016.
- [23] D. Cooper, C. D. Hodgson, and S. P. Kerckhoff. *Three-dimensional Orbifolds and Cone-Manifolds*. Math. Soc. Japan, 2000.

- [24] R. A. DeVore. Nonlinear approximation. *Acta Numer.*, pages 51–150, 1998.
- [25] S. Dieleman, K. W. Willett, and J. Dambre. Rotation-invariant convolutional neural networks for galaxy morphology prediction. *Monthly Not. Roy. Astronom. Soc.*, 450(2):1441–1459, 2015.
- [26] M. S. Dresselhaus, G. Dresselhaus, and A. Jorio. *Group theory: application to the physics of condensed matter*. Springer, 2007.
- [27] D. B. Dunson, H.-T. Wu, and N. Wu. Spectral convergence of graph Laplacian and heat kernel reconstruction in l_∞ from random samples. *Appl. Comput. Harmon. Anal.*, 55:282–336, 2021.
- [28] N. García Trillos, M. Gerlach, M. Hein, and D. Slepčev. Error estimates for spectral convergence of the graph Laplacian on random geometric graphs toward the Laplace–Beltrami operator. *Found. Comput. Math.*, 20(4):827–887, 2020.
- [29] G. H. Golub. Some modified matrix eigenvalue problems. *SIAM review*, 15(2):318–334, 1973.
- [30] P. M. Gruber. *Convex and Discrete Geometry*. Springer, 2007.
- [31] T. Hahn. *International tables for crystallography*, volume A. Wiley, 2011.
- [32] I. Harari and E. Turkel. Accurate finite difference methods for time-harmonic wave propagation. *J. Comput. Phys.*, 119(2):252–270, 1995.
- [33] D. Haussler and E. Welzl. ϵ -nets and simplex range queries. *Discrete Comput. Geom.*, 2(2):127–151, 1987.
- [34] M. Hein, J.-Y. Audibert, and U. v. Luxburg. From graphs to manifolds—weak and strong pointwise consistency of graph Laplacians. In *Proc. of COLT*, pages 470–485, 2005.
- [35] K. Hornik, M. Stinchcombe, and H. White. Multilayer feedforward networks are universal approximators. *Neural Networks*, 2(5):359–366, 1989.
- [36] D. Johnston. Group theory in solid state physics. *Rep. Progr. Phys.*, 23(1):66, 1960.
- [37] J. Killingbeck. Group theory and topology in solid state physics. *Rep. Progr. Physics*, 33(2):533, 1970.
- [38] I. R. Kondor. *Group Theoretical Methods in Machine Learning*. PhD thesis, Columbia Univ., 2008.
- [39] A. Krizhevsky, I. Sutskever, and G. E. Hinton. Imagenet classification with deep convolutional neural networks. *Communications of the ACM*, 60(6):84–90, 2017.
- [40] J. B. Kruskal. Multidimensional scaling by optimizing goodness of fit to a nonmetric hypothesis. *Psychometrika*, 29(1):1–27, 1964.
- [41] S. Lafon. *Diffusion maps and geometric harmonics*. PhD thesis, Yale University, 2004.
- [42] M. Lax. *Symmetry principles in solid state and molecular physics*. Courier Corporation, 2001.
- [43] P. D. Lax. *Functional Analysis*. Wiley, 2002.
- [44] Y. LeCun, B. Boser, J. Denker, D. Henderson, R. Howard, W. Hubbard, and L. Jackel. Handwritten digit recognition with a back-propagation network. *Adv. Neural Inf. Process. Systems*, 2, 1989.
- [45] D. J. C. MacKay. Introduction to Gaussian processes. *NATO ASI Series F*, 168:133–166, 1998.
- [46] M. B. Marcus and J. Rosen. *Markov processes, Gaussian processes, and local times*. Cambridge Univ. Press, 2006.
- [47] V. Maz'ya. *Sobolev Spaces*. Springer, 2nd edition, 2011.
- [48] W. McLean. *Strongly Elliptic Systems and Boundary Integral Equations*. Cambridge Univ. Press, 2000.
- [49] J. R. Munkres. *Topology*. Prentice Hall, 2nd edition, 2000.
- [50] A. R. Pears. *Dimension theory of general spaces*. Cambridge University Press, 1975.
- [51] A. Rahimi and B. Recht. Random features for large-scale kernel machines. *Adv. Neural Inf. Process. Systems*, 20, 2007.
- [52] J. Rahme, S. Jelassi, J. Bruna, and S. M. Weinberg. A permutation-equivariant neural network architecture for auction design. In *Proc. AAAI*, volume 35, pages 5664–5672, 2021.
- [53] J. G. Ratcliffe. *Foundations of Hyperbolic Manifolds*. Springer, 2nd edition, 2006.
- [54] P. Scott. The geometries of 3-manifolds. *Bull. London Math. Soc.*, 5:401–487, 83.
- [55] J. Seguel and D. Burbano. A scalable crystallographic FFT. In *Lecture Notes in Comput. Sci.*, volume 2840, pages 134–141. Springer, 2003.
- [56] A. Singer. From graph to manifold Laplacian: The convergence rate. *Appl. Comput. Harmon. Anal.*, 21(1):128–134, 2006.
- [57] J. Slater. Space groups and wave-function symmetry in crystals. *Rev. Modern Phys.*, 37(1):68, 1965.
- [58] A. Speiser. *Die Theorie der Gruppen endlicher Ordnung*. Birkhäuser, 1956.
- [59] I. Steinwart and A. Christmann. *Support Vector Machines*. Springer, 2008.
- [60] L. F. Ten Eyck. Crystallographic fast Fourier transforms. *Acta Cryst. A*, 29:183–191, 1973.
- [61] J. B. Tenenbaum, V. d. Silva, and J. C. Langford. A global geometric framework for nonlinear dimensionality reduction. *Science*, 290(5500):2319–2323, 2000.
- [62] W. P. Thurston. *Three-Dimensional Geometry and Topology, Vol. 1*. Princeton Univ. Press, 1997.

- [63] A. van der Vaart and J. H. van Zanten. Reproducing Hilbert spaces of Gaussian priors. In *Inst. Math. Stat. (IMS) Collect.*, volume 3, pages 200–222. 2008.
- [64] A. Vaswani, N. Shazeer, N. Parmar, J. Uszkoreit, L. Jones, A. N. Gomez, L. Kaiser, and I. Polosukhin. Attention is all you need. *Adv. Neural Inf. Process. Systems*, 30, 2017.
- [65] E. B. Vinberg and O. V. Shvartsman. Discrete groups of motions of spaces of constant curvature. In E. B. Vinberg, editor, *Geometry II. Spaces of Constant Curvature*. Springer, 1993.
- [66] H. Weinberger. Error estimation in the Weinstein method for eigenvalues. *Proc. Amer. Math. Soc.*, 3(4):643–646, 1952.
- [67] H. F. Weinberger. *Variational methods for eigenvalue approximation*. SIAM, 1974.
- [68] B. Wendroff. Bounds for eigenvalues of some differential operators by the Rayleigh-Ritz method. *Math. Comp.*, 19(90):218–224, 1965.
- [69] M. Zaheer, S. Kottur, S. Ravanbakhsh, B. Póczos, R. R. Salakhutdinov, and A. J. Smola. Deep sets. *Adv. Neural Inf. Process. Systems*, 30, 2017.
- [70] G. M. Ziegler. *Lectures on Polytopes*. Springer, 1995.

DEPARTMENT OF COMPUTER SCIENCE
PRINCETON UNIVERSITY
<https://www.cs.princeton.edu/~rpa>

GATSBY COMPUTATIONAL NEUROSCIENCE UNIT
UNIVERSITY COLLEGE LONDON
<https://www.gatsby.ucl.ac.uk/~porbanz>

Appendix

The first three sections of this appendix provide mathematical background on isometries (Appendix A), function spaces and smoothness (Appendix B), orbifolds (Appendix C), and spectral theory (Appendix D). The proof of the Fourier representation is subdivided into three parts: We first prove of the flux property, Proposition 28, in Appendix E, and Theorem 30 on self-adjointness of the Laplacian in Appendix F. Using these results, we then prove the Fourier representation in Appendix G. The proof of the embedding theorem (Theorem 15) follows in Appendix H. Appendix I collects all proofs on kernels and Gaussian processes.

A Background I: Isometries of Euclidean space

Isometries are invertible functions that preserve distance. To define an isometry between two sets V and W , both must be equipped with metrics, say d_V and d_W . A map $\phi : \mathbf{X} \rightarrow \mathbf{Y}$ is then an **isometry** if it is one-to-one and satisfies

$$d_W(\phi(v_1), \phi(v_2)) = d_V(v_1, v_2) \quad \text{for all } v_1, v_2 \in V .$$

Since this implies ϕ is Lipschitz, isometries are always continuous. If $W = V$, then ϕ is necessarily bijective. An isometry of \mathbb{R}^n is a bijection $\phi : \mathbb{R}^n \rightarrow \mathbb{R}^n$ that satisfies

$$d_n(\phi x, \phi y) = d_n(x, y) \quad \text{for all } x, y \in \mathbb{R}^n .$$

Identity (3) shows that every isometry can be uniquely represented as an orthogonal transformation followed by a shift. Loosely speaking, an isometry may shift, rotate, or flip M , but cannot change its shape or volume. Recall that a set \mathbb{G} of functions $\mathbb{R}^n \rightarrow \mathbb{R}^n$ is a **group** if it contains the identity map $\mathbf{1}$, and if $\phi, \psi \in \mathbb{G}$ implies $\phi \circ \psi \in \mathbb{G}$ and $\phi^{-1} \in \mathbb{G}$. The set of all isometries of \mathbb{R}^n forms a group, called the **Euclidean group** of order n .

A.1. More on crystallographic groups

Representation by shifts and orthogonal transformations. Since every isometry can be decomposed into an orthogonal transformation and a shift according to (3), every crystallographic group \mathbb{G} has two natural subgroups: One is the group

$$\mathbb{G}_o := \{ \phi \in \mathbb{G} \mid \phi(x) = Ax \text{ for some } A \in \mathbb{O}_n \} = \mathbb{G} \cap \mathbb{O}_n$$

of purely orthogonal transformations. This is an example of a **point group**, since all its elements have a common fixed point (namely the origin). It is always finite: Fix any x on the unit sphere in \mathbb{R}^n . Then $\phi(x)$ is also on the sphere for every $\phi \in \mathbb{G}_o$, since A_ϕ is orthogonal. However, discreteness requires there can only be finitely many such points $\phi(x)$ on the sphere. The other is the group of pure shifts,

$$\mathbb{G}_t := \{ \phi \in \mathbb{G} \mid \phi(x) = x + b \text{ for some } b \in \mathbb{R}^n \} .$$

One can show there are linearly independent vectors b_1, \dots, b_n such that

$$\mathbb{G}_t := \{ x \mapsto x + b \mid b = a_1 b_1 + \dots + a_n b_n \text{ for } a_1, \dots, a_n \in \mathbb{Z} \} .$$

Thus, the generating set for a crystallographic group on \mathbb{R}^n always includes n linearly independent shifts.

A.2. Equivalence to definitions in the literature

Our definition of a crystallographic group in Section 2 differs from those in the literature—we have chosen it for simplicity, but must verify it is equivalent. There are two standard definitions of crystallographic groups: Perhaps the most common one, used for example by Thurston [62], is as a discrete group of isometries for which \mathbb{R}^n/\mathbb{G} is compact in the quotient topology. Another is as a group of isometries of \mathbb{R}^n such that \mathbb{R}^n/\mathbb{G} has finite volume when identified with a subset of Euclidean space [65]. These are known to be equivalent [65, Corollary of Theorem 1.11]. Our definition is equivalent to both:

Lemma 32. *A group \mathbb{G} is crystallographic in the sense of Section 2 if and only if it is a discrete group of isometries of \mathbb{R}^n such that \mathbb{R}^n/\mathbb{G} is compact.*

Proof. If \mathbb{G} is crystallographic in our sense, it is discrete (see Section 2), and \mathbb{R}^n/\mathbb{G} is compact by Fact 4, so it satisfies the second definition above. Conversely, if \mathbb{G} satisfies Thurston’s definition, it tiles \mathbb{R}^n with some set Π . This set can always be chosen as a convex polytope [65, Theorem 2.5], so \mathbb{G} is crystallographic in our sense. \square

We note only en passe that there are tilings that cannot be described by a group of isometries. That is not at all obvious—the question was one of Hilbert’s problems—but counter-examples of such tilings (with non-convex polytopes) are now known [see 30, Chapter 32].

B Background II: Function spaces

This section briefly reviews concepts from functional analysis that play a role in the proofs. Helpful references include Aliprantis and Border [3], Brezis [19] on general functional analysis and Banach spaces, Adams and Fournier [2], Brezis [19] on Sobolev spaces, Steinwart and Christmann [59] on reproducing kernel Hilbert spaces, and Aliprantis and Burkinshaw [4] on compact operators.

B.1. Spans and their closures

Consider a Banach space V and a subset $\mathcal{F} \subset V$. The **span** of \mathcal{F} is the set

$$\text{span}(\mathcal{F}) = \left\{ \sum_{i \leq n} c_i f_i \mid n \in \mathbb{N}, c_i \in \mathbb{R}, f_i \in \mathcal{F} \right\}$$

of finite linear combinations of elements of \mathcal{F} . Since function spaces are typically infinite-dimensional, we also consider infinite linear combinations. These are defined with respect to a norm $\|\cdot\|$:

$$f = \sum_{i \in \mathbb{N}} c_i f_i \quad \text{means} \quad \|f - \sum_{i \leq n} c_i f_i\| \rightarrow 0 \text{ as } n \rightarrow \infty.$$

In other words, to get from the span to the set of infinite linear combinations, we take the closure in the relevant norm:

$$\left\{ \sum_{i \in \mathbb{N}} c_i f_i \mid c_i \in \mathbb{R}, f_i \in \mathcal{F} \right\} = \overline{\text{span}(\mathcal{F})}$$

B.2. Bases

A Hilbert space \mathbb{H} is a Banach space whose norm is induced by an inner product $\langle \cdot, \cdot \rangle_{\mathbb{H}}$, that is,

$$\|f\|_{\mathbb{H}} = \sqrt{\langle f, f \rangle_{\mathbb{H}}}.$$

A sequence f_1, f_2, \dots in a Hilbert space is an **orthonormal system** if $\langle f_i, f_j \rangle = \delta_{ij}$, where δ is the Kronecker symbol (the indicator function of $\{i = j\}$). An orthonormal system is **complete** if its span is dense in \mathbb{H} , that is, if

$$\mathbb{H} = \overline{\text{span}\{f_1, f_2, \dots\}},$$

where the closure is taken in the norm of \mathbb{H} . A complete orthonormal system is also called an **orthonormal basis**. If f_1, f_2, \dots is an orthonormal basis, \mathbb{H} can be represented as

$$\mathbb{H} = \left\{ \sum_{i \in \mathbb{N}} c_i f_i \text{ (convergence in } \|\cdot\|_{\mathbb{H}}) \mid c_1, c_2, \dots \in \mathbb{R} \text{ with } \sum_i c_i^2 < \infty \right\}.$$

B.3. \mathbf{L}_2 spaces

For any M and a σ -finite measure ν on M , the \mathbf{L}_2 -scalar product and pseudonorm are

$$\langle f, g \rangle_{\mathbf{L}_2(\nu)} := \int_M f(x)g(x)\nu(dx) \quad \text{and} \quad \|f\|_{\mathbf{L}_2(\nu)} := \sqrt{\langle f, f \rangle_{\mathbf{L}_2(\nu)}}.$$

To make $\|\cdot\|_{\mathbf{L}_2}$ a norm, one defines the equivalence classes $[f] := \{g \mid \|f - g\|_{\mathbf{L}_2} = 0\}$ of functions identical outside a null set, and the vector space

$$\mathbf{L}_2(\nu) := \{[f] \mid f : M \rightarrow \mathbb{R} \text{ and } \|f\|_{\mathbf{L}_2} < \infty\}$$

of such equivalence classes, which is a separable Hilbert space. Although its elements are not technically functions, we use the notation $f \in \mathbf{L}_2$ rather than $[f] \in \mathbf{L}_2$. We write $\mathbf{L}_2(\mathbb{R}^n)$ and $\mathbf{L}_2(\Pi)$ respectively if ν is Euclidean volume on \mathbb{R}^n or on Π . See Aliprantis and Border [3] or Brezis [19] for background on \mathbf{L}_2 spaces.

B.4. Reproducing kernel Hilbert spaces

Consider a set $M \subseteq \mathbb{R}^n$. A symmetric positive definite function $\kappa : M \times M \rightarrow \mathbb{R}$ is called a **kernel**. A kernel defines a Hilbert space as follows: The formula

$$\langle \sum_i a_i \kappa(x_i, \cdot), \sum_j b_j \kappa(y_j, \cdot) \rangle_{\mathbb{H}} := \sum_{i,j} a_i b_j \kappa(x_i, y_j) \quad \text{for } a_i, b_j \in \mathbb{R} \text{ and } x_i, y_j \in M$$

defines a scalar product on $\text{span}\{\kappa(x, \cdot) \mid x \in M\}$. The closure

$$\mathbb{H} := \overline{\text{span}\{\kappa(x, \cdot) \mid x \in M\}} \quad \text{with respect to the norm} \quad \|f\|_{\kappa} := \sqrt{\langle f, f \rangle_{\mathbb{H}}}$$

is a real, separable Hilbert space with inner product $\langle \cdot, \cdot \rangle_{\mathbb{H}}$, called the reproducing kernel Hilbert space or **RKHS** of k . Every RKHS satisfies the ‘‘reproducing property’’

$$(28) \quad f(x) = \langle f, \kappa(x, \cdot) \rangle_{\mathbb{H}} \quad \text{for all } f \in \mathbb{H} \text{ and all } x \in M.$$

In particular, $\kappa(x, y) = \langle \kappa(x, \cdot), \kappa(y, \cdot) \rangle_{\mathbb{H}}$. If f_1, f_2, \dots is an orthonormal basis of \mathbb{H} , then

$$(29) \quad \kappa(x, y) = \sum_{i \in \mathbb{N}} f_i(x) f_i(y) \quad \text{for all } x, y \in M.$$

If \mathbb{H} is an RKHS, the map $f \mapsto f(x)$ is continuous for each $x \in M$. Conversely, if \mathbb{H} is any Hilbert space of real-valued functions on M , and if the maps are continuous on \mathbb{H} for all $x \in M$, there is a unique kernel satisfying (28) that generates \mathbb{H} as its RKHS.

B.5. Spaces of continuous functions

For any set M , the vector space $\mathbf{C}(M)$ of continuous functions equipped with the norm $\|\cdot\|_{\text{sup}}$ is a Banach space. It is separable if M is compact [3]. In the proof of the spectral theorem, we must also consider the set

$$\mathbf{C}_u(M) := \{f \in \mathbf{C}(M) \mid f \text{ uniformly continuous}\},$$

and the compactly supported functions

$$\mathbf{C}_c(M) = \{f \in \mathbf{C}(M) \mid f = 0 \text{ outside a compact set } K \subset M\}.$$

We recall some basic facts from analysis that are used in the proofs:

Fact 33 (Aliprantis and Border [3]). *(i) Every continuous function on a compact set is uniformly continuous. (ii) Every uniformly continuous function f on a set $M \subseteq \mathbb{R}^n$ has a unique continuous extension \bar{f} to the closure \bar{M} . Its value at a boundary point $x \in \partial M$ is given by $\bar{f}(x) = \lim_j f(x_j)$ for any sequence of points $x_j \in M$ with $x_j \rightarrow x$.*

B.6. Smoothness spaces

Smoothness spaces quantify the smoothness of functions in terms of a norm. Two types of such spaces play a role in our results, namely \mathbf{C}^k spaces and Sobolev spaces. Both define smoothness via derivatives: We denote partial derivatives as

$$\partial^\alpha f := \frac{\partial^{|\alpha|} f}{\partial x_1^{\alpha_1} \dots \partial x_n^{\alpha_n}} \quad \text{where } \alpha = (\alpha_1, \dots, \alpha_n) \in \mathbb{N}^n \text{ and } |\alpha| := \alpha_1 + \dots + \alpha_n.$$

If we are taking a derivative with respect to the i th coordinate, we use a subscript,

$$\partial_i f := \frac{\partial f}{\partial x_i}$$

The set \mathbf{C}^k of k times continuously differentiable functions can then be represented as

$$\mathbf{C}^k(M) := \{f \in \mathbf{C}(M) \mid \partial^\alpha f \in \mathbf{C}(M) \text{ whenever } |\alpha| \leq k\} \quad \text{where } k \in \mathbb{N} \cup \{0, \infty\}.$$

Since that means the norm of \mathbf{C} is applicable to $\partial^\alpha f$, we can define

$$\|f\|_{\mathbf{C}^k} := \|f\|_{\text{sup}} + \sum_{|\alpha| \leq k} \|\partial^\alpha f\|_{\text{sup}}.$$

It can be shown that this is again a norm, and that it makes \mathbf{C}^k a Banach space [19]. \mathbf{C}^k functions are uniformly continuous, and even very smooth functions approximate elements of \mathbf{L}_2 to arbitrary precision:

Fact 34. *Let $M \subseteq \mathbb{R}^n$ be a set. (i) If $f \in \mathbf{C}^k(M)$ for $k \geq 1$, then f and its first $k - 1$ derivatives are uniformly continuous. (ii) The set $\mathbf{C}_c(M) \cap \mathbf{C}^\infty(M)$ is dense in $\mathbf{L}_2(M)$.*

The \mathbf{C}^k norms measure smoothness in a worst-case sense. To measure average smoothness instead, we can replace the sup norm by the $\mathbf{L}_2(M)$ -norm: The function

$$\|f\|_{\mathbf{H}^k} := \|f\|_{\mathbf{L}_2} + \sum_{|\alpha| \leq k} \|\partial^\alpha f\|_{\mathbf{L}_2},$$

is a norm, called the **Sobolev norm** of order k . It makes the set

$$\mathbf{H}^k(M) := \{f \in \mathbf{L}_2(M) \mid \|f\|_{\mathbf{H}^k} < \infty\} = \{f \in \mathbf{L}_2(M) \mid \partial^\alpha f \in \mathbf{L}_2(M)\}$$

a Banach space, and even a Hilbert space, called the **Sobolev space** of order k . We will only work with the spaces $\mathbf{H}^1(M)$. A inner product on $\mathbf{H}^1(M)$ is given by

$$\langle f, g \rangle_{\mathbf{H}^1} := \langle f, g \rangle_{\mathbf{L}_2} + \sum_{i \leq n} \langle \partial_i f, \partial_i g \rangle_{\mathbf{L}_2} .$$

The Sobolev norms are stronger than the \mathbf{L}_2 norm: We have

$$\|f\|_{\mathbf{L}_2(M)} \leq c_M \|f\|_{\mathbf{H}^1(M)} \quad \text{for all } f \in \mathbf{L}_2(M) \text{ and some } c_M > 0 .$$

Consequently, the approximation property in Fact 34(ii) does not necessarily hold in the Sobolev norm. Whether it does depends on whether the geometry of the domain M is sufficiently regular:

Fact 35. *Let Γ be a Lipschitz domain (such as a convex polytope). Then $\mathbf{C}_c(\Gamma) \cap \mathbf{C}^\infty(\Gamma)$ is dense in $\mathbf{H}^1(\Gamma^\circ)$.*

A readable introduction to Sobolev spaces is given by Brezis [19]. The monographs of Adams and Fournier [2] and Maz'ya [47] are comprehensive accounts.

B.7. Inclusion maps

If $V \subset W$ are two sets, the **inclusion map** or **injection map** $\iota : V \hookrightarrow W$ is the restriction of the identity on W to V . Loosely speaking, ι maps each point v in V to itself, but v is regarded as an element of V and its image $\iota(v)$ as an element of W . This distinction is not consequential if V and W are simply sets without further structure, but if both are equipped with topologies, the properties of ι encode relationships between these topologies.

Continuous inclusions. Suppose both V and W are equipped with topologies. Call these the V - and W -topology. The restriction of the W -topology to V , often called the relative W -topology, consists of all sets of the form $A \cap V$, where $A \subset W$ is open in W . Since $A \cap V$ is precisely the preimage $\iota^{-1}A$, and continuity means that preimages of open sets are open, we have

$$\iota \text{ continuous} \iff \text{the } V\text{-topology is at least as fine as the restricted } W\text{-topology.}$$

Inclusions between Banach spaces. Let $T : V \rightarrow W$ be a map from a Banach space V to another Banach space W . If such a map is linear, it is called a **linear operator**. It is continuous if and only if it is **bounded**,

$$(30) \quad \sup_{v \in V} \frac{\|T(v)\|_W}{\|v\|_V} < \infty \quad \text{or equivalently} \quad \|T(v)\|_W \leq c\|v\|_V \text{ for some } c > 0 .$$

If V is a vector subspace of W , then ι is automatically linear, so it is continuous iff

$$\|v\|_W = \|\iota(v)\|_W \leq c\|v\|_V .$$

Saying that ι is continuous is hence another way of saying that $\|\cdot\|_V$ is stronger than $\|\cdot\|_W$. If V and W are smoothness spaces, continuity of ι can hence often be interpreted as the elements V being smoother than those of W . A set $A \subset V$ is **norm-bounded** if

$$\sup_{v, v' \in A} \|v - v'\|_V < \infty .$$

A linear operator between Banach spaces is **compact** if the image $T(A)$ of every norm-bounded set $A \subset V$ has compact closure in W [4]. The inclusion is hence compact iff

$$A \subset V \text{ is bounded in } \|\cdot\|_V \implies \text{the } \|\cdot\|_W\text{-closure of } A \text{ in } W \text{ is compact.}$$

If V and W are smoothness spaces, the inclusion is often compact if V is in some suitable sense smoother than W . The well-known Arzela-Ascoli theorem [3], for example, can be interpreted in this way. For Sobolev spaces, a family of results known as Rellich-Kondrachov theorems [2] shows that, under suitable conditions on the domain, inclusions of the form $\mathbf{H}^{k+m} \hookrightarrow \mathbf{H}^k$ and $\mathbf{H}^{k+m} \hookrightarrow \mathbf{C}^k$ exist and are compact if the difference m in smoothness is large enough. The following version is adapted to our purposes:

Lemma 36. *Let Π be a polytope and $M \subseteq \Pi^\circ$ an open set. Then $\mathbf{H}^{k+1}(M) \subset \mathbf{C}^k(M)$ for $k \geq 0$, and the inclusion map is compact.*

Proof. Since Π is a polytope, it has the strong local Lipschitz property in the terminology of Adams and Fournier [2, 4.9]. By the relevant version of the Rellich-Kondrachov theorem, that implies that the set of restrictions of functions in $\mathbf{H}^{k+1}(\Pi^\circ)$ from Π° to M is a compactly embedded subset of $\mathbf{C}^k(M)$ [2, 6.3 III]. The image of $\mathbf{H}^{k+1}(\Pi^\circ)$ under the projection $f \mapsto f|_M$ is precisely $\mathbf{H}^{k+1}(M)$ [48, Chapter 3]. \square

C Background III: Orbifolds

In this section, we give a rigorous definition of orbifolds and review those results from the literature required for our proofs. For more background, see [15, 16, 23, 54, 62, 65]. Bonahon [15] provides an accessible introduction to gluing and quotient spaces. Most results below are adapted from the monograph of Ratcliffe [53]. Ratcliffe’s formalism is very general and can be simplified significantly for our purposes. We state results here in just enough generality to apply to crystallographic groups.

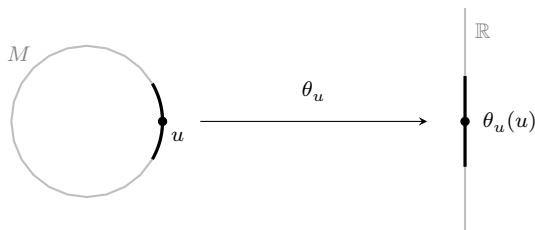
C.1. Motivation: Manifolds

To motivate the somewhat abstract definition of an orbifold, we start with that of a manifold, and then generalize to orbifolds below. Recall that a set M is a manifold if its topology “locally looks like \mathbb{R}^n ”. This idea can be formalized in a number of ways. We first give a definition using a metric, which is of the form often encountered in machine learning and statistics. We then generalize the metric definition to a more abstract one that brings us almost to orbifolds as we see in the following section.

Metric definition. Let M be a set equipped with a metric d_M . We then call M a manifold if, for every $u \in M$, we can choose a sufficiently small $\varepsilon(u) > 0$ such that the d_M -ball around u of radius ε is isometric to a d_n -ball of the same radius in \mathbb{R}^n . There is, in other words, an isometry

$$\theta_u : B_{\varepsilon(u)}(u, d_M) \rightarrow B_{\varepsilon(u)}(\theta_u(u), d_n) \subset \mathbb{R}^n \quad \text{for each } u \in M.$$

For example, the circle, equipped with the geodesic distance, is a manifold in the sense of this definition: It is not possible to map the entire circle isometrically to a subset of \mathbb{R} . However, the ball $B_{\varepsilon(u)}(u, d_M)$ around a point u is a semiarc, drawn in black below:



This semiarc can be mapped isometrically to an open interval in \mathbb{R} , and the same is true for the ball around any other point.

Coherence property. Before we generalize this definition, we observe that it implies a coherence property of the maps θ_u . Suppose the balls around two points v and w in M overlap, and u is in both balls. We can then find a sufficiently small $\varepsilon > 0$ such that $B_\varepsilon(u, d_M)$ is completely contained in both balls. Since both maps θ_v and θ_w are applicable to the points in this ball, the restrictions

$$\theta_v : B_\varepsilon(u, d_M) \rightarrow B_\varepsilon(\theta_v(u), d_n) \quad \text{and} \quad \theta_w : B_\varepsilon(u, d_M) \rightarrow B_\varepsilon(\theta_w(u), d_n)$$

are both isometries. The points $x = \theta_v(u)$ and $y = \theta_w(u)$ are images under different maps, and the balls around them are not required to overlap. Both are, however, Euclidean balls of the same radius. If $\psi = y - x$ is the (unique) shift of \mathbb{R}^n that maps x to y , we hence have

$$B_\varepsilon(\theta_v(u), d_n) = \psi B_\varepsilon(\theta_w(u), d_n).$$

Now observe that $\psi x = y = \theta_w \theta_v^{-1}(x)$. There is, in summary, a shift ψ such that

$$\psi x = y \quad \text{and} \quad \theta_w \theta_v^{-1}(z) = \psi z \quad \text{for all } z \text{ in the ball } B_\varepsilon(x, d_n).$$

The definition hence implies that the map $\theta_w \theta_v^{-1}$, often called a **coordinate change** in geometry, behaves like a shift on a sufficiently small neighborhood. When we drop the metric from the definition below, this property no longer arises automatically, and we must make it an explicit requirement.

Abstract definition. Let \mathbb{F} be a group of isometries of \mathbb{R}^n . The next definition generalizes the one above in two ways: It does not use a metric, and instead of requiring that coordinate changes look locally like shifts, it requires they look locally like elements of \mathbb{F} . A Hausdorff space M is a **\mathbb{F} -manifold** if:

1. There is a family $\{U_i\}_{i \in \mathcal{I}}$ of open connected subsets of M that cover M , i.e., each point of M is in at least one set U_i . The set \mathcal{I} is an arbitrary index set.
2. For each $i \in \mathcal{I}$, there is a homeomorphism $\theta_i : U_i \rightarrow V_i$ of U_i and an open set $V_i \subset \mathbb{R}^n$.
3. If two sets U_i and U_j overlap, the maps θ_i and θ_j cohere as follows: If x and y are points in \mathbb{R}^n that satisfy

$$\theta_j \theta_i^{-1}(x) = y,$$

then there is a transformation $\phi \in \mathbb{F}$ such that

$$\psi x = y \quad \text{and} \quad \theta_j^{-1} \theta_i(z) = \psi z \quad \text{for all } z \text{ in a neighborhood of } x.$$

We recover the metric definition if we make M a metric space (which is always Hausdorff), set $\mathcal{I} = M$, choose U_i as the ball around $i = u$ (which is always connected), and θ_i as the isometry θ_u (isometries are homeomorphisms).

C.2. Orbifolds

To capture the properties of the quotient \mathbb{R}^n/\mathbb{G} , the definition of a manifold is in general too restrictive. That follows from the following result:

Fact 37 (Bonahon [15] Theorem 7.8). *Let \mathbb{G} be a crystallographic group that tiles \mathbb{R}^n with a convex polytope. For every point $x \in \mathbb{R}^n$, there exists an $\varepsilon > 0$ such that the open metric ball $B_{d_{\mathbb{G}}}(\mathbb{G}(x), \varepsilon)$ in the quotient space \mathbb{R}^n/\mathbb{G} and the quotient $B_{d_n}(x, \varepsilon)/\text{Stab}(x)$ of the corresponding open ball in \mathbb{R}^n are isometric.*

We note this is precisely the metric definition of a manifold above if $\text{Stab}(x) = \{\mathbf{1}\}$ for all points in \mathbb{R}^n/\mathbb{G} . It follows that, for a crystallographic group \mathbb{G} ,

$$\mathbb{R}^n/\mathbb{G} \text{ is a manifold} \iff \text{no element of } \mathbb{G} \text{ has a fixed point.}$$

Let \mathbb{F} be a group of isometries of \mathbb{R}^n . An \mathbb{F} -**orbifold** is a Hausdorff space M with the following properties:

1. There is a family $\{U_i\}_{i \in \mathcal{I}}$ of open connected subsets of M that cover M , i.e., each point of M is in at least one set U_i .
2. For each $i \in \mathcal{I}$, there is a discrete group F_i of isometries of \mathbb{R}^n and a homeomorphism $\theta_i : U_i \rightarrow \mathbb{R}^n/F_i$ of U_i and an open subset of the quotient space \mathbb{R}^n/F_i .
3. If two sets U_i and U_j overlap, the maps θ_i and θ_j cohere as follows: If x and y are points in \mathbb{R}^n , and the corresponding points $F_i x \in \mathbb{R}^n/F_i$ and $F_j y \in \mathbb{R}^n/F_j$ satisfy

$$\theta_j \theta_i^{-1}(F_i x) = F_j y,$$

then there is a transformation $\phi \in \mathbb{F}$ such that

$$\psi x = y \quad \text{and} \quad \theta_j^{-1} \theta_i(F_i z) = F_j(\psi z) \quad \text{for all } z \text{ in a neighborhood of } x.$$

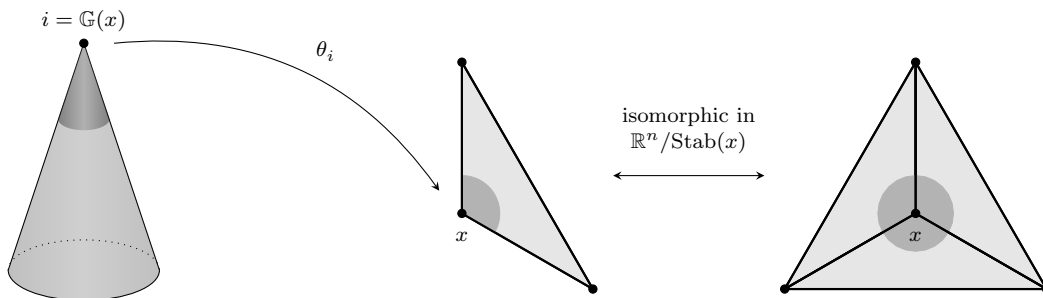
The family $\{\theta_i\}_{i \in \mathcal{I}}$ is called an **atlas**. Clearly, an \mathbb{F} -orbifold is an \mathbb{F} -**manifold** if and only if each F_i is the trivial group $F_i = \{\mathbf{1}\}$.

Lemma 38. *If \mathbb{G} is a crystallographic group that tiles \mathbb{R}^n with a convex polytope Π , then \mathbb{R}^n/\mathbb{G} is a \mathbb{G} -orbifold. At each point $i = \mathbb{G}(x)$, the group F_i is the stabilizer $\text{Stab}(x)$.*

This lemma is folklore in geometry—see e.g., Bonahon [15], Cooper et al. [23], Vinberg and Shvartsman [65] for results that are phrased differently but amount to the same. We give a proof here only to match our specific choices of definitions to each other.

Proof. Let $\tilde{\Pi}$ be a transversal. We choose $\mathcal{I} = \mathbb{R}^n/\mathbb{G}$, so each $i \in \mathcal{I}$ is the orbit $\mathbb{G}(x)$ of some point in \mathbb{R}^n , and hence of a unique point $x \in \tilde{\Pi}$. By Fact 37, there is hence a map θ_x with $\theta_x(\mathbb{G}(x)) = x$ that isometrically maps a ball $B_{d_{\mathbb{G}}}(\mathbb{G}(x), \varepsilon)$ with suitable radius to $B_{d_n}(x, \varepsilon)/\text{Stab}(x)$. We hence set $F_i = \text{Stab}(x)$, which is a finite subgroup of the discrete group \mathbb{G} , and hence discrete. What remains to be shown is the coherence property. Suppose x and y are points in \mathbb{R}^n with trivial stabilizers. If $\theta_y \theta_x^{-1}(x) = y$, then x and y are on the same orbit, so there is indeed a map $\psi \in \mathbb{G}$ with $\psi x = y$. The coherence property then follows by the same argument as for metric manifolds above. If the stabilizers are non-trivial, the same holds if points are substituted by their orbits under stabilizers. \square

Example 39. Consider again the triangle Π and rotation ϕ in Figure 13. Here, the stabilizer of the center of rotation x is $\text{Stab}(x) = \{\mathbf{1}, \phi, \phi^2\}$. The metric ball around the point $i = \mathbb{G}(x)$ on the orbifold (the tip of the cone) is a smaller cone:



Its image under θ_i can be identified with the intersection of Π with a Euclidean ball around x . Since Π and its image $\text{Stab}(x)\Pi$ under the stabilizer—the equilateral triangle on the right—are indistinguishable in $\mathbb{R}^n/\text{Stab}(x)$, that corresponds to the quotient of a metric ball in the plane.

C.3. Path metrics

An orbifold as defined above is a topological space. To work with the gluing results stated below, we must know it is also a metric space, and that this space is complete. Fact 40 shows that that is true. Before we state the fact, we briefly describe how to construct the relevant metric, which is the standard metric on orbifolds. Our definition is again adapted from that of Ratcliffe [53]. Bonahon [15] offers an accessible introduction to this type of metric.

Intuitively, the metric generalizes the geodesic on a smooth surface, by measuring the length of the shortest curve between two points. Formally, a **curve** connecting two points ω_1 and ω_2 in M is a continuous function

$$\gamma : [a, b] \subset \mathbb{R} \rightarrow X \quad \text{such that} \quad \gamma(a) = \omega_1 \text{ and } \gamma(b) = \omega_2 .$$

To define the **length** $\|\gamma\|$ of γ , first suppose ω_1 and ω_2 are in the same set U_i , and define

$$\|\gamma\| := \sup \{ \sum_{j \leq k} d_{F_i}(\theta_i \circ \gamma(t_{j-1}), \theta_i \circ \gamma(t_j)) \mid a = t_0 < t_1 < \dots < t_k = b \text{ for } k \in \mathbb{N} \} ,$$

that is, the supremum is taken over the sequences (t_0, \dots, t_k) . In words: For each $t_j \in [a, b]$, the point $\gamma(t_j)$ lies on the curve γ in M . By choosing a sequence t_0, \dots, t_k as above, we approximate the curve by k line segments $(\gamma(t_{j-1}), \gamma(t_j))$, and then approximate the length of γ by summing the lengths of these segments. Since each line segment lies in M , and we have no tool to measure distance in M , we map each point $\gamma(t_j)$ on the curve to a point $\theta_i(\gamma(t_j))$ in \mathbb{R}^n/F_i , where we know how to measure distance using d_{F_i} . We then record the length of the piece-wise approximation as the sum of lengths of the segments. The length $\|\gamma\|$ is the supremum over the lengths of all such approximations.

If there is no set U_i containing both points, one can always subdivide $[a, b]$ into finitely many segments $[t_{j-1}, t_j]$ such that every pair $\gamma(t_{j-1})$ and $\gamma(t_j)$ of consecutive points is in some set U_i (see [53]). One then defines

$$\|\gamma\| := \sum_{i \leq k} \|\gamma|_{[t_{i-1}, t_i]}\| ,$$

and it can be shown that $\|\gamma\|$ does not depend on the choice of subdivision.

Fact 40 (Ratcliffe [53] Lemma 1 of §13.2, Theorems 13.2.7 and 13.3.8). *If M is an \mathbb{F} -orbifold, any two points in M can be connected by a curve of finite length. The function*

$$d_{\text{path}}(\omega_1, \omega_2) := \inf \{ \|\gamma\| \mid \gamma \text{ is a curve connecting } \omega_1 \text{ and } \omega_2 \text{ in } M \}$$

is a metric on the set M , and metrizes the Hausdorff topology of M . The metric space so defined is complete.

C.4. Orbifolds constructed by abstract gluing

Let S_1, \dots, S_k be the facets of Π . A **side pairing** is a finite set $\mathcal{S} = \{\psi_1, \dots, \psi_k\}$ of isometries of \mathbb{R}^n if, for each $i \leq k$, there is a $j \leq k$ such that

$$(i) \ \psi_i(S_j) = S_i \quad (ii) \ \psi_i = \psi_j^{-1} \quad (iii) \ \Pi \cap \psi_i \Pi = S_i .$$

The definition permits $i = j$. A crystallographic group is determined by a side pairing:

Fact 41 (Bonahon [15] Theorem 7.11). *If a crystallographic group \mathbb{G} tiles with a convex polytope Π , the tiling is exact, and \mathcal{S} is a side pairing for Π and \mathbb{G} , the group generated by \mathcal{S} is \mathbb{G} .*

The side pairing defines an equivalence relation \equiv on points $x, y \in \Pi$, namely

$$x \equiv y \quad :\iff \quad \psi_i x = y \quad \text{for some } i \leq k .$$

Let M be the quotient space $M := \Pi / \equiv$, equipped with the quotient topology, that is,

$$A \subset M \text{ open} \quad :\iff \quad \{x \in \Pi \mid \text{equivalence class of } x \text{ is in } A\} \text{ is open set in } \Pi$$

We then refer to M as the quotient **obtained by abstract gluing** from Π and \mathcal{S} . We will be interested in a specific type of side pairing, called a **subproper** side pairing. The precise definition is somewhat involved, and can be found in §13.4 of Ratcliffe [53]. We omit it here, since we will see that all side pairings relevant to our purposes are subproper.

Fact 42 (Ratcliffe [53] Theorem 13.4.2). *Let \mathbb{F} be a group of isometries of \mathbb{R}^n and Π a convex polytope. Let M be the metric space obtained by abstract gluing from Π and a subproper \mathbb{F} -side pairing. Then M is an \mathbb{F} -orbifold. The natural inclusion $\Pi^\circ \hookrightarrow M$, i.e., the map that takes each point $x \in \Pi^\circ$ to its \equiv -equivalence class, is continuous.*

For the next result, recall the definition of $d_{\mathbb{G}}$ from Fact 3. We define a metric $d_{\mathbb{S}}$ for a group \mathbb{S} analogously, by substituting \mathbb{S} for \mathbb{G} .

Fact 43 (Ratcliffe [53] Theorem 13.5.3). *Let M be the orbifold in Fact 42, and \mathbb{S} be the group generated by all maps in the side pairing. If M is a complete metric space, the natural inclusion map $\Pi \hookrightarrow M$ induces an isometry from M to $(\mathbb{R}^n / \mathbb{S}, d_{\mathbb{S}})$.*

The final result on orbifolds we need gives a precise statement of the idea that the set of points around which an orbifold does not resemble a manifold is small. The next definition characterizes those points around which the manifold property breaks down as having order > 1 : Consider a point $z \in M$. Then we can find some $x \in \mathbb{R}^n$ that corresponds to z : We know that $z \in U_i$ for some i , and hence $\phi_i z = F_i x$ in the quotient space \mathbb{R}^n / F_i . The **order** of $z \in M$ is the number of elements of F_i that leave x invariant (formally, the order of the stabilizer of x in F_i). It can be shown that this number does not depend on the choice of i , so each $z \in M$ has a uniquely defined order.

Fact 44 (Ratcliffe [53] Theorem 13.2.4). *If M is an \mathbb{F} -orbifold, the set of points of order 1 in M is an open dense subset of M . The set of points of order > 1 is nowhere dense.*

C.5. Topological dimension

The notion of dimension we have used throughout is the algebraic dimension $\dim A$ of a set A in a vector space (see Section 2). For the proof of the embedding theorem, we also need another notion of dimension that does not require vector space structure, known variously as topological dimension, covering dimension, or Lebesgue dimension. The definition is slightly more involved: Consider a topological space X . An **open cover** of X is a collection \mathcal{A} of open sets in X that cover X , that is, each point of X is in at least one of the sets. The **order** of an open cover is

$$\text{order}(\mathcal{A}) := \sup \{ \text{number of elements of } \mathcal{A} \text{ containing } x \mid x \in X \} .$$

The **topological dimension** $\text{Dim } X$ of X is the smallest value $m \in \mathbb{N} \cup \{\infty\}$ such that, for every open covering \mathcal{B} of X , there is an open covering \mathcal{A} with $\text{order}(\mathcal{A}) = m + 1$ such that every set of \mathcal{B} contains a set of \mathcal{A} .

Fact 45 ([50, 3.2.7]). *The topological dimension of Euclidean space equals its algebraic dimension, $\text{Dim } \mathbb{R}^n = \dim \mathbb{R}^n = n$, and any closed metric balls $B \subset \mathbb{R}^n$ has $\text{Dim } B = n$.*

In general, however, the topological dimension of a set $A \subset \mathbb{R}^n$ may differ from its dimension $\dim A$ as defined in Section 2 (as the algebraic dimension of the linear hull), and even the proof that $\text{Dim } \mathbb{R}^n = n$ is not entirely trivial. Munkres [49] provides a readable overview. The reason why topological dimension is of interest in our context is the following classical result. Recall that, given topological spaces X and Y , an **embedding** of X into Y is an injective map $X \rightarrow Y$ that is a homeomorphism of X and its image.

Fact 46 ([49, 50.5]). *Every compact metrizable space X with $\text{Dim } X < \infty$ can be embedded into $\mathbb{R}^{2\text{Dim } X + 1}$.*

We also collect two additional facts for use in the proofs. Recall that a function is called closed if the image of every closed set is closed.

Fact 47 ([49, 50.2] and [50, 9.2.10]). *(i) If X is a topological space and Y_1, \dots, Y_k are closed and finite-dimensional subspaces, then*

$$X = Y_1 \cup \dots \cup Y_k \quad \text{implies} \quad \text{Dim } X = \max_i \text{Dim } Y_i .$$

(ii) Let $f : X \rightarrow Y$ be a continuous, closed and surjective map between metric spaces. If $|f^{-1}y| \leq m + 1$ for some $m \in \mathbb{N} \cup \{0\}$ and all $y \in Y$, then

$$\text{Dim } X \leq \text{Dim } Y \leq \text{Dim } X + m .$$

D Background IV: Spectral theory

The proof of the Fourier representation draws on the spectral theory of linear operators, and we now review the relevant facts of this theory. We are interested in an operator A (think $-\Delta$) defined on a space V (think $\mathbf{H}_{\mathbb{C}}$) which is contained in a space W (think \mathbf{L}_2). If V approximates \mathbf{L}_2 sufficiently well, and if A is self-adjoint on V , a general spectral result guarantees the existence of an orthonormal basis for \mathbf{L}_2 consisting of eigenfunctions (Fact 48). To apply the result to the negative Laplacian, we must extend Δ to an operator on $\mathbf{H}_{\mathbb{C}}$ (since Δ is defined on twice differentiable functions, and elements of $\mathbf{H}_{\mathbb{C}}$ need not be that smooth). Fact 49 shows that is possible. Once we have obtained the eigenfunctions, there is a generic way to show they are smooth (Fact 50).

D.1. Spectra of self-adjoint operators

Spectral decompositions of self-adjoint operators have been studied widely, see Brezis [19], McLean [48] for sample results. We use the following formulation, adapted from Theorem 2.37 and Corollary 2.38 of McLean [48].

Fact 48 (Spectral decomposition [48]). *Let Π be a polytope, and V a closed subspace of $\mathbf{H}^1(\Pi^\circ)$. Require that the inclusion maps*

$$(31) \quad V \hookrightarrow \mathbf{L}_2(\Pi^\circ) \hookrightarrow V^*$$

are both continuous and dense, and the first inclusion is also compact. Let $A : V \rightarrow V^$ be a bounded linear operator that is self-adjoint on V and satisfies*

$$(32) \quad \langle Af, f \rangle_V \geq c_V \|f\|_V^2 - c_L \|f\|_{\mathbf{L}_2}^2 \quad \text{for some } c_V, c_L > 0 \text{ and all } f \in V .$$

Then there is a countable number of scalars

$$\lambda_1 \leq \lambda_2 \leq \dots \quad \text{with} \quad \lambda_i \xrightarrow{i \rightarrow \infty} \infty$$

and functions $\xi_1, \xi_2, \dots \in V$ such that

$$A\xi_i = \lambda_i \xi_i \quad \text{for all } i \in \mathbb{N}.$$

The functions ξ_i form an orthonormal basis for V . For each $v \in V$,

$$\sum_{i \leq m} \lambda_i \langle v, \xi_i \rangle \xi_i \xrightarrow{m \rightarrow \infty} Av$$

holds in the dual V^* . If A is also strictly positive definite, then $\lambda_1 > 0$.

If the inclusions in (48) are continuous and dense, \mathbf{L}_2 is called a **pivot space** for V . See Remark 3 in Chapter 5 of Brezis [19] for a discussion of pivot spaces.

D.2. Extension of Laplacians to Sobolev spaces

Recall that the Laplace operator Δ on a domain Γ is defined on twice continuously differentiable functions. It can be extended to a continuous linear operator on $\mathbf{H}^1(\Gamma^\circ)$, provided the geometry of Γ is sufficiently regular. That is the case if Γ is a **Lipschitz domain**, which loosely speaking means it is bounded by a finite number of Lipschitz-smooth surfaces. Since a precise definition (which can be found in McLean [48]) is rather technical, we omit details and only note that every polytope is a Lipschitz domain [48, p 90].

Fact 49. *Let Γ be a Lipschitz domain, and denote by $\mathbf{H}^1(\Gamma^\circ)^*$ the dual space of $\mathbf{H}^1(\Gamma^\circ)$. There is a unique linear operator $\Lambda : \mathbf{H}^1(\Gamma^\circ) \rightarrow \mathbf{H}^1(\Gamma^\circ)^*$ that extends the Laplace operator. This operator is bounded on $\mathbf{H}^1(\Gamma^\circ)$.*

D.3. Smoothness of eigenfunctions

One hallmark of differential operators is that their eigenfunctions tend to be very smooth. The sines and cosines that make up the standard Fourier basis on the line are examples. Intuitively, that is due to the fact that the Laplacian is a second-order differential operator, and “removes two orders of smoothness”: If Δf is in \mathbf{C}^k , then f must be in \mathbf{C}^{k+2} . Since an eigenfunction appears on both sides of the spectral equation

$$-\Delta \xi = \lambda \xi,$$

one can iterate the argument: If ξ is in \mathbf{C} , it must also be in \mathbf{C}^2 , hence also in \mathbf{C}^4 , and so forth. This argument is not immediately applicable to the functions ξ constructed in Fact 48 above, since it does not guarantee the functions to be in \mathbf{C}^2 . It only shows they are in V , which in the context of differential operators (and specifically in the problems we study) is typically a Sobolev space. Under suitable conditions on the domain, however, one can show that argument above generalizes to Sobolev space, at least on certain open subsets. The following version is again adapted to our problem from a more general result.

Fact 50 ([48, 4.16]). *Let Π be a polytope and M an open set such that $\overline{M} \subset \Pi^\circ$. Let Λ be the extension of the Laplace operator guaranteed by Fact 49. Suppose $f \in \mathbf{H}^1(M)$ and $k \in \mathbb{N} \cup \{0\}$. Then $\Lambda f = g$ on M for $g \in \mathbf{H}^k(M)$ implies $f \in \mathbf{H}^{k+2}(M)$.*

E Proofs I: The flux property

This and the following two sections comprise the proof of Theorem 7, the Fourier representation. In this section, we prove the flux property of Proposition 28.

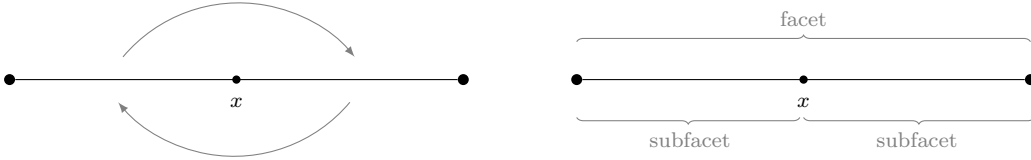
E.1. Tools: Subfacets

We next introduce a simple geometric tool to deal with non-exact tilings: Theorem 15 assumes the tiling is exact, but the the flux property and the Fourier representation make no such assumption. Although they do not use a gluing construction explicitly, they use the periodic boundary condition (6), which matches up points on the boundary $\partial\Pi$ as gluing does. Absent exactness, that requires dealing with parts of facets. We call each set of the form

$$\sigma := (\Pi \cap \phi\Pi)^\circ \quad \text{for some } \phi \in \mathbb{G} \text{ and } \sigma \neq \emptyset$$

a **subfacet** of Π . Let Σ be the (finite) set of subfacets of Π . Whereas the division of $\partial\Pi$ into facets is a property of the polytope that does not depend on \mathbb{G} , the subfacets are a property of the tiling.

Example 51. Consider an edge of a rectangle $\Pi \subset \mathbb{R}^2$. Suppose ϕ is a 180° rotation around the center x of the edge, as shown on the left:



Then ϕ maps the facet to itself, and maps the point x to itself, but no other point is fixed. In this case, x divides the interior of the facet into two subfacets (right). If ϕ is instead a reflection about the same edge, each point on the edge is a fixed point, and the entire interior of the edge is a single subfacet. Another example of a subfacet is the edge segment marked in Figure 12/left.

Lemma 52. *The subfacets are convex $(n-1)$ -dimensional open subsets of $\partial\Pi$, and their closures cover $\partial\Pi$. In particular,*

$$\text{vol}_{n-1}(\sigma) > 0 \quad \text{for all } \sigma \in \Sigma \quad \text{and} \quad \sum_{\sigma \in \Sigma} \text{vol}_{n-1}(\sigma) = \text{vol}_{n-1}(\partial\Pi) .$$

Each subfacet is mapped by \mathbb{G} to exactly one subfacet, possibly itself: For each $\sigma \in \Sigma$,

$$\phi_\sigma(\sigma) \in \Sigma \quad \text{for one and only one } \phi_\sigma \in \mathbb{G} \setminus \{\mathbf{1}\} ,$$

where $\phi_\sigma(\sigma) = \sigma$ if and only if σ contains a fixed point of ϕ_σ .

Proof of Lemma 52. Each subfacet is by definition of the form $\sigma = (\Pi \cap \psi\Pi)^\circ$, for some $\psi \in \mathbb{G}$. Since $\mathbb{G}(\Pi)$ is a tiling, Π and $\psi\Pi$ are the only tiles intersecting σ . We hence have

$$\sigma \cap \phi_\sigma^{-1}\Pi \neq \emptyset \quad \text{for one and only one } \phi_\sigma \in \mathbb{G} \setminus \{\mathbf{1}\} ,$$

namely for $\phi_\sigma = \psi^{-1}$. Since the set $\Pi \cap \phi_\sigma^{-1}\Pi$ is the intersection of two facets, and hence of two convex sets, it is convex. By the definition of subfacets, its relative interior σ is non-empty. That makes σ a $(n-1)$ -dimensional, convex, open subset of $\partial\Pi$.

1° *Volumes.* Since σ is open in $n-1$ dimensions,

$$\text{vol}_{n-1}(\sigma) > 0 .$$

The definition of a tiling implies each boundary point $x \in \partial\Pi$ is on the facet of some adjacent tile $\phi\Pi$. It follows that

$$\partial\Pi = \bigcup_{\phi \in \mathbb{G} \setminus \{1\}} \Pi \cap \phi\Pi = \bigcup_{\sigma \in \Sigma} \bar{\sigma}.$$

Since distinct subfacets do not intersect, applying volumes on both sides shows

$$\text{vol}_{n-1}(\partial\Pi) = \sum_{\sigma \in \Sigma} \text{vol}_{n-1}(\sigma).$$

2° *Each subfacet maps to exactly one subfacet.* We have already noted that σ intersects only the tiles Π and $\phi_\sigma^{-1}\Pi$. Since $\phi_\sigma^{-1}\Pi$ is adjacent to Π , so is $\phi_\sigma\Pi$. That implies $\phi(\sigma) = (\Pi \cap \phi_\sigma\Pi)^\circ$, and hence

$$\phi_\sigma(\sigma) \in \Sigma \quad \text{and} \quad \sigma \cap \phi^{-1}\Pi = \emptyset \quad \text{if } \phi \neq 1, \phi_\sigma.$$

Thus, σ maps to ϕ_σ and vice versa, and neither maps to any other subfacet.

3° *Fixed points.* We know that σ and $\phi_\sigma(\sigma)$ are either identical or disjoint. Suppose first that $\sigma \neq \phi_\sigma(\sigma)$. Then

$$\phi_\sigma^{-1}\Pi \neq \phi_\sigma\Pi \quad \text{and hence} \quad \phi_\sigma(\sigma) \cap \sigma = \emptyset,$$

so ϕ_σ has no fixed points in σ . On the other hand, suppose $\phi_\sigma(\sigma) = \sigma$. Then the restriction of ϕ_σ to the closure $\bar{\sigma}$ is a continuous map $\bar{\sigma} \rightarrow \bar{\sigma}$ from a compact convex set to itself. That implies, by Brouwer's theorem [3, 17.56], that the closure $\bar{\sigma}$ contains at least one fixed point, and we only have to ensure that at least one of these fixed points is in the interior σ . But if the boundary $\partial\sigma$ contains fixed points and σ does not, then $\phi_\sigma(\sigma) \neq \sigma$ since ϕ_σ is an isometry, which contradicts the assumption. In summary, we have shown that $\phi_\sigma(\sigma) = \sigma$ if and only if σ contains a fixed point. \square

E.2. Proof of the flux property

To establish the flux property in Proposition 28, we first show how the normal vector \mathbf{N}_Π of the boundary of a tile Π transforms under elements of the group \mathbb{G} .

Lemma 53 (Transformation behavior of normal vectors). *If a crystallographic group tiles \mathbb{R}^n with a convex polytope Π , then*

$$(33) \quad A_\phi \mathbf{N}_\Pi(x) = -\mathbf{N}_\Pi(\phi x) \quad \text{whenever } x, \phi x \in \Pi.$$

Proof. If $\phi\Pi$ is a tile adjacent to Π , its normal vector $\mathbf{N}_{\phi\Pi}$ satisfies

$$\mathbf{N}_\Pi(y) = -\mathbf{N}_{\phi\Pi}(y) \quad \text{if } y \in \Pi \cap \phi\Pi.$$

Since $x \sim \phi x$ holds, x is on at least one facet S of Π , and ϕx is hence on the facet ϕS of $\phi\Pi$. If \mathbf{N} is a normal vector of S (exterior to Π), then $A_\phi \mathbf{N}$ is a normal vector of ϕS (exterior to $\phi\Pi$). That shows

$$\mathbf{N}_{\phi\Pi}(\phi x) = A_\phi \mathbf{N}_\Pi(x) \quad \text{if } x, \phi x \in \Pi.$$

In summary, we hence have $A_\phi \mathbf{N}_\Pi(x) = -\mathbf{N}_\Pi(y)$ whenever x and ϕx are both in Π . \square

Proof of Proposition 28. 1° Let σ be a subfacet. Since \mathbf{N}_Π is constant on σ , we define the vectors

$$\mathbf{N}_\Pi(\sigma) := \mathbf{N}_\Pi(x) \text{ for any } x \in \sigma \quad \text{and} \quad I(\sigma) := \int_\sigma F(x) \text{vol}_{n-1}(dx).$$

By Lemma 52, the subfacets cover $\partial\Pi$ up to a null set. We hence have

$$\int_{\partial\Pi} F(x)^\top \mathbf{N}_\Pi(x) \text{vol}_{n-1}(dx) = \sum_{\sigma \in \mathcal{S}} \int_\sigma F(x)^\top \mathbf{N}_\Pi(x) \text{vol}_{n-1}(dx) = \sum_{\sigma \in \mathcal{S}} \mathbf{N}(\sigma)^\top I(\sigma).$$

We must show this sum vanishes.

2° If $\phi\sigma \in \Pi$, the ϕ -invariance of vol_{n-1} and condition (20) imply

$$\begin{aligned} I(\phi\sigma) &= \int_{\phi\sigma} F(x) \text{vol}_{n-1}(dx) = \int_\sigma F(\phi(x)) \text{vol}_{n-1}(dx) \\ &= A_\phi \int_\sigma F(x) \text{vol}_{n-1}(dx) = A_\phi I(\sigma). \end{aligned}$$

Lemma 53 implies $A_\phi \mathbf{N}_\Pi(\sigma) = -\mathbf{N}_\Pi(\phi\sigma)$ for $\phi\sigma \subset \Pi \cap \phi\Pi$. That shows

$$\mathbf{N}_\Pi(\phi\sigma)^\top I(\phi\sigma) = -(A_\phi \mathbf{N}_\Pi(\sigma))^\top A_\phi I(\sigma) = -\mathbf{N}_\Pi(\sigma)^\top A_\phi^\top A_\phi I(\sigma) = -\mathbf{N}_\Pi(\sigma)^\top I(\sigma),$$

since $A_\phi^\top = A_\phi^{-1}$. It follows that

$$\mathbf{N}_\Pi(\sigma)^\top I(\sigma) + \mathbf{N}_\Pi(\phi\sigma)^\top I(\phi\sigma) = 0 \quad \text{and even} \quad \mathbf{N}_\Pi(\sigma)^\top I(\sigma) = 0 \quad \text{if } \sigma = \phi\sigma.$$

3° By Lemma 52, the set Σ of subfacets can be sorted into pairs $(\sigma, \phi_\sigma\sigma)$ such that no subfacet occurs in more than one pair (though $\sigma = \phi_\sigma\sigma$ is possible). It follows that

$$\sum_{\sigma \in \Sigma} \mathbf{N}_\Pi(\sigma)^\top I(\sigma) = \frac{1}{2} \sum_{\sigma \in \Sigma} (\mathbf{N}_\Pi(\sigma)^\top I(\sigma) + \mathbf{N}_\Pi(\phi_\sigma\sigma)^\top I(\phi_\sigma\sigma)) = 0$$

as we set out to show. \square

F Proofs II: The Laplacian and its properties

The purpose of this section is to prove Theorem 30. We use the flux property to show that the symmetries imposed by a crystallographic group simplify the Green identity considerably. We can then use this symmetric form of the Green identity to show Λ has the desired properties.

F.1. Green's identity under crystallographic symmetry

That the extended Laplace operator is self-adjoint on $\mathbf{H}_\mathbb{G}$ for any crystallographic group derives from the fact that the symmetry imposed by the group makes the correction term in Green's identity vanish. That enters in the proof of Theorem 30 via the two identities in the following lemma. The first one is Green's identity under symmetry; the second shows that a similar identity holds for the Sobolev inner product.

Lemma 54 (Symmetric Green identities). *If a crystallographic group \mathbb{G} tiles \mathbb{R}^n with a convex polytope Π , the negative Laplace operator satisfies the identities*

$$(34) \quad \langle -\Delta f, h \rangle_{\mathbf{L}_2} = a(f, h)$$

$$(35) \quad \langle -\Delta f, h \rangle_{\mathbf{H}^1} = a(f, h) + \sum_{i \leq n} a(\partial_i f, \partial_i h)$$

for all functions f and h in \mathcal{H} .

Proof. Let \bar{f} and \bar{h} be the unique continuous extensions of f and h to the closure Π , and set $F := \bar{f}\nabla\bar{h}$. Since \bar{f} and \bar{h} satisfy the periodic boundary condition, (18) shows

$$F(\phi x) = \bar{h}(\phi x)\nabla\bar{f}(\phi x) = \bar{h}(x)A_\phi\nabla\bar{f}(x) = A_\phi F(x).$$

By the flux property (Proposition 28), we hence have

$$\int_{\partial\Pi} (\partial_{\mathbf{N}_\Pi}\bar{f})\bar{h} = \int_{\partial\Pi} \mathbf{N}_\Pi^\top F = 0,$$

and substituting into Green's identity (Fact 29) shows

$$(36) \quad \langle \Delta f, h \rangle_{\mathbf{L}_2} = a(f, h) - \int_{\partial\Pi} (\partial_{\mathbf{N}_\Pi} f)h = a(f, h),$$

so (34) holds. Now consider (35). Since f has three continuous derivatives, we have

$$\partial_i^2\partial_j f = \partial_j\partial_i^2 f \quad \text{and hence} \quad \Delta(\partial_j f) = \partial_j(\Delta f).$$

The \mathbf{H}^1 -product can then be written as

$$\langle \Delta f, h \rangle_{\mathbf{H}^1} = \langle \Delta f, h \rangle_{\mathbf{L}_2} + \sum_i \langle \partial_i(\Delta f), \partial_i h \rangle_{\mathbf{L}_2} = \langle \Delta f, h \rangle_{\mathbf{L}_2} + \sum_i \langle \Delta(\partial_i f), \partial_i h \rangle_{\mathbf{L}_2}.$$

Substituting the final sum into Green's identity shows

$$\sum_i \langle \Delta(\partial_i f), \partial_i h \rangle_{\mathbf{L}_2} = \sum_i a(\partial_i f, \partial_i h) + \int_{\partial\Pi} \sum_i (\partial_{\mathbf{N}_\Pi} \partial_i f) \partial_i h$$

Since $\nabla(\partial_i f)$ is precisely the i th row vector of the Hessian Hf , the integrand is

$$\sum_i (\partial_{\mathbf{N}_\Pi} \partial_i f) \partial_i h = \sum_i (\mathbf{N}_\Pi^\top (\nabla \partial_i f)) \partial_i h = \mathbf{N}_\Pi^\top (Hf) \nabla h.$$

Consider the vector field $F(x) := (Hf)\nabla h$. By Lemma 27, F transforms as

$$F(\phi x) = Hf(\phi x)\nabla h(\phi x) = A_\phi \cdot Hf(x) \cdot A_\phi^\top A_\phi \nabla h(x) = A_\phi \cdot F(x),$$

and hence satisfies (20). Another application of the flux property then shows

$$\sum_i \langle \Delta(\partial_i f), \partial_i h \rangle_{\mathbf{L}_2} = \sum_i a(\partial_i f, \partial_i h).$$

Substituting this identity and (34) into the \mathbf{H}^1 -product above yields (35). \square

F.2. Approximation properties of the space $\mathbf{H}_\mathbb{G}$

That we can use the space $\mathbf{H}_\mathbb{G}$ to prove results about continuous and \mathbf{L}_2 -functions relies on the fact that such functions are sufficiently well approximated by elements of $\mathbf{H}_\mathbb{G}$, and that $\mathbf{H}_\mathbb{G}$ can in turn be approximated by useful dense subsets. We collect these technical facts in the following lemma. Consider the space of functions

$$\mathbf{C}_{\text{pbc}}(\Pi^\circ) = \{f|_{\Pi^\circ} \mid f \in \mathbf{C}_\mathbb{G}\}$$

which we equip with the supremum norm. These are precisely those uniformly continuous functions on the interior Π° whose unique continuous extension to Π satisfies the periodic boundary conditions. Note that we can then express the definition of \mathcal{H} in (21) as

$$\mathcal{H} = \mathbf{C}_{\text{pbc}}(\Pi^\circ) \cap \mathbf{C}^\infty(\Pi^\circ).$$

Lemma 55. *If \mathbb{G} is crystallographic and tiles with Π , the inclusions*

$$\mathcal{H} \xrightarrow{\iota_1} \mathbf{H}_{\mathbb{G}} \xrightarrow{\iota_2} \mathbf{L}_2(\Pi^\circ) \xrightarrow{\iota_3} \mathbf{H}_{\mathbb{G}}^*,$$

are all dense, ι_2 and ι_3 are continuous, and ι_2 is compact. Moreover, if $\mathcal{F} \subset \mathbf{H}_{\mathbb{G}} \cap \mathbf{C}_{\text{pbc}}(\Pi^\circ)$ is dense in $\mathbf{H}_{\mathbb{G}}$, it is also dense in $\mathbf{C}_{\text{pbc}}(\Pi^\circ)$ in the supremum norm.

When we take closures in the proof, we write $\overline{\mathcal{F}}^{\text{sup}}$ and $\overline{\mathcal{F}}^{\mathbf{H}^1}$ to indicate the norm used to take the closure of a set \mathcal{F} .

Proof. That \mathcal{H} is dense in $\mathbf{H}_{\mathbb{G}}$ holds by definition, see (21).

1° *Inclusions ι_2 and ι_3 are dense and continuous.* Denote by $\mathbf{C}_c^\infty := \mathbf{C}_c(\Pi^\circ) \cap \mathbf{C}^\infty(\Pi^\circ)$ the set of compactly supported and infinitely differentiable functions on Π° . Denote by

$$\mathbf{H}_0^1 := \overline{\mathbf{C}_c^\infty}^{\mathbf{H}^1}$$

its \mathbf{H}^1 -closure. This is, loosely speaking, the Sobolev space of functions that vanish on the boundary [19, 48], and it is a standard result that

$$\mathbf{H}_0^1 \subset \mathbf{L}_2(\Pi^\circ) \subset (\mathbf{H}_0^1)^*,$$

where both inclusion maps are dense and bounded [19, Chapter 9.5]. Consider any $f \in \mathbf{C}_c^\infty$. Since f is uniformly continuous, it has a unique continuous extension \bar{f} to Π . This extension satisfies $\bar{f} = 0$ on the boundary $\partial\Pi$. (This fact is well known [e.g., 19], but also easy to verify: Since the support of f is a closed subset of the open set Π° , each point x on the boundary is the center of some open ball B that does not intersect the support, so $\bar{f} = 0$ on $\Pi^\circ \cap B$.) It therefore trivially satisfies the periodic boundary condition (6), which shows $\mathbf{C}_c^\infty \subset \mathcal{H}$. Taking \mathbf{H}_1 -closures shows $\mathbf{H}_0^1 \subset \mathbf{H}_{\mathbb{G}}$. We hence have

$$\mathbf{H}_0^1(\Pi^\circ) \subset \mathbf{H}_{\mathbb{G}} \subset \mathbf{H}^1(\Pi^\circ) \subset \mathbf{L}_2(\Pi^\circ) \subset \mathbf{H}^1(\Pi^\circ)^* \subset \mathbf{H}_{\mathbb{G}}^* \subset \mathbf{H}_0^1(\Pi^\circ)^*.$$

Since $\mathbf{H}_0^1 \hookrightarrow \mathbf{L}_2$ and $\mathbf{L}_2 \hookrightarrow (\mathbf{H}_0^1)^*$ are both dense and bounded, $\mathbf{H}_{\mathbb{G}} \hookrightarrow \mathbf{L}_2$ and $\mathbf{L}_2 \hookrightarrow \mathbf{H}_{\mathbb{G}}^*$ are dense and bounded (and hence continuous), and $\mathbf{H}_{\mathbb{G}} \hookrightarrow \mathbf{H}^1$ is bounded (and hence continuous).

2° *Inclusion ι_2 is compact.* We can decompose ι_2 as

$$\mathbf{H}_{\mathbb{G}} \hookrightarrow \mathbf{H}^1 \hookrightarrow \mathbf{L}_2.$$

It is known that $\mathbf{H}^1 \hookrightarrow \mathbf{L}_2$ is compact [2]. If one of two inclusions is compact, their composition is compact (see [2], or simply note that any bounded sequence in $\mathbf{H}_{\mathbb{G}}$ is also bounded in \mathbf{H}^1). That shows $\mathbf{H}_{\mathbb{G}} \hookrightarrow \mathbf{L}_2$ is compact.

3° *\mathcal{F} is dense in \mathbf{C}_{pbc} .* We know from Lemma 36 that $\mathbf{H}^1(\Pi^\circ) \subset \mathbf{C}(\Pi^\circ)$, and hence $\|h\|_{\mathbf{H}^1} \geq \|h\|_{\text{sup}}$ for all $h \in \mathbf{C}(\Pi^\circ)$. In other words, the sup-closure of the \mathbf{H}^1 -closure is the sup-closure, so

$$\overline{\mathcal{F}}^{\text{sup}} = \overline{(\overline{\mathcal{F}}^{\mathbf{H}^1})}^{\text{sup}} = \overline{\mathbf{H}_{\mathbb{G}}}^{\text{sup}} = \overline{(\overline{\mathcal{H}}^{\mathbf{H}^1})}^{\text{sup}} = \overline{\mathcal{H}}^{\text{sup}}.$$

It hence suffices to show \mathcal{H} is dense in \mathbf{C}_{pbc} . To this end, we use a standard fact: If we consider the closed set Π instead of the interior, $\mathbf{C}^\infty(\Pi)$ is dense in $\mathbf{C}(\Pi)$, since Π is compact. (One way to see this is that \mathbf{C}^∞ contains all polynomials, which are dense in $\mathbf{C}(\Pi)$ by the Stone-Weierstrass theorem [2].) Since $\mathbf{C}_{\text{pbc}}(\Pi)$ is a closed linear subspace of $\mathbf{C}(\Pi)$, it follows that

$$\mathbf{C}_{\text{pbc}}(\Pi) \cap \mathbf{C}^\infty(\Pi) \quad \text{is dense in} \quad \mathbf{C}_{\text{pbc}}(\Pi) \cap \mathbf{C}(\Pi) = \mathbf{C}_{\text{pbc}}(\Pi).$$

Consider a function $f \in \mathbf{C}_{\text{pbc}}(\Pi^\circ)$. Then f has a unique continuous extension \bar{f} to Π , which satisfies the periodic boundary condition. That shows that

$$(37) \quad f \mapsto \bar{f} \quad \text{is an isometric isomorphism} \quad \mathbf{C}_{\text{pbc}}(\Pi^\circ) \rightarrow \mathbf{C}_{\text{pbc}}(\Pi),$$

since the extension is unique and does not change the supremum norm. If f is also infinitely differentiable (and hence in \mathcal{H}), then \bar{f} is infinitely differentiable, so the same map is also an isometric isomorphism

$$\mathcal{H} = \mathbf{C}_{\text{pbc}}(\Pi^\circ) \cap \mathbf{C}^\infty(\Pi^\circ) \rightarrow \mathbf{C}_{\text{pbc}}(\Pi) \cap \mathbf{C}^\infty(\Pi).$$

In summary, we hence have

$$\mathcal{H} \xrightarrow{\text{isomorphic}} \mathbf{C}_{\text{pbc}}(\Pi) \cap \mathbf{C}^\infty(\Pi) \xleftarrow{\text{dense}} \mathbf{C}_{\text{pbc}}(\Pi) \xrightarrow{\text{isomorphic}} \mathbf{C}_{\text{pbc}}(\Pi^\circ),$$

and since isomorphisms preserve dense subsets, \mathcal{H} is indeed dense in $\mathbf{C}_{\text{pbc}}(\Pi^\circ)$. \square

F.3. Existence and properties of the Laplacian

Proof of Theorem 30. Since Π is a convex polytope, it is a Lipschitz domain, and Δ hence extends to a bounded linear operator Λ on $\mathbf{H}^1(\Pi^\circ)$, by Fact 49. The restriction of Λ to the closed linear subspace of $\mathbf{H}_{\mathbb{G}}$ is again a bounded linear operator that extends Δ . It remains to verify self-adjointness and (26) on $\mathbf{H}_{\mathbb{G}}$. Since Λ is bounded and hence continuous, it suffices to do so on the dense subset \mathcal{H} . For (26i), that has already been established in Lemma 54. To show (26ii), we note (25) implies

$$\|f\|_{\mathbf{H}^1}^2 = \langle f, f \rangle_{\mathbf{H}^1} = \langle f, f \rangle_{\mathbf{L}_2} + a(f, f) \quad \text{for } f \in \mathcal{H}$$

and hence

$$a(f, f) = \|f\|_{\mathbf{H}^1}^2 - \|f\|_{\mathbf{L}_2}^2.$$

Since $f \in \mathcal{H}$ and hence $\Lambda f = \Delta f$, we can substitute into (35), which shows

$$\langle -\Delta f, f \rangle_{\mathbf{H}^1} = a(f, f) + \sum_{i \leq n} a(\partial_i f, \partial_i f) \geq \|f\|_{\mathbf{H}^1}^2 - \|f\|_{\mathbf{L}_2}^2$$

where the last step uses the fact that a is positive semi-definite by (24). That proves coercivity. Since the bilinear form a is symmetric, (35) also shows

$$\langle -\Delta f, h \rangle_{\mathbf{H}^1} = a(f, h) + \sum_i a(\partial_i f, \partial_i h) = a(h, f) + \sum_i a(\partial_i h, \partial_i f) = \langle -\Delta h, f \rangle_{\mathbf{H}^1}$$

on \mathcal{H} , so Λ is self-adjoint on $\mathbf{H}_{\mathbb{G}}$. \square

G Proofs III: Fourier representation

We now prove the Fourier representation. We first restrict all function to a single tile Π . By Lemma 55, we can then choose the space V in the spectral theorem (Fact 48) as $\mathbf{H}_{\mathbb{G}}$. Since we also know the Laplacian is self-adjoint on $\mathbf{H}_{\mathbb{G}}$, we can use the spectral theorem to obtain an eigenbasis. We then deduce Theorem 7 by extending the representation from Π to the entire space \mathbb{R}^n .

G.1. Proof of the Fourier representation on a single tile

The eigenvalue problem (13) in Theorem 7 is defined on the unbounded domain \mathbb{R}^n . We first restrict the problem to the compact domain Π , that is, we consider

$$(38) \quad \begin{array}{ll} -\Delta h = \lambda h & \text{on } \Pi^\circ \\ \text{subject to } h(x) = h(y) & \text{whenever } x \sim y \text{ on } \partial\Pi. \end{array}$$

That allows us to apply Fact 48 and 50 above, which hold on compact domains. (The deeper relevance of compact domains is that function spaces on such domains tend to have better approximation properties than on unbounded domains.) The restricted version of Theorem 7 we prove first is as follows.

Lemma 56. *Let \mathbb{G} be a crystallographic group that tiles \mathbb{R}^n with a convex polytope Π . Then (38) has solutions for countably many distinct values of λ , which satisfy*

$$0 = \lambda_1 < \lambda_2 < \lambda_3 < \dots \quad \text{and} \quad \lambda_i \xrightarrow{i \rightarrow \infty} \infty.$$

Each solution h is infinitely often differentiable on Π° . There exists a sequence of solutions h_1, h_2, \dots that is an orthonormal basis of $\mathbf{L}_2(\Pi)$, and satisfies

$$|\{j \in \mathbb{N} \mid h_j \text{ solves (38) for } \lambda_i\}| = k(\lambda_i).$$

In the proof, we again use the notation $\overline{M}^{\mathbf{L}_2}$ and $\overline{M}^{\mathbf{H}^1}$ to indicate the norm used to take the closure of a set M .

Proof of Lemma 56. We apply the spectral decomposition result (Fact 48), with $A = \Lambda$ and $V = \mathbf{H}_{\mathbb{G}}$. We have already established its conditions are satisfied (except for the optional assumption of strict positive definiteness): By Theorem 30, Λ exists, is a bounded and self-adjoint linear operator on $\mathbf{H}_{\mathbb{G}}$, and satisfies (32). By Lemma 55, $\mathbf{H}_{\mathbb{G}}$ approximates $\mathbf{L}_2(\Pi^\circ)$ in the sense of (31). Fact 48 hence shows that there is an orthonormal basis of eigenfunctions for $\mathbf{H}_{\mathbb{G}}$, i.e., functions ξ_1, ξ_2, \dots that satisfy

$$(39) \quad \begin{array}{lll} \text{(i) } \Lambda \xi_i = \lambda_i \xi_i & \text{(ii) } \langle \xi_i, \xi_j \rangle_{\mathbf{H}^1} = \delta_{ij} & \text{(iii) } \overline{\text{span}\{\xi_1, \xi_2, \dots\}}^{\mathbf{H}^1} = \mathbf{H}_{\mathbb{G}}. \end{array}$$

What remains to be shown are the properties of the eigenvalues and eigenfunctions, and that the ONB of $\mathbf{H}_{\mathbb{G}}$ can be translated into an ONB of \mathbf{L}_2 .

Non-negativity of eigenvalues. The operator Λ is positive semi-definite, but not strictly positive definite, on V . To show this, it again suffices to consider $-\Delta$ on \mathcal{H} . By (35), we have

$$(40) \quad \begin{aligned} \langle \Lambda f, f \rangle_{\mathbf{H}^1} &= a(f, f) + \sum_i a(\partial_i f, \partial_i f) \\ &= \int \|\nabla f(x)\|_{\mathbb{R}^n}^2 \text{vol}(dx) + \sum_i \int \|\nabla \partial_i f(x)\|_{\mathbb{R}^n}^2 \text{vol}(dx) \geq 0. \end{aligned}$$

That shows Λ is positive semi-definite. Now consider, for any $\varepsilon > 0$, the operator

$$\Lambda_\varepsilon : \mathbf{H}_{\mathbb{G}} \rightarrow \mathbf{H}_{\mathbb{G}} \quad \text{defined by} \quad \Lambda_\varepsilon f := \Lambda f + \varepsilon f.$$

This operator is still bounded, coercive and self-adjoint, so Fact 48 is applicable. Clearly, Λ_ε has the same eigenfunctions as Λ , with eigenvalues $\lambda_i + \varepsilon$. It is also strictly positive definite, since

$$\langle \Lambda_\varepsilon f, f \rangle_{\mathbf{H}^1} = \langle \Lambda f, f \rangle_{\mathbf{H}^1} + \langle \varepsilon f, f \rangle_{\mathbf{H}^1} \geq \varepsilon \|f\|_{\mathbf{H}^1}.$$

It hence follows from Fact 48 that the smallest eigenvalue satisfies $\lambda_1 + \varepsilon > 0$. Since that holds for every $\varepsilon > 0$, we have $\lambda_1 \geq 0$.

The smallest eigenvalue and its eigenspace. If a function f is constant on Π° , then

$$f \in \mathbf{H}_{\mathbb{G}} \quad \text{and} \quad \Lambda f = -\Delta f = 0.$$

That shows the smallest eigenvalue is $\lambda_1 = 0$, and its eigenspace $\mathcal{H}(0)$ contains all constant functions. To show that it contains no other functions, note that

$$\langle \Lambda f, f \rangle = 0 \quad \text{and by (40) hence} \quad \|\nabla f(x)\|^2 = 0 \text{ for almost all } x \in \Pi^\circ.$$

That implies f is piece-wise constant. Since the only piece-wise constant function contained in \mathbf{H}^1 are those that are strictly constant (see Adams and Fournier [2]), $\mathcal{H}(0)$ is the set of constant functions, and $\dim \mathcal{H}(0) = 1$.

Regularity of eigenfunctions. We now use the strategy outlined in Appendix D.3. Let ξ be an eigenfunction. We have shown that implies $\xi \in \mathbf{H}_{\mathbb{G}}$, and hence $\xi \in \mathbf{H}^1(\Pi^\circ)$. Consider any $x \in \Pi^\circ$. Since the interior is open, we can find $\varepsilon > 0$ such that the open ball $B = B_\varepsilon(x)$ of radius ε centered at x satisfies $\bar{B} \subset \Pi^\circ$. The restriction $\xi|_B$ of ξ to B then satisfies

$$f|_{B_\varepsilon(x)} \in \mathbf{H}^1(B) \quad \text{and} \quad \Lambda f|_B = \lambda f|_B.$$

Since $\xi|_B$ appears on both sides of the equation, Fact 50 implies that $f|_B$ is also in $\mathbf{H}^{1+2}(B)$, hence also in $\mathbf{H}^{1+4}(B)$, and so forth, so $\xi|_B \in \mathbf{H}^k(B)$ for all $k \in \mathbb{N}$. Lemma 36 then shows that $\xi|_B$ is even in $\mathbf{C}^k(B)$ for each $k \in \mathbb{N}$, and hence in $\mathbf{C}^\infty(B)$. We have thus shown that ξ has infinitely many derivatives on a neighborhood of each $x \in \Pi^\circ$, and hence that $\xi \in \mathbf{C}^\infty(\Pi^\circ)$.

Turning the Sobolev basis into an \mathbf{L}_2 basis. The functions ξ_i form an orthonormal basis of $\mathbf{H}_{\mathbb{G}}$, by (39). To obtain an orthonormal basis for $\mathbf{L}_2(\Pi^\circ)$, we substitute (25) into (39ii), and obtain

$$\delta_{ij} = \langle \xi_i, \xi_j \rangle_{\mathbf{H}^1} = \langle \xi_i, \xi_j \rangle_{\mathbf{L}_2} + a(\xi_i, \xi_j) = \langle \xi_i, \xi_j \rangle_{\mathbf{L}_2} + \langle \Lambda \xi_i, \xi_j \rangle_{\mathbf{L}_2}.$$

Since ξ_i is an eigenfunction, it follows that

$$\delta_{ij} = \langle \xi_i, \xi_j \rangle_{\mathbf{L}_2} + \lambda_i \langle \xi_i, \xi_j \rangle_{\mathbf{L}_2} \quad \text{and hence} \quad \frac{1}{1 + \lambda_i} \langle \xi_i, \xi_j \rangle_{\mathbf{L}_2} = \delta_{ij}.$$

The functions $h_i := \xi_i / \sqrt{1 + \lambda_i}$ then satisfy

$$-\Delta h_i = \lambda_i h_i \text{ on } \Pi^\circ \quad \text{and} \quad \langle h_i, h_j \rangle_{\mathbf{L}_2} = \delta_{ij}.$$

Since we have merely scaled the functions ξ_i , we also have

$$\text{span}\{h_1, h_2, \dots\} = \text{span}\{\xi_1, \xi_2, \dots\}.$$

That implies

$$\begin{aligned} \mathbf{L}_2\text{-closure of } \text{span}\{h_1, h_2, \dots\} &= \mathbf{L}_2\text{-closure of } \mathbf{H}^1\text{-closure of } \text{span}\{h_1, h_2, \dots\} \\ &= \mathbf{L}_2\text{-closure of } \mathbf{H}_{\mathbb{G}}, \end{aligned}$$

and since the inclusion $\mathbf{H}_{\mathbb{G}} \hookrightarrow \mathbf{L}_2(\Pi^\circ)$ is dense by Lemma 55, we have

$$\overline{\text{span}\{h_1, h_2, \dots\}}^{\mathbf{L}_2} = \mathbf{L}_2(\Pi^\circ).$$

In summary, we have shown that $\{h_1, h_2, \dots\}$ is an orthonormal basis of $\mathbf{L}_2(\Pi^\circ)$ consisting of eigenfunctions of $-\Delta$.

Extending the basis on Π° to a basis on Π . Each h_i is in $\mathbf{C}^\infty(\Pi^\circ)$, and hence has a unique continuous extension \bar{h}_i to Π° . Since $\text{vol}_n(\partial\Pi) = 0$, we can isometrically identify $\mathbf{L}_2(\Pi^\circ)$ with $\mathbf{L}_2(\Pi)$: Under this identification, each function h_i on the interior Π° is equivalent to any measurable extension of h_i to Π , so

$$\overline{\text{span}\{h_1, h_2, \dots\}}^{\mathbf{L}_2} = \mathbf{L}_2(\Pi) .$$

The extended functions also satisfy

$$-\Delta\bar{h}_i = \lambda_i\bar{h}_i \text{ on } \Pi \quad \text{and} \quad \langle \bar{h}_i, \bar{h}_j \rangle_{\mathbf{L}_2(\Pi)} = \delta_{ij} ,$$

where the first identity extends from Π° to Π by \mathbf{C}^∞ -continuity, and the second holds since the boundary does not affect the integral. The functions \bar{h}_i are hence eigenfunctions of $-\Delta$ on Π , and form an orthonormal basis of $\mathbf{L}_2(\Pi)$. \square

G.2. Proof of the Fourier representation on \mathbb{R}^n

Proof of Theorem 7. To deduce the theorem from Lemma 56, we must (1) extend the basis constructed on Π above to a basis on \mathbb{R}^n , and (2) show that every continuous invariant function can be represented in this basis.

1° Consider the function \bar{h}_i in the proof of Lemma 56. Recall each \bar{h}_i is infinitely smooth on Π and satisfies the periodic boundary condition. It follows by (12) that

$$e_i := \bar{h}_i \circ p$$

is in $\mathbf{C}_\mathbb{G}$. Let Δ^k denote the k -fold application of Δ . By Lemma 27, the fact that \bar{h}_i satisfies the periodic boundary condition (6) implies that the continuous extension $\overline{\Delta\bar{h}_i}$ also satisfies (6). Iterating the argument shows that the same holds for the continuous extension of $\Delta^k\bar{h}_i$ for any $k \in \mathbb{N}$. We hence have

$$\Delta^k e_i = \Delta^k(\bar{h}_i \circ p) = \overline{(\Delta^k \bar{h}_i)} \circ p \quad \text{and} \quad \overline{(\Delta^k \bar{h}_i)} \circ p \in \mathbf{C}_\mathbb{G} \quad \text{for all } k \in \mathbb{N} ,$$

so e_i has infinitely many continuous derivatives on \mathbb{R}^n . Since it is also \mathbb{G} -invariant, it solves the constrained eigenvalue problem (13) on \mathbb{R}^n . That extends Lemma 56 to \mathbb{R}^n .

2° It remains to be shown that a function f on \mathbb{R}^n is in $\mathbf{C}_\mathbb{G}$ if and only if $f = \sum c_i e_i$ for some sequence (c_i) , where the series converges in the supremum norm. Combining Corollary 17 and (37) shows that

$$h \mapsto \bar{h} \circ p \quad \text{is an isometry} \quad \mathbf{C}_{\text{pbc}}(\Pi^\circ) \rightarrow \mathbf{C}_\mathbb{G} .$$

For any $f : \mathbb{R}^n \rightarrow \mathbb{R}$, we hence have

$$f = \sum c_i e_i \quad \iff \quad f|_{\Pi^\circ} = \sum c_i e_i|_{\Pi^\circ} .$$

In other words, we have to show that

$$h \in \mathbf{C}_{\text{pbc}}(\Pi^\circ) \iff h = \sum c_i e_i|_{\Pi^\circ} \quad \text{and hence that} \quad \mathbf{C}_{\text{pbc}}(\Pi^\circ) = \overline{\text{span}\{e_i|_{\Pi^\circ} \mid i \in \mathbb{N}\}}^{\text{sup}} .$$

Since the proof of Lemma 56 shows $\{e_i|_{\Pi^\circ} \mid i \in \mathbb{N}\}$ is a rescaled orthonormal basis of $\mathbf{H}_\mathbb{G}$, and hence a subset of $\mathbf{H}_\mathbb{G} \cap \mathbf{C}_{\text{pbc}}(\Pi^\circ)$ that is dense in $\mathbf{H}_\mathbb{G}$, that holds by Lemma 55. \square

H Proofs IV: Embeddings

To prove Theorem 15, we first establish two auxiliary results on topological dimensions of quotient spaces. Recall from Fact 37 that \mathbb{R}^n/\mathbb{G} is locally isometric to quotients of metric balls. The first lemma considers the effect of taking a quotient on the dimension of a ball. The second lemma combines this result with Fact 37 to bound the dimension of \mathbb{R}^n/\mathbb{G} .

Lemma 57 (Quotients of metric balls). *Let B be an open metric ball in \mathbb{R}^n , and G a finite group of isometries of \mathbb{R}^n . Then the quotient B/G has topological dimension*

$$n \leq \text{Dim}(B/G) < n + |G|.$$

Proof. The quotient map $q : B \rightarrow B/G$ is, by definition, continuous and surjective. Recall that preimages of points under q are orbits: If $\omega \in \mathbb{R}^n/\mathbb{G}$ is the orbit $G(x)$ of some $x \in \mathbb{R}^n$, then $q^{-1}\omega = G(x)$. We show q is also closed: Let $A \subset B$ be a subset. First observe that

$$qA \text{ closed} \Leftrightarrow B/G \setminus qA \text{ open} \Leftrightarrow q^{-1}(B/G \setminus qA) \text{ open},$$

by continuity of q . This set can be expressed as

$$q^{-1}(B/G \setminus qA) = B \setminus q^{-1}qA = B \setminus \left(\bigcup_{\phi \in G} \phi A \right) = \bigcap_{\phi \in G} \phi(B \setminus A),$$

and is therefore open whenever A is closed, since each ϕ is an isometry and G is finite. Consider any element $\omega \in B/G$. Then there is some $x \in B$ with $\omega = q(x)$, and

$$q^{-1}\omega = \{\phi x \mid \phi \in G \text{ and } \phi x \in B\} \quad \text{which shows that} \quad |q^{-1}\omega| \leq |G|.$$

Fact 47(ii) is now applicable, and shows

$$\text{Dim } B \leq \text{Dim}(B/G) < \text{Dim } B + |G|,$$

and by Fact 47(i), $\text{Dim } B = n$. □

Lemma 58 (Topological dimension of the quotient space). *Let \mathbb{G} be a crystallographic group that tiles \mathbb{R}^n with a convex polytope Π . Then \mathbb{R}^n/\mathbb{G} is a \mathbb{G} -orbifold, of topological dimension*

$$n \leq \text{Dim } \mathbb{R}^n/\mathbb{G} < n + \max_{x \in \Pi} |\text{Stab}(x)|$$

Proof. Choose the index set in the orbifold definition as $\mathcal{I} = \Pi$. By Fact 37, we may then choose $U_x = B_{d_{\mathbb{G}}}(q(x), \varepsilon)$, the group H_x as $\text{Stab}(x)$, and the map

$$\theta_x : B_{d_{\mathbb{G}}}(q(x), \varepsilon) \rightarrow B_{d_n}(x, \varepsilon)$$

as the isometry guaranteed by Fact 37. That makes \mathbb{R}^n/\mathbb{G} an orbifold. Isometry of the open balls also implies for the corresponding closed balls of radius $\delta = \varepsilon/2$ that

$$\overline{B}_{d_{\mathbb{G}}}(q(x), \delta) \quad \text{is homeomorphic to} \quad \overline{B}_{d_{\mathbb{G}}}(x, \delta)/\text{Stab}(x) \quad \text{for each } x \in \Pi.$$

Since homeomorphic spaces have the same topological dimension, Lemma 57 shows

$$\overline{B}_{d_{\mathbb{G}}}(q(x), \delta) = \overline{B}_{d_{\mathbb{G}}}(x, \delta)/\text{Stab}(x) < n + |\text{Stab}(x)|.$$

Since \mathbb{G} is crystallographic, the quotient space is compact, and we can hence cover it with a finite number of the closed balls above. Applying Fact 47(i) then shows the result. □

Proof of Theorem 15. Let \mathcal{S} be the side pairing defined by \mathbb{G} for Π . Since \mathbb{G} is by definition a discrete group of isometries, \mathcal{S} is subproper (see [53], 13.4, problem 2). The gluing construction hence constructs a set M that is a \mathbb{G} -orbifold, according to Fact 42. By definition of M as a quotient, the gluing construction also defines a quotient map

$$q_M : \Pi \rightarrow M ,$$

which is continuous and surjective. By Fact 40, the quotient topology is metrized by d_{path} . By Fact 40, the metric space (M, d_{path}) is complete. It hence follows by Fact 43 that there exists a isometry

$$\gamma_M : (M, d_{\text{path}}) \rightarrow (\mathbb{R}^n/\mathbb{S}, d_{\mathbb{S}}) ,$$

where \mathbb{S} is the group generated by \mathcal{S} . In our case, $\mathbb{S} = \mathcal{S}_{\Pi}$, and by Fact 41, the generated group is $\mathbb{S} = \mathbb{G}$. That shows γ_M in fact an isometry

$$\gamma_M : (M, d_{\text{path}}) \rightarrow (\mathbb{R}^n/\mathbb{G}, d_{\mathbb{G}}) .$$

Since isometric spaces have the same topological dimension, Lemma 58 shows

$$\text{Dim } M < n + \max_{x \in \Pi} |\text{Stab}(x)| .$$

By Fact 47(ii) there is an embedding $e : M \rightarrow \mathbb{R}^N$ with $N \leq 2(n + \max |\text{Stab}(x)|) - 1$. Since \mathbb{G} is crystallographic, and \mathbb{R}^n/\mathbb{G} hence compact, M and $\Omega := e(M)$ are compact. Using the restriction $q : \Pi \rightarrow \mathbb{R}^n/\mathbb{G}$ of the quotient map to Π , we can define

$$\rho_{\Pi} : \Pi \rightarrow \Omega \quad \text{as} \quad \rho_{\Pi} := e \circ \gamma^{-1} \circ q .$$

By the properties of the constituent maps, ρ_{Π} is continuous and satisfies the periodic boundary condition (6). That makes $\rho := \rho_{\Pi} \circ p$ continuous and \mathbb{G} -invariant. If $h : \mathbb{R}^N \rightarrow Y$ is a continuous function, the composition $f = h \circ \rho$ is hence continuous and \mathbb{G} -invariant on \mathbb{R}^n . Conversely, suppose $f : \mathbb{R}^n \rightarrow Y$ is continuous and \mathbb{G} -invariant. For each $z \in \Omega$, the preimage $\rho^{-1}\{z\}$ is precisely the orbit $\mathbb{G}(x)$ of some $x \in \Pi$. Since \mathbb{G} -invariant function are constant on orbits, the assignment

$$\hat{h}(z) := \text{the unique value of } f \text{ on the orbit } \rho^{-1}\{z\}$$

is a well-defined and continuous function $\hat{h} : \Omega \rightarrow Y$. Since Ω is compact, \hat{h} has a (non-unique) continuous extension to a function $h : \mathbb{R}^N \rightarrow Y$, which satisfies $f = h \circ \rho$. \square

I Proofs V: Kernels and Gaussian processes

I.1. Kernels

Proof of Proposition 19. Suppose κ is invariant. For any $f \in \mathbb{H}$, (28) implies

$$f(\phi x) = \langle f, \kappa(\phi x, \cdot) \rangle_{\mathbb{H}} = \langle f, \kappa(x, \cdot) \rangle_{\mathbb{H}} = f(x) ,$$

so f is \mathbb{G} -invariant. Conversely, suppose all $f \in \mathbb{H}$ are \mathbb{G} -invariant. Let f_1, f_2, \dots be a complete orthonormal system. Then all f_i are \mathbb{G} -invariant, so (29) shows

$$\kappa(\phi x, \psi y) = \sum_{i \in \mathbb{N}} f_i(\phi x) f_i(\psi y) = \sum_{i \in \mathbb{N}} f_i(x) f_i(y) = \kappa(x, y)$$

and κ is invariant. Suppose κ is also continuous. If κ is invariant, its infimum and supremum on \mathbb{R}^n equal its infimum and supremum on the compact set Π , and since κ is continuous, that implies it is bounded. That shows all functions in \mathbb{H} are continuous [59, 4.28]. \square

The main ingredient in the proof of Proposition 23 is the following lemma, which shows that the RKHS of κ is isometric to that of $\hat{\kappa}$, and that an explicit isometric isomorphism between them is given by composition with the embedding map ρ .

Lemma 59. *Let $\hat{\kappa}$ be a continuous kernel on Ω with RKHS $\hat{\mathbb{H}}$. Set*

$$\kappa := \hat{\kappa} \circ (\rho \otimes \rho) \quad \text{and} \quad \mathbb{H} := \text{RKHS defined by } \kappa .$$

Then κ is a continuous kernel on \mathbb{R}^n , is \mathbb{G} -invariant in both arguments, and $\mathbb{H} \subset \mathbf{C}_{\mathbb{G}}$. The map

$$I : \hat{\mathbb{H}} \rightarrow \mathbb{H} \quad \text{defined by} \quad \hat{f} \mapsto \hat{f} \circ \rho$$

is a linear isometric isomorphism, and two functions \hat{f} and \hat{g} in $\hat{\mathbb{H}}$ are orthogonal if and only if $\hat{f} \circ \rho$ and $\hat{g} \circ \rho$ are orthogonal in \mathbb{H} .

Proof. 1° The kernel κ is clearly continuous, since $\hat{\kappa}$ and ρ are. Since Ω is compact, $\hat{\kappa}$ is bounded, and since $\|\kappa\|_{\text{sup}} = \|\hat{\kappa}\|_{\text{sup}}$, it follows that κ is bounded. Bounded continuity of κ implies all elements of \mathbb{H} are continuous [59, Lemma 4.28]. That shows $\mathbb{H} \subset \mathbf{C}_{\mathbb{G}}$.

2° Next, consider the map I . Linearity of I is obvious. To show it is bijective, write

$$S := \text{span}\{\kappa(x, \cdot) \mid x \in \mathbb{R}^n\} \quad \text{and} \quad \hat{S} := \text{span}\{\hat{\kappa}(\omega, \cdot) \mid \omega \in \Omega\} .$$

Note that makes \mathbb{H} the norm closure of S , and $\hat{\mathbb{H}}$ the norm closure of \hat{S} (see Appendix B.4).

3° Consider any $\hat{f} \in \hat{S}$. Then $\hat{f} = \sum a_i \hat{\kappa}(\omega_i, \cdot)$ for some scalars a_i and points ω_i in Ω . Since ρ is surjective by Theorem 15, we can find points x_i in \mathbb{R}^n such that $\omega_i = \rho(x_i)$. It follows that

$$f = \hat{f} \circ \rho = \left(\sum a_i \hat{\kappa}(\rho(x_i), \cdot) \right) \circ \rho = \sum a_i \kappa(x_i, \cdot) \in S \quad \text{and hence} \quad I(\hat{S}) \subset S .$$

Reversing the argument shows $I^{-1}(S) \subset \hat{S}$. Thus, I is a linear bijection of \hat{S} and S .

4° Substituting $\hat{f} \in \hat{S}$ as above into the definition of the scalar product shows

$$\langle \hat{f}, \hat{g} \rangle_{\hat{\mathbb{H}}} = \sum a_i a_j \hat{\kappa}(\rho(x_i), \rho(x_j)) = \sum a_i a_j \kappa(x_i, x_j) = \langle f, g \rangle_{\mathbb{H}}$$

and hence $\|f\|_{\mathbb{H}} = \|\hat{f}\|_{\hat{\mathbb{H}}}$ for all $\hat{f} \in \hat{S}$. In summary, we have shown that the restriction of I to \hat{S} is a bijective linear isometry $\hat{S} \rightarrow S$.

5° Since I is an isometry on a dense subset, it has a unique uniformly continuous extension to the norm closure $\hat{\mathbb{H}}$, which takes the norm closure $\hat{\mathbb{H}}$ to the norm closure \mathbb{H} of the image and is again an isometry [3, 3.11]. \square

Proof of Proposition 23. 1° By Theorem 15, there is a unique continuous function

$$\hat{\kappa} : \Omega \times \Omega \rightarrow \mathbb{R} \quad \text{that satisfies} \quad \kappa = \hat{\kappa} \circ (\rho \otimes \rho) .$$

Lemma 59 then implies all $f \in \mathbb{H}$ are \mathbb{G} -invariant and continuous.

2° We next show the inclusion is compact. Consider first the map $I : \hat{f} \mapsto \hat{f} \circ \rho$ as in Lemma 59, but now defined on the larger space $\mathbf{C}(\Omega)$. We know from Theorem 15 that I is an isometric isomorphism $\mathbf{C}(\Omega) \rightarrow \mathbf{C}_{\mathbb{G}}$ (with respect to the supremum norm). By Lemma 59 its restriction to a map $\hat{\mathbb{H}} \rightarrow \mathbb{H}$ is also an isometric isomorphism (with respect to the RKHS norms). It follows that the inclusion maps

$$\iota : \mathbb{H} \rightarrow \mathbf{C}_{\mathbb{G}} \quad \text{and} \quad \hat{\iota} : \hat{\mathbb{H}} \rightarrow \mathbf{C}(\Omega) \quad \text{satisfy} \quad \iota = I \circ \hat{\iota} \circ I^{-1} .$$

Since $\hat{\kappa}$ is a continuous kernel by step 1, and its domain Ω is compact by Theorem 15, the inclusion $\hat{\iota}$ is compact [59, 4.31]. The composition of a compact linear operator with

any continuous linear operator is again compact [4, Theorem 5.1]. Since I and its inverse are linear and continuous, that indeed makes ι compact.

3° Since $\hat{\kappa}$ is a continuous kernel on a compact domain, Mercer's theorem [59, 4.49] holds for $\hat{\kappa}$. It shows there are functions $\hat{f}_1, \hat{f}_2, \dots$ and scalars $c_1 \geq c_2 \geq \dots > 0$ such that

$$(\sqrt{c_i} \hat{f}_i)_{i \in \mathbb{N}} \text{ is an ONB for } \hat{\mathbb{H}} \quad \text{and} \quad \hat{\kappa}(\omega, \omega') = \sum_i c_i \hat{f}_i(\omega) \hat{f}_i(\omega') \quad \text{for all } \omega, \omega' \in \Omega .$$

The functions $f_i := \hat{f}_i \circ \rho$ then satisfy

$$\kappa(x, y) = \hat{\kappa}(\rho(x), \rho(y)) = \sum_i c_i \hat{f}_i(\rho(x)) \hat{f}_i(\rho(y)) = \sum_i c_i f_i(x) f_i(y) .$$

Since the map $\hat{f} \mapsto \hat{f} \circ \rho$ preserves the scalar product by Lemma 59, the sequence $(\sqrt{c_i} f_i)$ is an ONB for \mathbb{H} .

4° It remains to verify the representation

$$\mathbb{H} = \{ f = \sum_{i \in \mathbb{N}} a_i \sqrt{c_i} f_i \mid a_1, a_2, \dots \in \mathbb{R} \text{ with } \sum_i |a_i|^2 < \infty \} .$$

Since Mercer's theorem applies to $\hat{\kappa}$, the analogous representation

$$\hat{\mathbb{H}} = \{ \hat{f} = \sum_{i \in \mathbb{N}} a_i \sqrt{c_i} \hat{f}_i \mid a_1, a_2, \dots \in \mathbb{R} \text{ with } \sum_i |a_i|^2 < \infty \}$$

holds on Ω , by Steinwart and Christmann [59, 4.51]. As $\hat{f} \mapsto \hat{f} \circ \rho$ is an isometric isomorphism by Lemma 59, that yields the representation for \mathbb{H} above. \square

I.2. Gaussian processes

Proof of Proposition 24. That F is continuous and \mathbb{G} -invariant almost surely follows immediately from Theorem 15. Let $\tilde{\Pi}$ be a transversal. Our task is to show that the restriction $F|_{\tilde{\Pi}}$ is a continuous Gaussian process on $\tilde{\Pi}$. To this end, suppose h is a continuous function on \mathbb{R}^N . Then $h \circ \rho$ is continuous by Theorem 15, and the restriction is again continuous. That means

$$\tau : h \mapsto (h \circ \rho)|_{\tilde{\Pi}} \quad \text{is a map} \quad \mathbf{C}(\Omega) \rightarrow \mathbf{C}(\tilde{\Pi}) .$$

Since both composition with a fixed function and restriction to a subset are linear as operations on functions, τ is linear, and since neither composition nor restriction can increase the sup norm, it is bounded. The restriction

$$F|_{\tilde{\Pi}} = \tau(H)$$

is hence the image of a Gaussian process with values in the separable Banach space $\mathbf{C}(\Omega)$ under a bounded linear map into the Banach space $\mathbf{C}(\tilde{\Pi})$. That implies it is a Gaussian process with values in $\mathbf{C}(\tilde{\Pi})$, and that κ and μ transform accordingly [63, Lemma 7.1]. \square